FIELD PERFORMANCE EVALUATION OF SUSTAINABLE AGGREGATE BY-PRODUCT APPLICATIONS

Prepared By
Issam Qamhia
Erol Tutumluer, PhD.
Hasan Ozer, PhD.
University of Illinois at Urbana-Champaign

ILLINOIS CENTER FOR TRANSPORTATION

1. Report No. FHWA-ICT-18-016	2. Government Accession No. N/A	3. Recipient's Catalog No. N/A
4. Title and Subtitle Field Performance Evaluation of Sustainable Aggregate By-product Applications		**5. Report Date** October 2018
		6. Performing Organization Code N/A
7. Author(s) Issam Qamhia, Erol Tutumluer, and Hasan Ozer		**8. Performing Organization Report No.** ICT-18-019 UILU-ENG-2018-2019
9. Performing Organization Name and Address Illinois Center for Transportation Department of Civil and Environmental Engineering University of Illinois at Urbana-Champaign 205 North Mathews Avenue, MC-250 Urbana, IL 61801		**10. Work Unit No.** N/A
		11. Contract or Grant No. R27-168
12. Sponsoring Agency Name and Address Illinois Department of Transportation Bureau of Research 126 East Ash Street Springfield, IL 62704		**13. Type of Report and Period Covered** Final Report 9/1/15 – 10/3/18
		14. Sponsoring Agency Code FHWA

15. Supplementary Notes

Conducted in cooperation with the U.S. Department of Transportation, Federal Highway Administration.

16. Abstract

Research efforts at the Illinois Center for Transportation (ICT) focused on evaluating new sustainable applications of Quarry By-products (QB) or QB mixed with other marginal, virgin, or recycled aggregate materials in pavements, as unbound or chemically stabilized pavement layers. Sixteen full-scale test sections were constructed to evaluate the use of QB in base, subbase, and aggregate subgrade applications. The chemically stabilized test sections utilizing QB were stabilized with 3% cement or 10 % Class 'C' fly ash by dry weight and were constructed over a subgrade having an engineered unsoaked California bearing ratio (CBR) of 6% to study their effectiveness in low to medium volume flexible pavements. The unbound applications of QB investigated the use of QB to fill the voids between large aggregate subgrade rocks commonly used for rockfill applications on top of very soft subgrade soils, as well as using dense-graded aggregate subgrade layers with higher fines content up to 15% passing No. 200 sieve for soft subgrade remediation. These unbound test sections were constructed over a CBR=1% subgrade soil to investigate their effectiveness in both construction platforms and low volume road applications. All the field test sections were then evaluated in rutting and fatigue by applying traffic loading using a super-single wheel in Accelerated Pavement Testing (APT). Following APT, forensic analysis tests were conducted to further evaluate the test section performances; these tests included: Falling Weight Deflectometer (FWD) tests before and after trafficking, hot mix asphalt coring, Dynamic Cone Penetrometer (DCP) profiling of subsurface layers, and trenching to expose the cross sections of the constructed sections. In general, results from APT and forensic analyses indicated that satisfactory results and improved rutting performance were obtained from all the test sections utilizing QB applications. Therefore, the proposed QB applications are deemed to be readily implementable and can be successfully incorporated into standard pavement construction and rehabilitation practices.

17. Key Words Quarry by-product, Accelerated Pavement Testing, Field Performance, Recycled Aggregates, Sustainability, Sustainable Construction Practice, Aggregate Subgrade, Chemical Stabilization	18. Distribution Statement No restrictions. This document is available through the National Technical Information Service, Springfield, VA 22161.		
19. Security Classif. (of this report) Unclassified	**20. Security Classif. (of this page)** Unclassified	**21. No. of Pages** 83 pp + appendices	**22. Price** N/A

Form DOT F 1700.7 (8-72)   **Reproduction of completed page authorized**

ACKNOWLEDGMENTS, DISCLAIMER, MANUFACTURERS' NAMES

EXECUTIVE SUMMARY

Quarry by-products (QB), usually less than 0.25 in. (6 mm) in size, are the residual deposits from the production of required grades of aggregates, and are often stockpiled in excess quantities at the quarries. Estimates in 2012 indicated that more than 4 billion US tons of QB were accumulated from the 3,000 operating quarries around the US. QB poses environmental and economic challenges as they accumulate in large quantities in landfills or interfere with quarry operations. With recent focus on sustainable construction practices and the scarcity of natural resources, more common and sustainable uses of by-product materials such as QB are becoming imperative.

This research effort, conducted at the Illinois Center for Transportation (ICT), focused on introducing and evaluating new sustainable applications of QB and/or QB mixed with other marginal, virgin or recycled aggregate materials in pavements. The selected QB applications were evaluated through the construction of full-scale pavement test sections utilizing QB in targeted sustainable applications, and testing them with heavy wheel loads through accelerated pavement testing (APT). The QB applications studied included both unbound and bound (chemically stabilized) pavement subsurface/foundation layers. The QB pavement layer applications studied were in five different categories:

1. Using QB for filling voids/gaps between large stones as aggregate subgrade on soft subgrades. Aggregate subgrade refers to a term used by the Illinois Department of Transportation (IDOT) linked to furnishing, transporting, and placing granular materials for weak subgrade remediation and regular subbase applications.

2. Increased fines content (e.g. 15% QB fines passing No. 200 sieve) in dense-graded aggregate subbase over soft subgrade soils with California Bearing Ratio (CBR) = 1%. The current IDOT specifications allow for a maximum of 12% passing the No. 200 sieve for such applications.

3. Using QB as a cement or fly ash-treated subbase (e.g., in inverted pavements).

4. Using QB as a cement or fly ash-treated base material.

5. For base course application, blending QB with coarse aggregate fractions of recycled materials [Fractionated Reclaimed Asphalt Pavements (FRAP) or Fractionated Recycled Concrete Aggregates (FRCA)] and stabilizing the blends with 3% cement or 10% class C fly ash by weight.

Prior to the field evaluations of the above QB applications in full-scale pavement test sections, several complementary laboratory studies were conducted to prepare and finalize the intended QB applications. The main laboratory studies in this category are: (1) A packing study of QB with FRAP/FRCA to determine the optimum blending ratio by weight that maximizes density and reduces voids; (2) A packing study to construct layers of large aggregate subgrade and use vibratory action to drive the QB into the inherent voids to determine the optimum quantity of QB that can be packed; and, (3) Unconfined Compressive Strength (UCS) tests to determine the strength characteristics of stabilized QB and QB blends with 3% cement and 10% class C fly ash. Other laboratory tests were also conducted such as grain size distribution, moisture-density, and aggregate morphological shape properties.

The laboratory tests indicated that an optimum blending ratio of QB with recycled coarse materials was 70% QB and 30% course recycled aggregates (FRAP or FRCA) blends by weight. A 3% cement or 10% class C fly ash were found to provide the appropriate compressive strength levels for chemically stabilized QB and QB blends, with blends of QB, FRAP, and cement achieving the highest strength; which was statistically different from chemically stabilized QB blends without coarse aggregates. The packing tests of QB into the voids of large aggregate subgrades indicated that 25% QB by the dry weight of the large rocks is the optimum QB quantity to be used, after consideration of QB stockpiles with an excess of 2.5% moisture contents.

Fifteen full-scale pavement test sections utilizing QB applications and one additional control (conventional flexible) section were constructed in three 'Test Cells.' Cell 1 had four paved and four unpaved test sections. Construction platforms and low volume road applications of QB were studied. Particularly, there were two applications studied: (1) QB used to fill the voids of large aggregate subgrade rocks by shaking the QB from the surface in one or two lifts; and (2) Dense-graded aggregate subgrade layers with 15% plastic and nonplastic fines.

Cells 2 and 3 studied chemically stabilized QB applications for base and subbase layers, and one control section constructed with dense-graded unbound aggregate layer conforming to IDOT's CA06 gradation requirements. The QB applications studied for base materials included QB + FRAP + cement, QB + FRCA + cement, QB + FRAP + fly ash, and QB + cement. For the QB + cement application, two test sections with QB from two sources were constructed to investigate the effect of the QB source on performance. The QB applications studied for subbase applications included a cement-stabilized QB subbase and a CA06 base, as well as a fly ash-stabilized QB subbase and CA06 base.

Construction activities included engineering the top 305 mm (12 in.) existing subgrade to a CBR = 1% for Cell 1 test sections and to a CBR = 6% for all the pavement test sections in Cells 2 and 3. Subgrade modification was achieved through moisture adjustment and compaction. Quality assurance measures included checking for subgrade strength and uniformity with a Dynamic Cone penetrometer (DCP), and measuring subgrade density with a nuclear density gauge. Satisfactory strength/density values were achieved for target soil strengths.

The construction of the QB layers were successfully achieved and extensively monitored throughout construction. The data for nuclear density measurements and moisture contents indicated that nearly all the test sections were constructed with near optimum moisture contents and/or achieved proper densities. A Lightweight Deflectometer (LWD) was used to assess the stiffness/modulus of the constructed layers after the construction of each lift. It was also used to monitor the increase in stiffness of the chemically stabilized layers for up to 11 days after construction. Satisfactory modulus values were achieved for Cell 1 test sections, and the increase in stiffness of the chemically stabilized layers was the highest for cement-stabilized test sections and usually lower for fly ash-stabilized sections. Particularly, the section with the cement-stabilized QB/FRAP blend had the highest back-calculated modulus.

Following the paving of test sections with hot mix asphalt, Falling Weight Deflectometer (FWD) tests were conducted on all finished surfaces. Significantly low deflection values were measured for the sections with stabilized QB, particularly the ones constructed with QB blends with FRAP/FRCA.

Accelerated Pavement Testing (APT) was conducted using the Advanced Transportation Loading Assembly (ATLAS). For the purpose of this study, a constant unidirectional wheel load of 10 kips (44.5 kN), a tire pressure of 110 psi (760 kPa), and a constant speed of 5 mph (8 km/h) were assigned. Construction platforms in Cell 1 South (Cell 1S) were trafficked with 20,000 passes. Flexible pavement sections in Cell 1 North (Cell 1N) were trafficked with up to 90,000 passes. The exceptionally good performance of some of the stabilized QB applications in Cells 2 and 3 necessitated trafficking with more passes (135,000 passes total), and increasing the load/pressure for the latter 35,000 passes to 14 kip (62.3 kN)/ 125 psi (862 kPa) in order to have more consistent and meaningful comparisons among the test sections.

Measurements for rutting progression for the construction platform test sections in Cell 1S showed good performance for the sections constructed with 15% nonplastic fines and with blends of large aggregate subgrade rocks with QB. The section constructed with 15% plastic fines showed quick deterioration and a significant increase in rutting rate progression in the events of rain (i.e. high moisture contents). For the flexible pavement sections in Cell 1N, a similarly good performance was observed in all the test sections with relatively low rut amounts for a total of 90,000 ATLAS passes.

Measurements of rutting progression in Cells 2 and 3 indicated exceptionally good performance of sections with blends of QB and FRAP/FRCA stabilized with cement; which had very low rutting progression after 135,000 passes, despite the increase in load/pressure levels at 100,000 passes. Generally, sections stabilized with cement accumulated lower rutting than those stabilized with fly ash. For cement-stabilized QB sections with QB from different sources, no significant differences in rutting performance was detected, indicating a negligible effect of QB sources. For the inverted section with a cement-stabilized QB base, measured rut amounts were significantly lower than those in the test section with the fly ash-stabilized QB base, and the overall rut measurements were relatively low. None of the stabilized sections showed any signs of cracks despite the increased load and the high number of ATLAS passes.

The control section constructed with unbound aggregates in Cell 3 showed the earliest signs of failure, with cracks starting to appear in the transition zone after 30,000 passes. The early failure, and high rutting accumulation, which is not typical for such sections from the experience of IDOT, was attributed to the as-constructed low HMA thickness, resulting in lower structural capacity and premature cracking. Moisture seepage through the thin, low density HMA resulted in higher moisture contents in the base, which contributed to pumping of fines under the heavy loading. The resulting loss of support further accelerated the cracking and rut accumulation with dipping of the ATLAS wheel in this section.

Four of the test sections in Cells 2 and 3 were instrumented with soil pressure cells on top of the engineered CBR = 6% subgrade. Data collected from these pressure cells showed that significantly low vertical pressures were transmitted to the subgrade for sections with stabilized bases/subbases (i.e. Cell 2 Section 1, Cell 2 Section 4, and Cell 3 Section 2). In fact, subgrade pressures recorded for

the control section in Cell 3 were 3-5 times higher than those recorded for the other three cement-stabilized test sections in both Cells 2 and 3 instrumented with subgrade pressure cells.

Additional testing and forensic analyses were conducted after the APT study to better understand and assess the performance of the constructed test sections. These tests included: (1) FWD testing to track changes in deflections before and after APT; (2) HMA coring; (3) DCP testing for the aggregate subgrade/subbase/base layers to assess the strength; (4) Flooded tests for the aggregate subgrade/QB test sections to assess the effect of flooding on FWD deflections; and (5) Trenching of the test sections to assess uniformity of construction and determine as-constructed layer thicknesses. Results from these forensic tests and analyses further supported the conclusions from the APT study indicating the overall quite satisfactory performance results of these sustainable QB applications.

TABLE OF CONTENTS

LIST OF FIGURES

LIST OF TABLES

LIST OF ACRONYMS

APT	Accelerated Pavement Testing
ATLAS	Advanced Transportation Loading Assembly
ATREL	Advanced Transportation Research and Engineering Laboratory
CBR	California Bearing Ratio
C#S#	Cell # - Section # (Number of Cell and Section)
DCP	Dynamic Cone Penetrometer
FRAP	Fractionated Reclaimed Asphalt Pavements
FRCA	Fractionated Recycled Concrete Aggregate
FWD	Falling Weight Deflectometer
IBV	Immediate Bearing Value
ICT	Illinois Center for Transportation
IDOT	Illinois Department of Transportation
LL	Liquid Limit
LWD	Lightweight Deflectometer
MDD	Maximum Dry Density
OMC	Optimum Moisture Content
PI	Plasticity Index
QB	Quarry By-products

CHAPTER 1: INTRODUCTION

1.1 BACKGROUND AND MOTIVATION

Quarry by-products (QB) are an industrial by-product of aggregate quarry processes. They are typically less than 0.25 in. (6 mm) in size and consist of coarse, medium, and fine sand particles, and a clay/silt fraction. Quarry by-products are found abundantly all over the United States due to the vast network of crushed rock extraction facilities. Quarry by-products are produced during crushing, washing, and screening operations. QB exists in three types, resulting from these operations: screenings, pond fines, and baghouse fines (Chesner et al., 1998). During the crushing stages, QBs are generally carried out in three stages: primary crushing, secondary crushing, and tertiary crushing (Petavratzi and Wilson 2007). Research conducted in the early 1990s showed that stockpiled fines comprised an average of approximately 12% of the total annual aggregate production of the surveyed companies (Kumar and Hudson 1992). The more recent NCHRP Synthesis 435 (volume 4) reports that, depending on the type of rock quarried, QB can make up to 25% of the total aggregates produced (Stroup-Gardiner and Wattenberg-Komas, 2013). Due to the high accumulation of QB that exceeds 4 billion US tons (3.6 billion metric tons) of quarry by-products from 3,000 quarries in the US (Chesner et al., 1998), and the high quantities of QB produced yearly, which can be as high as 950,000 tons in Illinois alone (Tutumluer et al., 2015), a more common use of QB as a sustainable pavement construction material becomes imperative.

In a recent ICT R27-125 project, entitled, "Sustainable Aggregates Production – Green Applications for Aggregate By-Product," QB production in Illinois was evaluated through questionnaires distributed to the aggregate producers. The amount of QB accumulated in the quarries, the annual production rate, excess QB generated, and the current application areas of QB were among the survey questions [5]. Ninety percent of the survey respondents indicated that they were producing QB. Among the quarries that produced quarry fines in Illinois, 55% of them produced in excess of 100,000 tons of QB in a year (Tutumluer et al., 2015).

As part of the ICT R27-125 project, a detailed laboratory study was also conducted to characterize the engineering properties of QB materials produced in the primary, secondary, and tertiary aggregate production stages from four different major quarries operating in the State of Illinois. Property tests were conducted for determining aggregate gradation, particle shape characteristics, and mineralogical analyses of the QB samples. Differences in shape and gradation properties of QB materials produced in each crushing stage were observed. Because the unconfined compressive strength for QB materials is typically low (less than 11 psi [76 kPa]), two chemical admixture stabilizers (Portland cement and Class C fly ash) were used to improve the strength properties of QB materials. In general, 2% cement and 10% Class C fly ash-treated QB materials were 10 to 30 times stronger than the virgin QB samples (Tutumluer et al., 2015). Such significant increases observed in the strength of stabilized QB materials have indicated suitability of QBs for sustainable pavement applications.

Another recent ICT project R27-124, titled, "Evaluation of Aggregate Subgrade Materials Used as Pavement Subgrade/Granular Subbase," had the objective of evaluating and validating the existing

IDOT 'Aggregate Subgrade' gradation bands through full-scale field testing (Kazmee and Tutumluer, 2015). Aggregate subgrades are large-sized rocks used in the IDOT Standard Specifications for Road and Bridge Construction linked to furnishing, transporting, and placing granular materials for subgrade improvement and subbase.

As part of the findings of the ICT R27-124 project, the penetration of aggregate subgrade into a very soft subgrade was demonstrated to be effective in improving the weak subgrade and preparing a fairly stable working platform layer in pavement construction (Kazmee and Tutumluer, 2015). Nevertheless, the uniformly graded materials, such as the railway ballast or large primary crusher run aggregates with 6-8 in. (150-200 mm) top size, exhibited a wider variation in rutting performance because of the presence of large inherent voids (Kazmee and Tutumluer, 2015). Therefore, one of the recommendations of the ICT R27-124 project was to consider the inclusion of smaller sized aggregate materials to fill voids, improve aggregate interlock, and improve the performance of the uniformly graded large size aggregate subgrade materials. Low cost QB or non-plastic fines were especially recommended for such beneficial and sustainable pavement applications. The challenge was to ensure uniformity by avoiding segregation among different blended aggregate sizes.

Given the high production and accumulation rates of QB, and the negative environmental/ economical consequences that result from its accumulation at the quarries, various pavement applications can provide opportunities to utilize mass quantities of QB (Tutumluer et al., 2018). This project therefore, aimed to evaluate sustainable pavement applications to incorporate QBs by adequately evaluating their field performance as recommended by both the R27-124 and R27-125 research project outcomes. In order to assess the field performance of such applications, both unsurfaced and hot mix asphalt (HMA) surfaced pavements were constructed as test sections at the Advanced Transportation Research and Engineering Laboratory (ATREL) and were tested to failure using the Advanced Transportation Loading Assembly (ATLAS) equipment. Following accelerated pavement testing (APT), forensic analysis tests (such as Falling Weight Deflectometer or FWD testing, HMA coring, Dynamic Cone Penetration or DCP testing, and trenching) were conducted to further evaluate the constructed test section performances. The results of APT and forensic analyses are used in this report to recommend the most successful and sustainable QB applications studied in the field for pavement construction practice.

1.2 QB APPLICATIONS STUDIED

Given the potential of using QB materials in pavement applications, in light of the recommendations of the previous R27-124 and R27-125 research project outcomes, the following applications were selected for studying in the field the QB usage as unbound aggregate materials and as chemically stabilized materials:

1. Using QB for filling voids/gaps between large stones as aggregate subgrade on soft subgrades.

2. Increased fines content (e.g. 15% passing No. 200 sieve) in dense-graded aggregate base layer over soft subgrade soils with CBR 1% or less.

3. Using QB as a cement or fly ash-treated subbase (e.g., in inverted pavements).

4. Using QB as a cement or fly ash-treated base material.

5. For base course application, blending QB with coarse aggregate fractions of recycled materials [Fractionated Reclaimed Asphalt Pavements (FRAP) or Fractionated Recycled Concrete Aggregates (FRCA)] and stabilizing the blends with 3% cement or 10% class C fly ash by weight.

These selected promising QB applications were investigated by constructing 16 full-scale test sections, and evaluating their performance through APT, and other nondestructive and destructive testing techniques during construction, and forensic analyses after APT.

1.3 RESEARCH OBJECTIVES

The primary objective of this research project was to investigate and document potential successful uses of quarry by-products in subsurface/foundation layers for pavement applications. The following specific goals were determined for the study:

- Develop and evaluate laboratory characterization techniques to select and investigate the proper construction of aggregate subgrade/QB layers, and proper mix proportioning of QB, with and without recycled coarse materials, and chemical admixtures, i.e., cement and fly ash.

- Evaluate the field performances of the proposed unstabilized and chemically stabilized QB applications for weak subgrade replacement, and subbase and base layers through the accelerated testing of full-scale test sections: both unsurfaced working platform applications and asphalt-surfaced low to medium volume pavements.

- Use the study findings of the field performance evaluations to recommend implementation projects and draft revisions to existing material specifications governing the use of QB materials in pavement applications.

1.4 RESEARCH METHODOLOGY

To fulfill the above stated research objectives, the following tasks and methodology are considered in this study:

- Characterizing the properties and engineering behavior of the selected construction materials by collecting and testing adequate amounts of the selected QB and other construction materials to determine their engineering properties. Properties such as grain size distribution, morphological shape properties, moisture-density relationships, packing of QB with other recycled/marginal materials, and unconfined compressive strength tests were conducted.

- Constructing and instrumenting full-scale pavement test sections using the selected sustainable applications of QB materials. Sixteen test sections were constructed in three test 'Cells' to evaluate a unique set of QB applications. Soil pressure cells were used to collect pressure values on top of the subgrade under some of the stabilized QB test sections and the conventional flexible control section.

- Accelerated pavement testing and performance monitoring of the constructed test sections, through frequent mesurements of rutting progression, subgrade pressures, and visual inspection of the test sections.

- Testing and monitoring the full-scale pavement sections during construction, testing, and after trafficking. The quality and strength of the constructed test sections were investigated by collecting data for the achieved nuclear gauge densities, dynamic cone penetrometer (DCP) testing, Light Weight Deflectometer (LWD) modulus measurements, Falling Weight Deflectometer (FWD) deflection measurements, HMA coring, and trenching.

- Analyses of the field section performances, and the recommendations for implementation of research findings. The recommendations were documented based on the construction and accelerated testing stages, and the interpretation of the study results in comparison with results from previously conducted field studies.

1.5 REPORT ORGANIZATION

This report consists of seven chapters, including this introduction chapter.

Chapter 2, titled 'Literature Review,' provides a brief literature of the past studies associated with using QB, recycled materials, and marginal aggregates in pavement applications.

Chapter 3, titled 'Materials Selection, Characterization & Laboratory Studies,' provides a discussion of the materials selection criteria and the laboratory component of this project. Laboratory tests such as grain size distribution, moisture-density tests, packing studies of QB with recycled coarse aggregates and with large aggregate subgrade rocks, and unconfined compressive strength testing of chemically stabilized QB applications are discussed in this chapter.

Chapter 4, titled 'Construction of Full-Scale Pavement Test Sections, and Quality Assurance Measures,' provides details of the layouts of the field pavement test sections, and a detailed description of construction activities such as subgrade strength modification, various construction phases of the full-scale test sections, pavement instrumentation with subgrade soil pressure cells, and associated quality control tests.

Chapter 5, titled 'Performance Monitoring with Accelerated Pavement Testing,' provides a summary of the performance records of the constructed working platform and flexible pavement test sections. This includes the rutting progression in all test sections and the measured top of subgrade wheel load deviator stresses for sections instrumented with soil pressure cells.

Chapter 6, titled 'Full-Scale Test Study Results and Interpretations,' provides a summary of the tests conducted after the APT, and an interpretation of the performance of the test sections in light with the different datasets collected during the stages of construction, trafficking, and forensic analysis.

Chapter 7, titled 'Summary and Conclusions,' provides a summary of the test results, the main recommendations and conclusions from the field evaluations of QB applications. This chapter also

discusses promising implementation projects as the next steps to further study, as well as some recommendations for future research.

CHAPTER 2: LITERATURE REVIEW

2.1 INTRODUCTION

This chapter presents a brief summary of some of the previous research studies related to the laboratory characterization of Quarry by-Products (QB), and their utilization in pavement applications. The use of other recycled/marginal aggregates, and a brief review of the current design practices for low volume roads and construction platforms, are also discussed in this chapter.

2.2 LABORATORY CHARACTERIZATION OF QUARRY BY-PRODUCTS

Due to the high production and accumulation rates of QB, potential application areas in the construction and rehabilitation of the transportation infrastructure were reported in the literature. Several past research studies focused on laboratory property testing and evaluating field applications of QB. Kalcheff and Machemehl (1980) conducted particle size distribution tests for different types of QB. It was reported that screenings generally contain freshly fractured faces, have fairly uniform gradation, and contain few plastic fines. The particle distributions of the tested QB followed a similar gradation trend, with particles smaller than sieve No. 200 (0.075 mm) ranging from 6% to 12%. Kumar and Hudson (1992) examined the unconfined compressive strength, tensile modulus of elasticity, and Poisson's ratio of cement-treated QB. Their study concluded that stabilizing QB with cement could produce the adequate compressive strength, modulus of elasticity, and tensile strength required for subbase materials.

It is generally agreed that the properties of QB could not be easily predicted or generalized due to the natural variability of parent rock and the different crushing technologies employed (Stroup-Gardiner and Wattenberg-Komas, 2013; Wood and Marek, 1995; Manning, 2004). Stokowski (1992) has shown that QB are rich in $CaCO_3$, SiO_2, Al_2O_3, and Fe_2O_3 relative to $MgCO_3$. As a result of this finding, quarry by-products have lower specific gravity and are relatively soft because of calcite ($CaCO_3$) and being rich in clay minerals (SiO_2, Al_2O_3, and Fe_2O_3). According to Dumitru et al. (2001), mineralogical tests such as X-ray diffraction analysis need to be conducted to determine the compositions of secondary minerals and to quantify the amounts of harmful content that can be detrimental to some applications.

Petavratzi and Wilson (2007) concluded that QB were composed of the same mineral substances as the soil and solid rock from which they are derived, and that they are usually inert or non-hazardous by their nature. Puppala et al. (2008) reported that the liquid limit, plastic limit, and specific gravity of a QB material in Texas were found to be 21.5%, 11.7% and 2.65, respectively. They also concluded that the compressive strength of untreated (virgin) QB can be very low. Puppala et al. (2012) conducted one-dimensional vertical free-swelling test of QB. In their study, the QB samples were found to be of moderately swelling potential. Mwumvaneza et al. (2015) conducted unconfined compressive strength tests on QB obtained from different sources, and concluded that the strength of untreated QB is relatively low.

Based on laboratory testing results, some researchers have utilized chemical stabilization and accordingly recommended specific field applications for QB. According to Kalcheff and Machemehl (1980), the stabilization of QB with cement developed relatively high rigidity with a small amount of Portland cement compared with granular soil-cement stabilization. The use of low-cement content has the advantage of decreasing the shrinkage cracking. In 1992, Kumar and Hudson examined the unconfined compressive strength, tensile modulus of elasticity, and Poisson's ratio of cement-treated QB materials. It was concluded that stabilizing QB with cement could produce the adequate compressive strength, modulus of elasticity, and tensile strength required for subbase materials. They proposed a base course material additive, flowable fill, under slab granular fill, and cement-stabilized subbase/base layers as possible pavement applications of QB.

According to the results presented in the study by Wood and Marek (1995), using 3% cement, 8% fly ash, and 89% QB resulted in a flowable fill with adequate performance. Naik et al. (2005) examined the use of QB in Self-Consolidating Concrete (SCC). They found that the addition of QB minimized the addition of the admixture without reducing the strength of the SCC. Puppala et al. (2008) reported that the addition of 2.3% cement increased the unconfined compressive strength to 174 psi (1,200 kPa). It is concluded that the strength and resilient modulus of the cement-treated QB are similar to those of sandy materials with very few fines. Mwumvaneza et al. (2015) conducted unconfined compressive strength tests on 10% Class 'C' fly ash and 2% Portland cement-stabilized QB samples, and they examined that the chemically stabilized QB specimens exhibited up to 30 times strength improvement when compared with untreated QB materials.

Finally, in a laboratory study conducted by LaHucik et al. (2016), various proportions of cement-treated mixes of QB and fractionated RAP were evaluated. Based on the aggregate packing tests on blends of QB and FRAP, an optimal blend was determined to minimize the void content. The blend consisted of 70% QB with 30% FRAP, by weight. Additionally, LaHucik et al. (2016) evaluated mixture design performances through strength tests (compression and split tension) and modulus tests. Higher cement content increased both the strength and elastic modulus of all the tested mixes. Mixtures containing virgin aggregates with QB yielded statistically greater elastic moduli than mixtures with FRAP and QB. Fibers did not have a statistical effect on strength or elastic modulus but did provide residual shear capacity across cracks. The QB and FRAP or QB and virgin aggregate mixtures with 3% to 4% cement content exceeded the strengths for typical cement-stabilized base materials in the literature (LaHucik et al., 2016).

2.3 QUARRY BY-PRODUCT APPLICATIONS IN PAVEMENTS

The use of QB as a subsurface material, in a base or a subbase layer, was evaluated through field studies. The QB was used as an 8-in. (203-mm) thick base layer, topped with 1.2 in. (30 mm) of surface treatment for a low traffic volume roadway in Brazil (de Rezende and de Carvalho, 2003). No significant structural damages were observed for more than three years of service. However, the QB that was used had around 45% of material passing the No. 4 sieve (4.75 mm) and had a relatively high percentage of silts and clays (22%). Lab-measured resilient modulus values ranged from 28.5 to 68.4 ksi (196.6 to 471.6 MPa).

The use of QB in a stabilized base layer has also been investigated by researchers (Tutumluer et al., 2018a). In a study in Lynn County, Iowa, the use of emulsion-stabilized limestone screening was investigated as a base material (Nelson et al., 1994). Several test sections with base thicknesses of 4-6 in. (100-150 mm) and asphalt cement contents of 2.5%, 3.5%, and 4.5% were inspected. The 4-in. (100-mm) base thickness did not produce a satisfactory low cost maintenance roadway. It was recommended that a 6-in. (150-mm) emulsion-stabilized QB base with more than 3.5% asphalt cement, topped with 50-mm (2-in.) HMA surface could provide a low maintenance roadway (Nelson et al., 1994).

In a study in Arlington, Texas, the use of limestone QB was evaluated as a base material for sections of a State Highway 360 (Puppala et al., 2008). A 36-in. (914-mm) thick quarry fines layer stabilized with 2.3% cement was used as the base layer, topped with 4-in. (102-mm) HMA and 8-in. (203-mm) Continuously Reinforced Concrete Pavement (CRCP) surface. Field monitoring using horizontal inclinometers showed that the sections experienced low permanent deformation during service. Additionally, the International Roughness Index (IRI) values were measured to be within 0.5-2.5 m/km after 30 months of service, which is lower than the threshold value of 3.15 m/km, thus indicating good performance (Puppala et al., 2012).

In several other research studies, various field applications to utilize QB were proposed based on their mechanical and physical properties and laboratory performance. In a 1992 study by Kumar and Hudson, the unconfined compressive strength, tensile modulus of elasticity, and Poisson's ratio of QB treated with 8% cement were examined for use as a subbase material. They proposed base course material additive, flowable fill, under slab granular fill, and cement-stabilized subbase/base layers as possible pavement applications of QB. McClellan et al. (2002) sampled QB from several quarries in Florida, and reported engineering backfill and direct addition to concrete mixes as a filler or fine aggregates as potential sustainable applications of QB that required the usage of mass quantities of QB. Other potential use areas for QB include self-consolidating concrete (Wood and Marek, 1995; Naik et al., 2005), and the replacement of sand in concrete to enhance pozzolanic reactions and durability (Lohani, 2012). NCHRP synthesis 435 (volume 4) summarizes the different uses of QB in pavement applications by the different states in the US. More details can be found in the original reference (Stroup-Gardiner and Wattenberg-Komas, 2013).

2.4 RECYCLED / MARGINAL AGGREGATE APPLICATIONS IN PAVEMENTS

Due to the wide use of recycled materials in pavement foundation and subsurface (base/subbase/subgrade) applications, researchers have focused on the evaluation of the engineering properties and field performance of recycled materials in unbound and bound pavement layers. Bennert et al. (2000) evaluated recycled concrete aggregate (RCA) and recycled asphalt pavement (RAP) aggregate for resilient modulus and permanent deformation trends, and compared performance with dense-graded aggregate base coarse (DGABC) materials in New Jersey. Both RCA and RAP were mixed at various percentages with the DGABC. They reported that RAP, RCA, and DGABC blended materials obtained higher resilient modulus values than the currently used virgin aggregates, while RCA mixed samples obtained the lowest amount of permanent deformation.

Similarly, Arulrajah et al. (2012) reported that in terms of usage in pavement subbases, RCA and waste rock have geotechnical engineering properties equivalent or superior to those of typical quarry granular subbase materials. More research has reported similar findings for the use of RAP, RCA, or blends with virgin aggregates for unbound applications (Arulrajah et al., 2013) and cement-treated applications (Mohammadinia et al., 2014).

IDOT has recently introduced open-ended gradation bands allowing the inclusion of large rocks with a maximum dimension in the range of 6 to 8 in. (152 to 203 mm). These large rocks can be originated from both the primary crushing stage at quarries and recycled sources, and are often referred to as "aggregate subgrade" materials by IDOT. In a recent full-scale accelerated pavement testing study, such application of large rocks was proven to be beneficial in terms of pavement rutting performance (Kazmee and Tutumluer, 2015). However, the researchers also concluded that uniformly graded large rocks could exhibit variable performance in strength and deformation characteristics due to significant particle reorientation in the presence of large voids in the granular matrix.

2.5 SUMMARY

This Chapter provided a literature review of the past studies associated with using QB, recycled materials, and marginal aggregates in pavement applications. Since the 1980s, several research studies focused on the quantification of QB production rates, and the characterization of their mechanical and physical properties in the laboratory. Many researchers have proposed applications for QB in pavements based on the laboratory characteristics. The proposed applications were mainly in concrete mixes or as chemically stabilized subsurface layers. Such applications included: cement-stabilized base/subbase QB layers, flowable fills, replacement of sand in concrete, and engineering backfill.

Despite proposing many applications for QB, only a few research and field studies were conducted to incorporate QB in pavement design, or to evaluate the field performance of QB materials under heavy wheel loading. The current field effort described in this report serves as a continuity of a recent research project which primarily focused on studying QB applications that demonstrated through laboratory testing to be potentially beneficial to use for improved pavement foundation.

CHAPTER 3: MATERIALS SELECTION, CHARACTERIZATION & LABORATORY STUDIES

3.1 INTRODUCTION

This chapter presents a discussion of the materials selected for the field APT study, and the laboratory testing and characterization results conducted for these materials. The materials were selected to cover different geographical regions and sources in the state of Illinois. The laboratory tests that are deemed necessary for characterizing the collected materials and ensuring good quality construction were performed at ICT. Laboratory testing included grain size distribution, compaction characteristics (moisture-density relationships), unconfined compressive strength tests for the stabilized QB samples, a packing study for a primary crusher run aggregate subgrade material and QB, and a packing study of QB with coarse recycled aggregates (FRAP & FRCA). The results and conclusions from these laboratory tests are summarized in this chapter.

3.2 SELECTION OF MATERIALS

In total, nine aggregate materials were selected from across the state of Illinois to construct the full-scale pavement test sections. Out of the nine materials, three are QB materials obtained from three different quarries that have excess quantities of QB stored on-site. Three materials are aggregate base course materials, referred to here by CA06_R, CA06_15NPF, and CA06_15PF. The CA06_R (R stands for regular) material falls in the IDOT CA06 gradation band for coarse aggregates (see Table 3.1). The other two aggregate materials (CA06_15NPF, and CA06_15PF) conform to the IDOT CA06 gradation, except that they have 15% nominal non-plastic and plastic fines content, respectively, passing the No. 200 sieve, or finer than 0.075 mm. The plastic fines had a plasticity index (PI) of 8%, and a liquid limit (LL) of 21%. The current IDOT specification permits a maximum of 12% fines passing No. 200 sieve.

A Primary Crusher Run (PCR) virgin aggregate conforming to IDOT CS02 gradation for aggregate subgrade materials (see Table 3.2) was obtained to study an application of QB as a filler material for the voids in these large aggregates for increased stability. In addition, two recycled materials (FRAP and FRCA) were obtained to study chemically stabilized applications of QB mixed with these recycled materials and stabilized with cement or class 'C' fly ash. A summary of the nine materials and three source locations in the state of Illinois is shown in Table 3.3.

In addition to the nine aggregate materials, Type I Portland cement, and self-cementitious Class 'C' fly ash materials were obtained from local vendors in Urbana to be used as stabilizing agents or chemical admixtures in the pavement test sections for studying chemically stabilized applications of QB. The hot mix asphalt (HMA) used to pave the test sections comprised an asphalt binder with a Superpave performance grade of PG 64-22, and a 0.375-in. (9.5-mm) nominal aggregate size.

Table 3.1. IDOT Gradation Band for CA06 Coarse Aggregate Material

Sieve Size	1 ½"	1"	1/2"	# 4	# 16	# 200
Sieve Size (mm)	38 mm	25 mm	12.7 mm	4.75 mm	1.19 mm	0.075 mm
Percent Passing (%)	100	95±5	75±15	43±14	25±15	8±4

Table 3.2. IDOT Gradation Band for CS02 Aggregate Subgrade Material

Sieve Size	6"	4"	3"	2"	#4	# 200
Sieve Size (mm)	152 mm	102 mm	76 m	51 mm	4.75 mm	0.075 mm
Percent Passing (%)	100	80 ± 10		25 ± 15		

Table 3.3. Selected Aggregate Materials and Quarry Locations

Material ID	Quarry Location	Materials Collected	Quarry Locations (Illinois)
QB1	(A) Bolingbrook	Quarry By-product	
QB2	(B) Thornton	Quarry By-product	
QB3	(C) Dupo	Quarry By-product	
CA06_R	(D) Fairmont	Aggregate material, conforming to CA06 Gradations	
CA06_15NPF	(E) Aurora	Aggregate material, conforming to IDOT CA06 gradations, 15% nonplastic fines Passing No. 200 sieve	
CA06_15PF	(F) Milan	Aggregate material, conforming to IDOT CA06 gradations, 15% plastic fines Passing No. 200 sieve	
PCR (CS02)	(G) Lisbon	Primary Crusher Run aggregates, conforming to IDOT CS02 gradations	
FRAP	(H) Urbana	Fractionated RAP	
FRCA	(H) Urbana	Fractionated RCA	

3.3 LABORATORY CHARACTERIZATIONS OF SELECTED MATERIALS/APPLICATIONS

Several laboratory tests were conducted to determine the properties of the construction materials selected to build the full-scale test sections for the unbound and chemically stabilized applications of QB. These laboratory tests were deemed necessary to ensure high quality construction, and to correlate with expected field performance. The laboratory tests discussed in this section include: (1) Grain size distribution; (2) Compaction characteristics, i.e. moisture-density relationships; (3) Packing study of QB2 with recycled coarse FRAP and FRCA aggregates; (4) Unconfined compressive strength (UCS) tests for the chemically stabilized materials; and (5) Packing study of PCR with QB1 shaken from the top to fill the voids of the large rocks for increased stability.

3.3.1 Particle Size Distributions

The particle size distributions of four aggregate materials (QB1, QB2, QB3, and FRAP) were determined by dry sieve analyses in accordance with the ASTM C136 / C136M Standard (ASTM, 2014). For the other four materials that conform to IDOT's CA06 aggregate gradation specifications, namely FRCA, CA06_15NPF, CA06_15PF, and CA06_R, the gradations were determined with washed sieve analyses using a mechanical apparatus as per ASTM C117 Standard (ASTM, 2017). For the primary crusher run aggregate material having a nominal maximum aggregate particle size of 6 in. (152 mm), representative samples were separated on the 3 in. (76 mm) sieve, and the gradation of aggregate particles passing the 3 in. (76-mm) sieve was determined with conventional dry sieve analysis. For particles retained on the 3 in. (76-mm) sieve, the field imaging technique previously used by Kazmee and Tutumluer (Kazmee and Tutumluer, 2015), was used to determine the particle sizes and aggregate shape morphological properties. Figure 3.1 shows the particle size distributions of the nine selected aggregate materials, and the corresponding IDOT aggregate gradation bands.

Figure 3.1(a) presents the particle size distributions for the three QB materials. All three materials have similar gradation curves, and are relatively well-graded. The fines content passing sieve No. 200 (0.075 mm) ranges between 12% and 13% for all QB materials. Overall, QB1 exhibited the finest gradation among all three materials, which can facilitate the percolation to fill up the voids between large PCR stones. QB2 has a relatively coarser gradation compared to QB1 and QB3.

Figure 3.1(b) shows the gradations of the CA06_15NPF, CA06_15PF, and CA06_R materials. The particle size distribution for CA06_R conforms with IDOT's CA06 gradation band limits, while the gradations of CA06_15NPF and CA06_15PF have higher fines content than the currently accepted limit for CA06 of 12%. The fines content passing sieve No. 200 (0.075 mm) for CA06_R is 8.8%, determined by washed sieving. The fines contents for CA06_15NPF and CA06_15PF were 14.2% and 16.2%, respectively, slightly lower/higher than the target 15% fines content.

The particle size distribution of the PCR aggregate is shown in Figure 3.1(c). The gradation falls within the CS02 gradation band specified by IDOT. These aggregates have a nominal maximum aggregate size of 6 in. (152 mm), and are mostly larger than 0.5 in. (12.5 mm) in size. The gradation curves for QB1 that was used to fill the voids of the PCR aggregates, and the CA06_R used as a capping material are shown as superimposed for comparison.

Finally, Figure 3.1(d) shows the gradation curves of the FRCA and FRAP materials that are used as coarse aggregates and blended with QB2 in the construction of three stabilized base pavement test sections. The FRAP material has a relatively coarser gradation with very little fines, and a smaller nominal aggregate size (0.75 in. or 19 mm). The FRCA material, on the other hand, has a grain size distribution that complies with IDOT's CA06 gradation, larger top size particles up to 1.5 in. (38.1 mm), and a higher fines content of 9.1%, determined from washed sieve analysis. Additionally, the FRCA is relatively well-graded while the FRAP material is more uniformly graded.
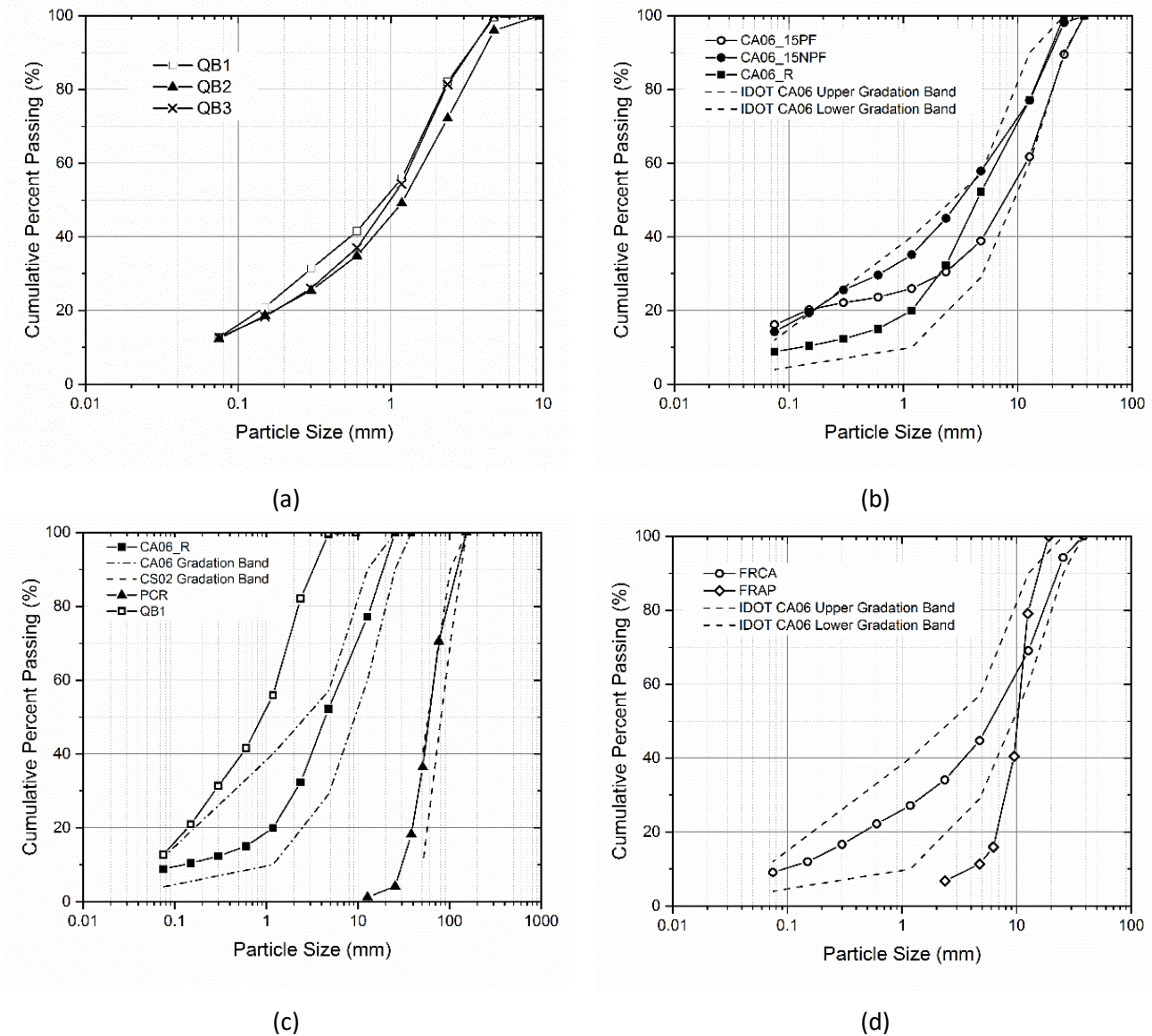
Figure 3.1. Grain size distribution curves for the different construction materials used in this study: (a) QB materials; (b) CA06 materials; (c) Cell '1' materials, including PCR, QB1 and CA06_R; and (d) FRCA and FRAP.

3.3.2 Packing Study of QB2 with Coarse Recycled Materials (FRAP & FRCA)

As part of the chemically stabilized applications that utilize large quantities of QB, some of the constructed applications utilize QB mixed with coarse recycled aggregates (FRAP or FRCA). A study was performed to determine a suitable mix ratio that maximizes the packing density (minimizes voids content) and utilizes high quantities of QB in the mix. The tests were performed by dry-mixing QB2 in different percentages by weight with FRAP or FRCA, and compacting the mixes using the modified compactive effort in a standard CBR mold in five equal lifts. The quantity of QB varied from 30% to 100% by the weight of the total mix, in increments of 10%.

The results are given in Figure 3.2(a), which shows that the density starts to stabilize/maximize at 70% QB and 30% FRAP mix, while the density continues to increase linearly as the amount of QB2 was increased for the case of QB blended with FRCA. A similar laboratory study performed by LaHucik et al. (2016) to determine the optimum blending ratio of QB:FRAP as per ASTM C29 Standard (ASTM, 2017a) concluded that 70% QB by weight maximizes the packing density. However, the trend with changing the QB content was quite different from the one in this study, which was expected due to differences in the gradation of the used FRAP material. For this study, it was decided to use a 70% QB and 30% FRAP or FRCA mixes for the field construction. The mix design provides an opportunity to utilize high quantities of QB within a skeleton of coarse aggregates to achieve higher strength. Figure 3.2(b) shows the combined gradations of 70% QB2 and 30% FRAP/FRCA mixes. It is shown that the QB2/FRAP blend is relatively coarser and has lower fines content compared to the QB2/FRCA blend. The difference is due to the gradations of FRAP and FRCA employed in the respective mix designs.

(a)   (b)
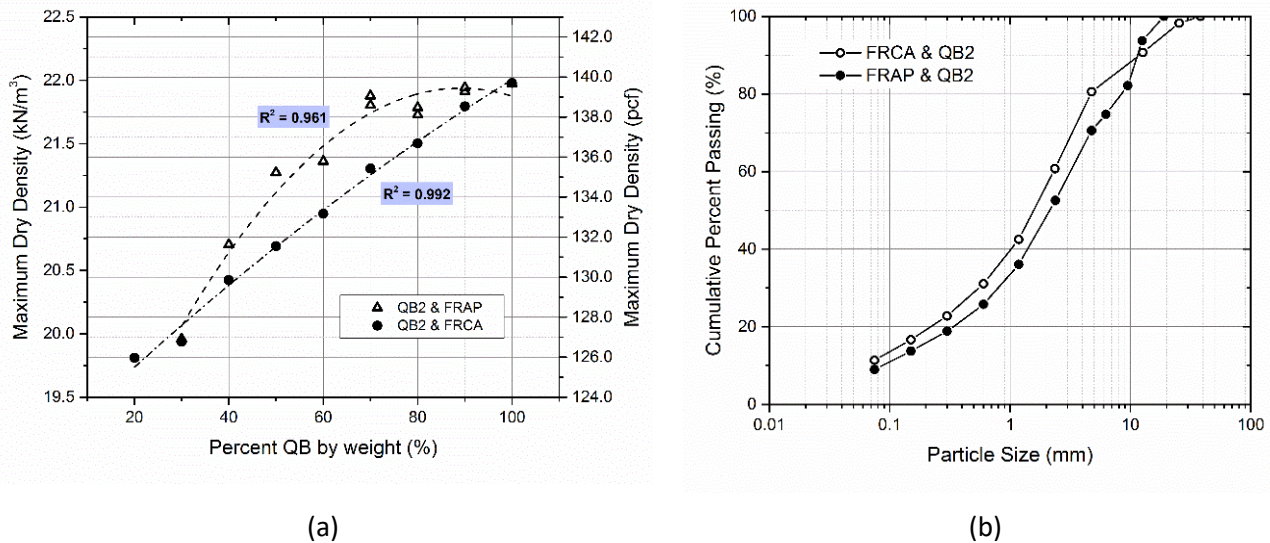
Figure 3.2. QB2 Packing study with FRAP or FRCA: (a) Achieved maximum dry density at different blending ratios; and (b) Grain size distribution curves for QB2:FRAP/FRCA with a 70% QB and 30% FRAP/FRCA mixes.

3.3.3 Moisture-Density Relationships

The maximum dry densities (MDD) and corresponding optimum moisture contents (OMC) were obtained for all materials using the standard compactive effort test procedure as per ASTM D698 Standard (ASTM, 2012). The determination of the moisture-density relationships is deemed critical for the construction phase because the constructed test sections were compacted at the optimum moisture content, and the field densities were checked for the relative compaction, which had to exceed 95% of the MDD as specified by IDOT standards for a passing field density. The compaction characteristics of all the materials that were used in the construction of field test sections are shown in Figure 3.3, grouped by similarity in material or application.

Figure 3.3(a) shows the compaction curves for the three CA06 materials (CA06_R, CA06_15NPF, CA06_15PF). Material CA06_15NPF has the highest MDD and OMC of 138.4 pcf (21.7 kN/m^3) and 6.8%, respectively. Material CA06_15PF exhibited a lower MDD of 134.7 pcf (21.2 kN/m^3) and a slightly lower OMC of 6.5%, which can be attributed to the significantly coarser gradation and the clumping of fines, resulting in less particle exposure and lowering the OMC. The CA06_R material had the lowest MDD and OMC of 132 pcf (20.75 kN/m^3) and 5.4%, respectively. The lower moisture content can be attributed to the lower fines content.

Figure 3.3(b) and Figure 3.3(c) present the moisture-density relationships for the QB2 and QB3 materials, respectively, both for the stabilized and unstabilized QB applications. From Figure 3.3(b), the highest MDD and OMC were for QB2 stabilized with 3% cement, followed by QB2 stabilized by 10% class 'C' fly ash. The MDDs achieved were 137.9, 137.2, and 136 pcf (21.7, 21.6, and 21.4 kN/m^3) for the cement-stabilized, fly ash-stabilized, and unstabilized QB2, respectively; while the OMC values were 9.1%, 8.0%, and 7.9%, respectively. The order of decreasing OMC values is comparable to the one presented in a recent study by Tutumluer et al. (Tutumluer et al., 2015); while the orders of MDD are different and the researchers reported the highest MDD for the fly ash stabilized materials. For QB3 material, the QB3 stabilized with 3% cement had a higher OMC than the unstabilized QB3 (8.4% vs. 7.8%), while the MDD values achieved showed an opposite trend (130 pcf [20.4 kN/m^3] vs. 132 pcf [20.7 kN/m^3]).

Figure 3.3(d) shows the moisture-density curves of the QB2 samples, blended with FRAP or FRCA in a 70% QB and 30% FRAP/FRCA mixes, and stabilized with 3% cement or 10% fly ash. These materials showed similar trends to that seen for stabilized QB2 material, where the fly ash-stabilized QB2/FRAP had a lower OMC compared to the 3% cement-stabilized QB2/FRAP (7.5% vs. 8.0% respectively). However, the fly ash-stabilized QB2/FRAP showed a higher MDD than the cement-stabilized QB2/FRAP (136 pcf or 21.4 kN/m^3 vs. 134.8 pcf or 21.2 kN/m^3), which is more consistent with the previous research (Tutumluer et al., 2015). For the 3% cement-stabilized QB2/FRCA material, the OMC of 9.8% is significantly higher than the cement-stabilized QB2/FRAP material, while the MDD of 129 pcf (20.3 kN/m^3) is significantly lower. One possible explanation is the higher fines content, and the finer grain size distribution of the QB2/FRCA blends. The lower OMC for samples containing FRAP is consistent with other study findings in the literature reported by several other researchers (Bennert and Maher, 2005; MacGregor et al., 1999; Sayed et al., 1993).
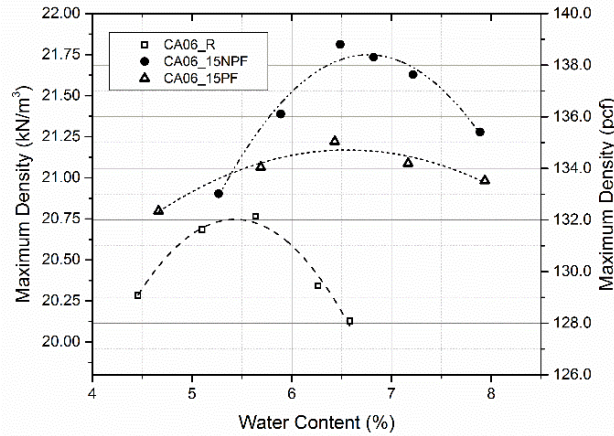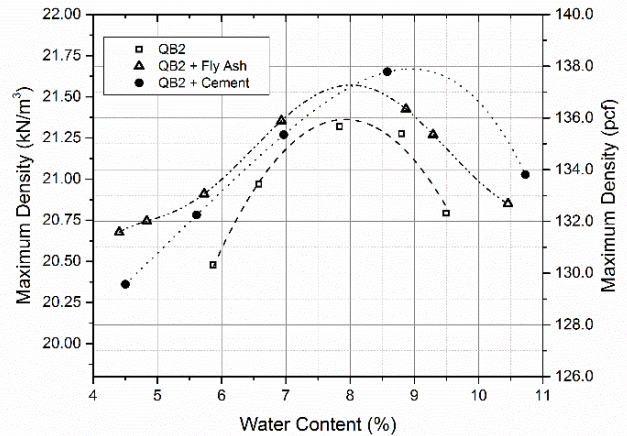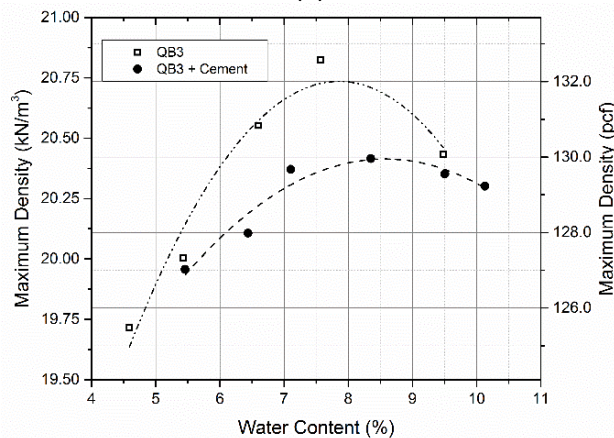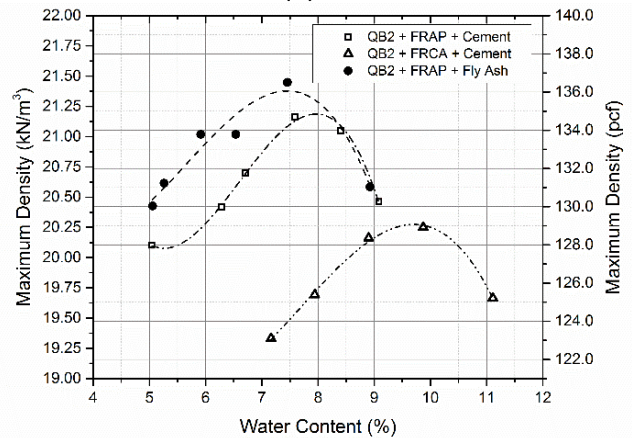
Figure 3.3. Moisture-density curves for the materials used in the construction of field test sections.

3.3.4 Unconfined Compressive Strength Tests for Stabilized QB Applications

Due to the significantly low strength of untreated QB (Tutumluer et al., 2015), the stabilization of QB and QB-FRAP/FRCA blends were necessary for achieving sufficient strength for pavement applications (Qamhia et al., 2016). Accordingly, the QB samples were stabilized with either 3% Type I Portland cement or 10% class 'C' fly ash and tested for their 7-day unconfined compressive strength (UCS). Sample preparations for the QB2 and QB3 materials were carried out according to the procedure outlined in ASTM D1632 Standard (ASTM, 2007). The samples were compacted into a 2.8 in. (71 mm) diameter and 5.6 in (142 mm) tall cylinder in three equal lifts using the standard Proctor hammer. Additionally, cylinders for UCS testing for the QB2/FRAP and QB2/FRCA blends were compacted as per ASTM C1435/ C1435M Standard (ASTM, 2014), with a small change; 4 in. x 8 in. (102 mm x 203 mm) cylinders were made instead of 6 in. x 12 in. (152 mm x 305 mm) cylinders due to the smaller

size of QB. All samples were then cured unsealed in a moisture-controlled room at 100% relative humidity and at room temperature for seven days.

Stabilized samples were tested for the 7-day UCS using the recommendations and procedure outlined in ASTM D1633 standard (ASTM, 2007a). Prior to testing, the samples were completely soaked in water for four hours, surface-dried and capped at the ends using a sulfuric compound, then tested for compressive strength on a Forney loading frame at a rate of 4,000-11,000 lb./minute (18-49 kN/minute). Figure 3.4 compares the seven-day achieved unconfined compressive strength properties of the stabilized samples. Excluding the samples for [FRCA + QB2 + 3% Cement], which had a coefficient of variation of 22.9%, all the other samples had a coefficient of variation lower than 13.5%. Additionally, samples for [FRAP + QB2 + 3% Cement] achieved the highest 7-day UCS, and their strength was statistically different from all other combinations except [FRCA + QB2 + 3% Cement]; using a two-sided t-test with a 95% confidence interval. The mean UCS for [FRAP + QB2 + 10% Fly ash] and [FRCA + QB2 + 3% Cement] are also statistically different from all stabilized QB2 and QB3 samples, while the strength of stabilized QB2 and QB3 samples are not statistically different. The UCS values of [FRAP + QB2 + 10% Fly ash] and [FRCA + QB2 + 3% Cement] are not statistically different, partly due to the high variability in the achieved strengths of the [FRCA + QB2 + 3% Cement] samples.
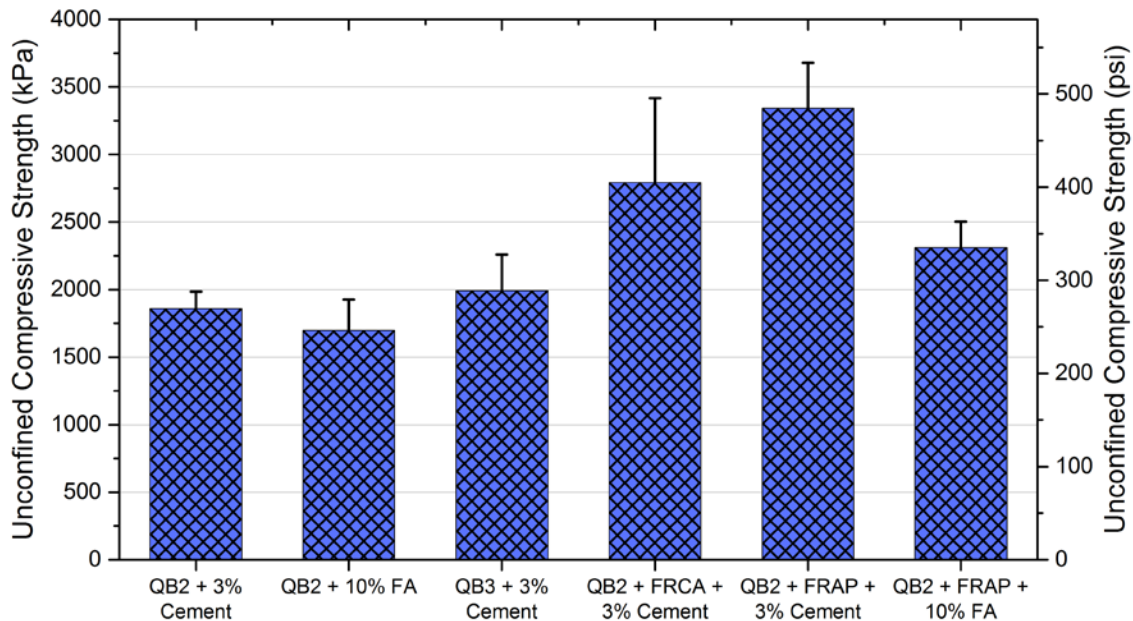
Figure 3.4. Average 7-day unconfined compressive strength (UCS) values of the different chemical admixture stabilized material combinations used in constructing field test sections.

3.3.5 Packing Study of the Aggregate Subgrade and QB

Prior to the construction of test sections utilizing PCR rocks and QB, a laboratory investigation was conducted to ascertain the optimized blend of the large PCR rocks and QB1 in a single lift and in two lifts. A customized compaction steel box (called the UIUC packing box) was built according to the ASTM size specifications to investigate the packing efficiency of the two materials. The steel box, shown in Figure 3.5(a), is 24 in. (610 mm) x 24 in. x 21 in. (530 mm) in height. One side of the box has

a removable steel door, which can be pulled up to expose the cross-section to a Plexiglass side after compaction. A high-resolution image of the cross-section was taken to further study the packing and percolation of QB1 through the large rocks. The goal was to obtain a consistent and meaningful qualitative assessment of QB1 blends to select the optimized QB1 percentage for field applications.

<div align="center">(a)   (b)</div>
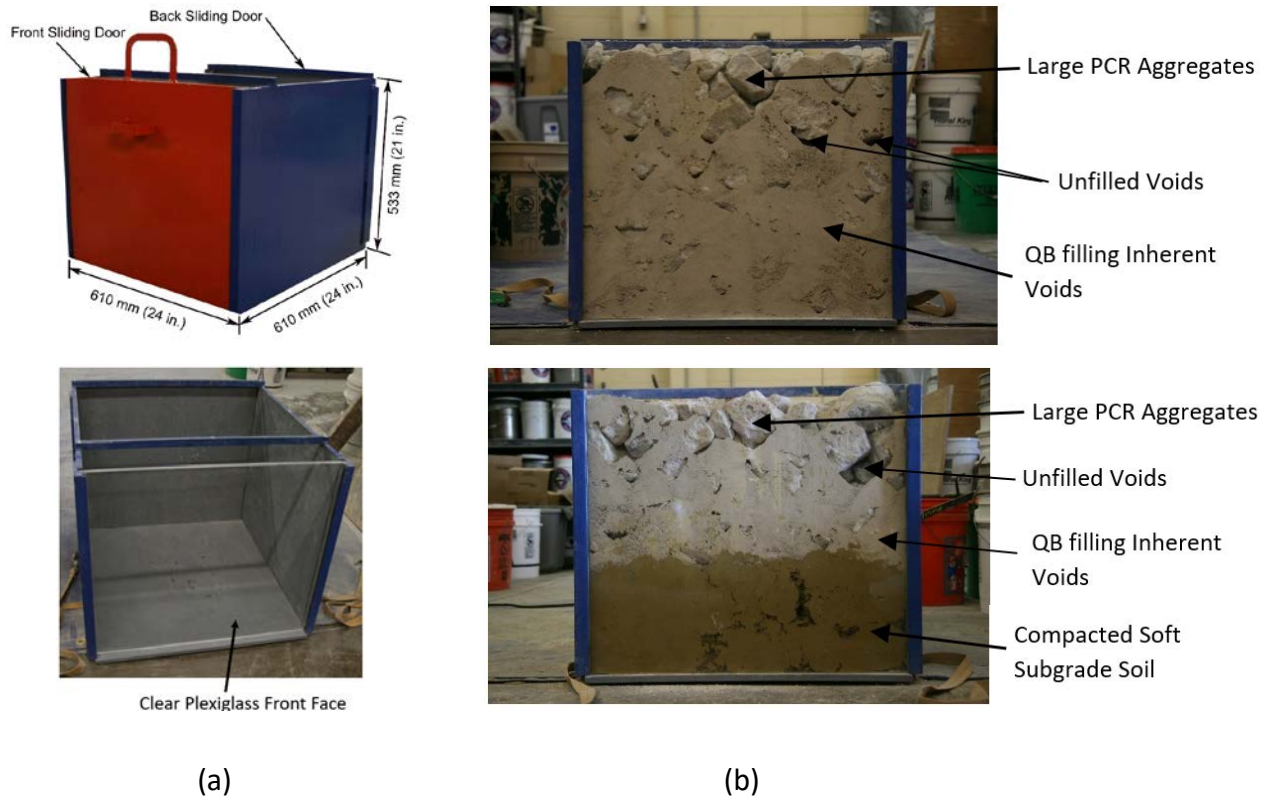
Figure 3.5. (a) UIUC packing box; and (b) Cross-section of the tests with 25% of wet QB (w% = 2.5-2.6%) two lifts (top) and in a single lift on top of soft compacted subgrade (bottom).

The test matrix studied in the laboratory consisted of conducting fourteen different tests using the UIUC packing box. Several variables were studied to examine factors that might affect the packing of the QB with the large rocks, and the maximum quantity of QB that could be intermixed by shaking from the top of the lift. Table 3.4 presents a summary of the variables studied using the test matrix. More details are presented in Appendix A and elsewhere (Qamhia et al., 2017). Vibration was achieved using a laboratory-sized vibratory roller (VIBCO US-1600 model), at a vibration frequency of 9000 rpm, to simulate the field construction procedure.

As a first step, tests for the compaction of the large PCR rocks in a single lift and in two lifts were conducted to measure the void ratios or porosities. The bulk specific gravity of the CS02 PCR aggregate material was measured as per ASTM C127 Standard (ASTM, 2015) to be 2.67. Using this specific gravity and based on the packing arrangement of the large rocks in the box (with no particle crushing or breakage), void ratios of 77.5% and 83.1% were calculated (e = V_v/V_s) for the large rocks compacted in two lifts and in one lift, respectively. These corresponded to porosity values (n = V_v/V_T) of 43.6% and 45.4% for the two- and one-lift arrangements, respectively. Based on these calculations,

the maximum possible QB quantity to be used was determined to be approximately 40% of the weight of the dry large rocks.

Table 3.4. Summary of the Test Matrix for Tests Conducted Using the UIUC Packing Box

Test No.	Percentage of QB (%)	No. of lifts	Moisture Content of QB (%)	Support Condition	Achieved Density pcf (kN/m³)
1	0 (PCR Only)	2	0 (oven-dried)	Steel Bottom	93.8 (14.73)
2	0	2	0	Steel Bottom	93.9 (14.75)
3	0	1	0	Steel Bottom	90.1 (14.15)
4	0	1	0	Steel Bottom	91.9 (14.43)
5	20	2	0	Steel Bottom	113.3 (17.80)
6	40	2	0	Steel Bottom	124.6 (19.57)
7	30	2	0	Steel Bottom	120.6 (18.95)
8	30	1	0	Steel Bottom	119.0 (18.69)
9	30	2	0	Steel Bottom	121.4 (19.07)
10	40	2	0	Steel Bottom	129.1 (20.28)
11	35	1	0	Soft Loose Subgrade	118.3 (18.58)
12	30	2	2.6	Steel Bottom	120.4 (18.91)
13	25	2	2.5	Steel Bottom	116.6 (18.32)
14	25	1	2.6	Soft Compacted Subgrade	118.3 (18.58)

Following the determination of the void ratios, the effects of the following four study variables on the packing arrangements of QB were mainly investigated in the laboratory:

1. Number of lifts: A single 21-in. (530-mm) lift and two approximately equal 10.5-in. (265-mm) lifts with the QB1 were used. Appropriate amounts of QB1 were dropped and vibrated on top of each lift (either single lift or two-lift application) of the PCR rocks.

2. The quantity of the QB1: The quantity was varied from 20% all the way up to 40% of the dry weight of the large rocks.

3. The moisture content (w %) of the QB1: Moisture content represents the dryness or wetness variability of the natural state of QBs obtained from a quarry source and used during pavement construction application. It varied from oven-dried QB1 (0%) to the as-received moisture content of the QB1 material from the source quarry (2.5±0.2%).

4. Reaction support in the experimental setup: The support conditions or foundation rigidity on top of which the samples are compacted need to address varying degrees of subgrade support. The support condition was varied from a rigid steel bottom to a very soft subgrade soil placed at the bottom of the packing box and engineered to a CBR of less than 1% through moisture adjustment.

The heights of the loose large rocks, loose large rocks and QB1 on the surface, and the compacted mix were measured at nine locations (center, midpoint of each face, and each corner), and averaged for density calculations. To minimize variability, the same large aggregates were used for all tests.

Laboratory experiments did not show significant differences in densities and characteristic trends of percolation between the single-lift and two-lift experiments with dry QB1. However, the results are expected to differ for wet QB as higher moisture contents reduce the ability of the QB1 to percolate and fill the voids at shallower depths with a single lift arrangement. For tests with varying QB1 content, 30% was found to be the optimum quantity of QB1 to be mixed with the PCR in the case of dry QB1. However, this same quantity was found to result in a relatively large amount of QB1 left on the surface for wet QB1 with a moisture content of 2.5%. Over the CBR=1% engineered subgrade, the optimum quantity of QB1 that could be packed was found to be 25% by dry weight of the large rocks for single lift arrangement. Moisture content was thus found to be the most dominant factor governing the selection of the maximum allowable percentage of QB1 and optimum packing of inherent voids in PCR aggregates**.** Figure 3.5(b) showed the cross-section of the compacted large rocks with 25% of QB by dry weight of the PCR aggregates, at a moisture content of 2.5-2.6% and (1) compacted in two lifts on top of a rigid steel foundation, and (2) compacted in one lift on top of compacted soft subgrade with CBR of 1%.

3.4 SUMMARY

This chapter provided a discussion of the materials selection criteria and the laboratory research components of this project. Laboratory tests described include grain size distibution, moisture-density tests, packing studies of QB with recycled coarse aggregates and with large aggregate subgrade rocks, and unconfined compressive strength testing of chemically stabilized QB applications.

The laboratory tests indicated that an optimum mixing ratio of QB with recycled coarse materials was 70% QB and 30% FRAP or FRCA by weight. Either 3% cement or 10% class C fly ash was found to provide appropriate compressive strength levels for chemically stabilized QB and QB blends with FRAP and cement achieving the highest strength; which was statistically different from chemically stabilized QB blends without coarse aggregates. The packing tests of QB into the voids of large aggregate subgrades indicated that 25% QB by the dry weight of the large rocks was approximately an optimum QB quantity to be used considering moist or wet conditions of QB delivery in the field. The next chapter will discuss the field designs and construction of the full-scale test sections based on the information from the laboratory studies.

CHAPTER 4: CONSTRUCTION OF FULL-SCALE PAVEMENT TEST SECTIONS, AND QUALITY ASSURANCE MEASURES

4.1 INTRODUCTION

This chapter presents details for the layout of the constructed test sections, the step-by-step construction procedures, and the associated quality assurance procedures followed to assess the quality of the constructed test sections. In total, sixteen different full-scale test sections encompassing four construction platforms and twelve flexible pavements were constructed over weak subgrades of controlled (engineered) strength. Seven of the constructed flexible pavements were aimed at studying mechanically stabilized applications of QB in base and subbase layers. Quality assurance tests included as-constructed nuclear gauge densities and lightweight deflectometer testing.

4.2 LAYOUT OF CONSTRUCTED TEST SECTIONS

The construction took place at the Illinois Center for Transportation's (ICT) accelerated pavement testing facility. The Google satellite image of the construction site, showing the plan view of the constructed pavements is shown in Figure 4.1. A detailed plan view of the test sections is also given in Figure 4.2 of this report. In total, 16 test sections were constructed. The constructed roads were divided into four test blocks (Cells) designated by: Cell 1 (Cell 1S, and Cell 1N), Cell 2, and Cell 3. Each Cell marks one testing location with ATLAS, and is further subdivided into four test sections, each studying a different QB application.

Figure 4.1. Google satellite view of the construction site showing overall the constructed test cells.

Cell '1' (Figure 4.2 and Table 4.1) was constructed 119 ft. (35.6 m) long and 18 ft. (5.4 m) wide. Four test sections, each approximately 20 ft. (6.1 m) long and wide 9 ft. (2.7 m) were constructed to study the 'subgrade modification' applications of QB; namely, PCR/QB1 mixed by shaking and compacting the QB on top of large rocks in a single lift and in two lifts, and the dense-graded aggregate subgrade layers with 15% plastic and nonplastic fines passing the No. 200 sieve. For each section, a 21-in. (530-mm) thick aggregate cover and a 3-in. (76-mm) of dense-graded CA06_R capping material were constructed. The 9-ft. (2.7-m) wide north test sections were topped with an additional 4-in. (100-mm)

thick HMA layer to evaluate low volume road applications, and are denoted as Cell '1N'. The 9-ft. (2.7-m) south test sections were built to evaluate construction platform applications and was called Cell '1S'. Cell 1 was constructed on top of a subgrade soil with an engineered CBR of 1%.

Table 4.1. Constructed Test Sections for Cell 1 Utilizing Unstabilized Applications of QB

Section	Description and Construction Details*	Typical Cross Sections
C1S1	Primary Crusher Run (PCR) rocks with 25% QB1 by weight, constructed in **two** equal lifts using a vibratory roller compactor. QB1 is placed into the voids of the PCR from the top of **each** lift.	
C1S2	PCR with 16.7% QB1 by weight, constructed in **one** single lift in a similar manner as C1S1.	
C1S3	CA06_15PF: Dense-graded CA06 aggregates with 15% plastic fines content (passing No. 200 sieve) with a plasticity index (PI) of 8 constructed in **three** equal lifts.	
C1S4	CA06_15NPF: Dense-graded CA06 aggregates with 15% nonplastic fines content (passing No. 200 sieve) constructed in **three** equal lifts.	
* All test sections in Cell 1 were overlain by a 3-in. (76-mm) thick dolomite capping (CA06_R material). For Cell 1N, a 4 in. (100-mm) thick HMA layer was paved on top of the capping layer.		

Cell '2' (Figure 4.2 and Table 4.2) was constructed 119 ft. (35.6 m) long and 12 ft. (3.6 m) wide. Four test sections, each approximately 20 ft. (6.1 m) long, were constructed to study the 'base' applications of QB; namely, [70% QB2 + 30% FRAP] + 3% Cement of the total weight, [70% QB2 + 30% FRCA] + 3% Cement base, [70% QB2 + 30% FRAP] + 10% Fly ash, and [100% QB2] + 3% Cement base. The base layers were 12 in. (305 mm) thick and were topped with 4-in. (100-mm) of HMA to evaluate low to medium volume road applications. Cell 2 was constructed on top of a subgrade soil with an engineered CBR of 6%.

Cell '3' (Figure 4.2 and Table 4.2) was constructed 130 ft. (39.0 m) long and 12 ft. (3.6 m) wide. Four test sections, each approximately 20 ft. (6.1 m) long, were constructed to study the base and subbase applications of QB. The first test section was constructed with [100% QB3 + 3% Cement] base, to evaluate the effect of the QB type (QB2 vs QB3 differences). Two of the sections evaluated inverted pavement applications of QB, and were constructed with a 6-in. (152-mm) thick QB2 subbase layer stabilized with 3% cement and 10% fly ash respectively, and topped with 6-in. (152-mm) of dense-graded CA06_R aggregate base. The last section was a control section, constructed with 12 in. (305

mm) of regular dense-graded base course material. All four sections were overlain by 4 in. (100 mm) of HMA to evaluate low to medium volume roads applications. Cell 3 was constructed on top of a subgrade soil with an engineered CBR of 6%.

Table 4.2. Constructed Test Sections for Cells 2 and 3 with Admixture Stabilized Applications of QB

	Section	Description and Construction Details*	Typical Cross Sections
Cell 2	**C2S1**	A blend of 70% QB2 and 30% FRAP by weight, mixed with 3% Type I cement by weight.	
	C2S2	A blend of 70% QB2 and 30% FRCA by weight, mixed with 3% Type I cement by weight.	
	C2S3	A blend of 70% QB2 and 30% FRAP by weight, mixed with 10% Class 'C' fly ash by weight.	
	C2S4	A Blend of QB2 and 3% Type I cement by weight.	**Cells 2 and 3**
Cell 3	**C3S1**	A Blend of QB3 and 3% Type I cement by weight.	
	C3S2	Subbase layer: A Blend of QB2 and 3% Type I cement by weight. Base layer: CA06_R (A dense-graded unbound dolomite aggregate layer)	
	C3S3	Subbase layer: A Blend of QB2 and 10% Class 'C' fly ash by weight. Base layer: CA06_R	**Cell 3 (C3S2 and C3S3)**
	C3S4	CA06_R dense-graded dolomite base	

Longitudinal and transverse drainage lines were installed to drain water efficiently from the test sections (Figure 4.2). Longitudinal drainage lines ran along the north side of each cell, and a transverse drainage line ran from south to north along the west side of Cell 3 and connected to the longitudinal drainage line. Perforated, plastic drainage pipes were covered with an open-graded granular material that follows IDOT CA07 gradation band for grain size distribution. A storage basin and a sump pump were utilized to store and divert the water from the test sections (see Figure 4.2). Additionally, the beginning and end parts of each cell were designed to have 22.5 ft. (6.8 m) long crawler zones (where the crawlers of ATLAS were placed) and a 7.5 ft. (2.3 m) speed stabilization zone. The speed stabilization zones were for acceleration/deceleration to ensure that all test sections were tested at a constant speed of 5 mph (8 km/h). A 10 ft. (3 m) long transition zone was also added at the middle of each cell, to minimize any possible influence of changing materials on the APT

results. Figure 4.3 shows the details of the transition and buffer zones for each cell. Further, the transverse rut profile measurement lines are also indicated in each test section at one third lengths.
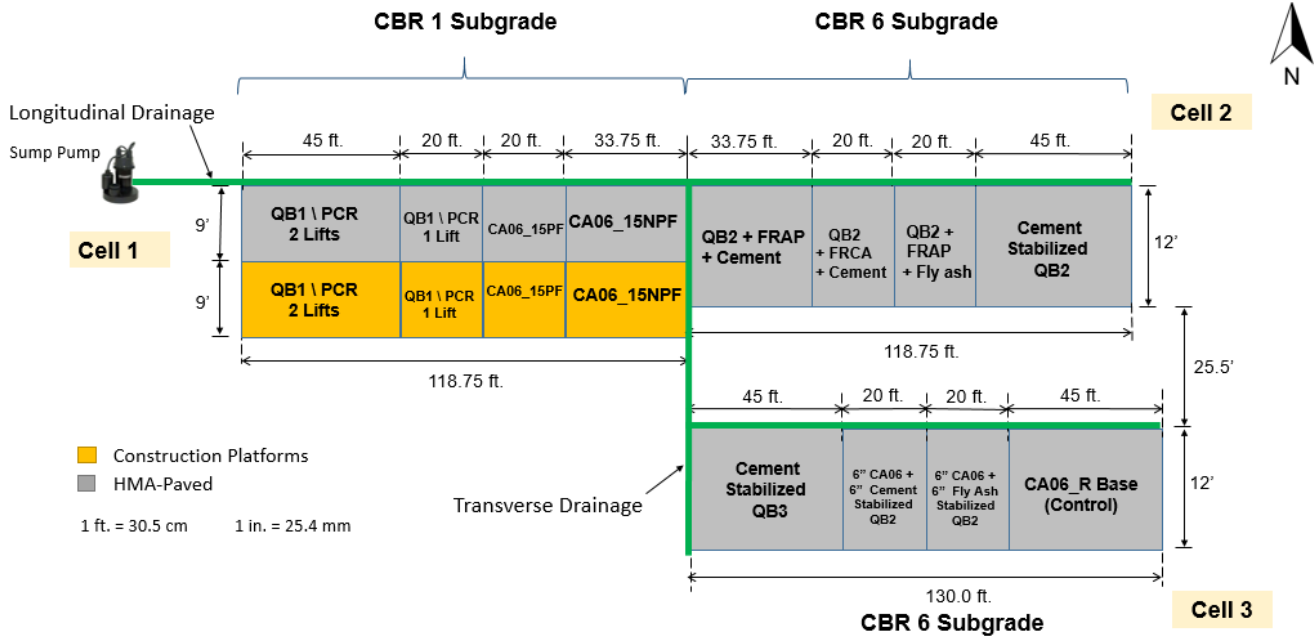
Figure 4.2. Plan view of the constructed test sections encompassing different QB applications.
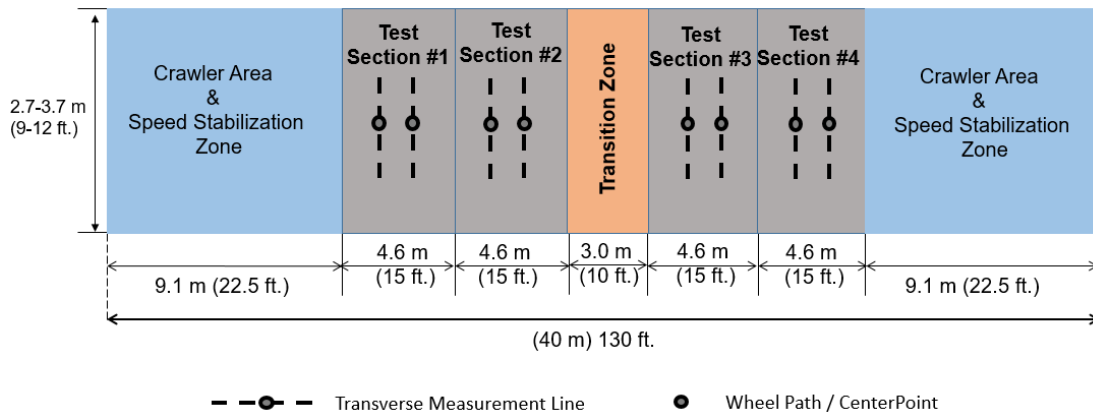
Figure 4.3. Plan view of a typical test cell showing the transition and buffer zones and the transverse measurement lines.

4.3 CONSTRUCTION OF FULL-SCALE TEST SECTIONS

Prior to starting construction activities, existing unsurfaced pavement test sections at the construction site were milled to a depth of 24 in. (60 cm). Further, to prevent any possible contamination from the existing test sections, the existing subgrade soil was scraped off an additional 9 in. (0.2 m) below the existing grade and replaced with fill materials. The drainage lines were repaired and installed next. Following that, the three test cells were constructed. First, the existing

subgrade soil was engineered to a subgrade strength of CBR = 1% for Cell 1, and CBR = 6% for Cells 2 and 3. Then, the base/subbase layers were constructed and the HMA surface was placed in two equal lifts in test sections of Cells 1N, 2 and 3. The detailed construction activities, including QA/QC measures to ensure high quality construction, are discussed in this section.

4.3.1 Engineering Subgrade Strength and Subgrade Preparation

The process of engineering subgrade strength and modifying the existing in situ soil to a CBR less than or equal to 1% for Cell 1 and a CBR of 6% for Cells 2 and 3 was achieved through a moisture adjustment procedure adopted similarly in earlier studies of ICT projects R27-81 and R27-124. The process is iterative (Qamhia et al, 2017a; Qamhia et al., 2018), and each time an iteration/trial is performed, the achieved CBR profile was tested using Dynamic Cone Penetrometer (DCP) tests to a depth of 12 in. (305 mm) to assess subgrade strength and uniformity.

The subgrade soil at the ATREL site is typically classified as low plasticity clayey silt (CL – ML) by the Unified Soil Classification System or an A-4 soil by the AASHTO classification. The in situ subgrade soil also has a Plasticity Index (PI) of 6% (range: 5%-7%). The relationship between CBR and moisture content for this subgrade was adequately established in the laboratory in a previous research study (Mishra, 2012). Accordingly, a moisture content of 15% and a dry density of 115.2 pcf (18.1 kN/m^3) corresponds to a CBR of 1%, while a moisture content of 12% and a dry density of 121.6 pcf (19.1 kN/m^3) corresponds to a CBR of 6%.

The following procedure was employed for subgrade strength modification:

- First, the top 14 in. (355 mm) of the existing subgrade soil was tilled with a tiller to achieve better homogeneity. Each cell was then divided into four zones (four zones each for Cells 1N and 1S), and representative soil samples were then collected from at least two spots in each zone and tested for the in situ moisture contents using a microwave test method, as outlined in ASTM D4643 Standard (ASTM, 2008).

- The amounts of water required to increase the moisture contents to obtain a CBR of 1% for Cell 1 and a CBR of 6% for Cells 2 and 3 were estimated from the volume of earthwork (see Figure 4.2 of plan view dimensions and 14 in. depth) and the in situ moisture content of the soil in each zone separately. The soil layer was again tilled and compacted to the desired laboratory density level (approximately) using a sheepsfoot roller compactor, for water retention in the sheepsfoot marks. Knowing the flow rate, the estimated additional amount of water was sprayed uniformly over each zone using a fire hose connected to a water truck.

- The soil was then uniformly mixed, and re-compacted with a sheepsfoot roller compactor (see Figure 4.4). More soil samples were collected and tested for moisture content to ensure uniformity and check that the target moisture content was achieved. Note that for Cells 2 and 3, the mixing was done using a tiller, while for Cell 1 it was done with the bucket of an excavator due to the sinking of the tiller in the soft soil. Additionally, for Cell 2, the existing and part of the borrow soil were more wet than desired, so the soil was tilled and sun-dried several times to engineer the soil moisture content and the CBR = 6% subgrade strength.

Following subgrade soil compaction using a sheepsfoot roller compactor, Dynamic Cone Penetrometer (DCP) tests were carried out on the compacted soil to a depth of 12 in. (305 mm) to assess subgrade strength and uniformity in terms of the CBR profile (see Figure 4.4); which is related to the Penetration Rate (PR) of the DCP in mm/blow using the original South African Kleyn equation, which is referred to as equation 4.1 below (Kleyn, 1975):

$$Log\ (CBR) = 2.61 - 1.26 \log_{10}(PR) \tag{4.1}$$

- The steps outlined above were repeated until a uniform subgrade foundation with a CBR of less than or equal to 1% for Cell 1 and a CBR of 6% for Cells 2 and 3 to a depth exceeding 12 in. (305 mm) was achieved.

Subgrade Soil Tilling and Mixing	Subgrade Compaction
Moisture Adjustment	DCP Profiling for Top 305 mm (12 in.)

Figure 4.4. Construction activities for engineering subgrade strength and subgrade preparation.

- Finally, the surface of the subgrade was sprayed with a prime coat at a rate of 3.6 lb./yd^2 (1.95 kg/m^2) for Cell 1 and a rate of 3.2 lb./yd^2 (1.73 kg/m^2) for Cells 2 and 3 in order to minimize any moisture loss and thus maintain the desired subgrade strength levels. For the same reason, the test Cells were further covered with plastic sheets until the subsurface layers were constructed (see Figure 4.5).

Subgrade Surface after Application of Tack Coat   Test Cells Covered with Plastic Sheets

Figure 4.5. Subgrade protection and mitigation from moisture loss.

The achieved average DCP values at each measuring point in Cells 1N, 1S, 2 and 3 are shown in Figure 4.6. An average CBR of less than 1% was achieved for all points in Cell 1, while the achieved CBR values for Cell 2 and 3 varied between 5% and 8%. Cell 3 had slightly higher CBR values than Cell 2 at many measurement points. Figure 4.6 shows the average CBR (back-calculated using the Kleyn equation) obtained at each measuring point. This average was computed by considering the top 12 in. (305 mm) subgrade profile, and the iterative subgrade engineering process ensured that the depth profile had a uniform subgrade at each of the measuring points, which was achieved by multiple rounds of tilling and compaction. Also note that the results are only shown for the last trial (i.e. final CBR profile), on top of which the pavements were constructed. For the earlier and intermediate trials, the DCP profile varied significantly across the cells, and varied from the desired target values.
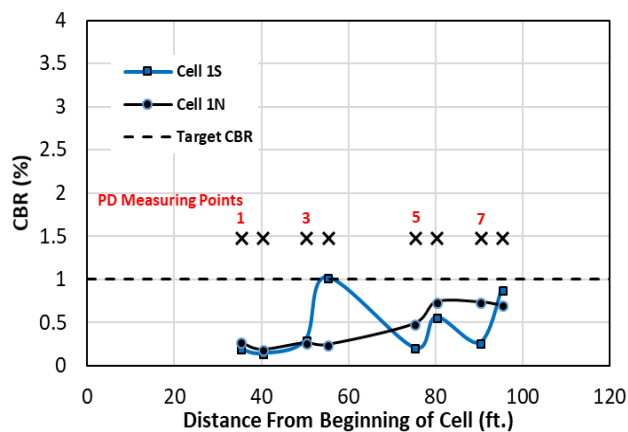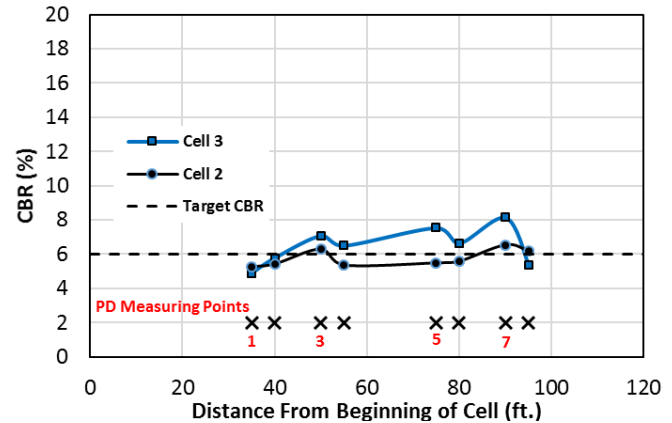
(a)   (b)

Figure 4.6. Average CBR values for the top 12 in. (30.5 cm) subgrade for (a) Cells 1N and 1S, showing the final trial with CBR values < 1%, and (b) Cells 2 and 3 showing final achieved CBR of ~6%.

Following the final trial, the achieved subgrade densities for Cells 2 and 3 were measured using a nuclear gauge. At least one density measurement was taken for each section at one of the measuring points. The results for the achieved dry densities, moisture contents, and relative compaction are shown in Figure 4.7, which shows the 100% laboratory density of 121.6 pcf (19.1 kN/m^3) as the target density. IDOT considers 95% of the target density as satisfactory; thus, all dry densities exceeding 115.5 pcf (18.1 kN/m^3) are considered satisfactory, which is the case for all test sections. The lowest measured subgrade density was for section 1 in Cell 3, which was also satisfactory (i.e. exceeding 95% of target density). Subgrade density measurements were conducted for Cells 2 and 3 only. For Cell 1, density measurements were not possible due to the very soft nature of the engineered subgrade.

Cell / Section	Achieved Density Pcf (kN/m^3)	Achieved Moisture Content (%)	Relative Field Compaction* (%)
C2S1	121.6 (19.1)	11.9	100.1
C2S2	126.0 (19.8)	10.4	103.5
C2S3	121.0 (19.0)	11.1	99.7
C2S4	124.8 (19.6)	10.8	102.7
C3S1	117.8 (18.5)	10.8	96.8
C3S2	125.4 (19.7)	10.3	103.4
C3S3	127.3 (20.0)	9.3	104.9
C3S4	122.9 (19.3)	10.4	100.8

*Based on ASTM D698
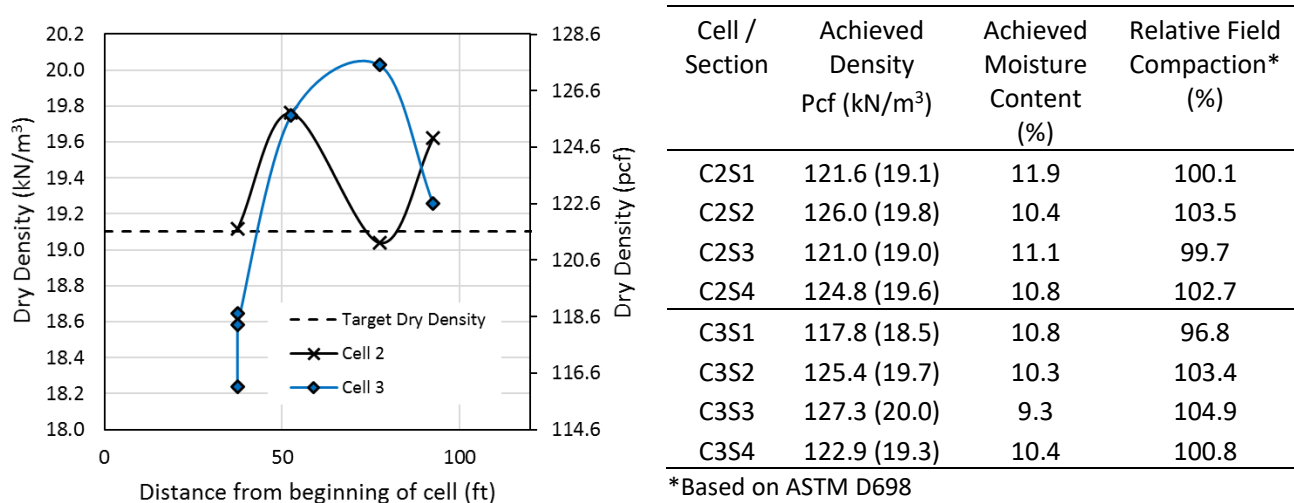
Figure 4.7. Average nuclear gauge densities on top of the subgrade for Cells 2 and 3.

4.3.2 Construction of the Unbound Aggregate Test Sections

This section covers the construction of the test sections in Cell 1 and Cell 3 with unbound aggregate materials. These sections are mainly the aggregate subgrade sections in Cell 1 (PCR / QB test sections and test sections with 15% fines content) as well as the CA06_R layers in Cell 3 used as base layers in C3S2, C3S3, and the control section (C3S4). The details for these test sections were previously given in Figure 4.2, Table 4.1 and Table 4.2.

4.3.2.1 Construction of PCR/QB1 Test Sections (C1S1 and C1S2)

Two test sections were constructed in Cell 1 to study the use of QB to fill the voids of large primary crusher run aggregates for increased stability and lower settlement potential. Such rockfill applications of PCR aggregates are common on top of very soft subgrades (e.g. CBR = 1%). They are built in thick lifts to act as construction working platforms on top of which the pavement sections are constructed. However, these open-graded aggregate layers contain large voids and are prone to variable settlement due to the high porosity. The goal of the constructed test sections was to study the incorporation of QB1 into the voids between PCR aggregates to provide increased stability. They

were placed by adding the QB from the surface in one single 21 in. (530 mm) lift or in two 10.5 in. (265 mm) lifts and with the help of vibratory action from a vibratory compactor.

From the UIUC packing box study of PCR/QB1 discussed in Chapter 3, the target QB1 quantity to be added was 25% by weight of the large rocks. This recommendation was based on single 10.5 in. (265 mm) lift compacted on top of the subgrade with CBR = 1%, and with a QB1 moisture content of 2.5%.

Similarly in the field, representative samples of QB1 were first collected and tested for their field moisture contents, and the average moisture content was found to be 3.2%. The field moisture content was even higher than the moisture content obtained during the laboratory tests.

During the construction of the first lift in the two-lift test section (C1S1), the large rocks were placed first and then the full amount of QB1 (25% QB materials by the dry weight of the PCR lift) were evenly distributed on the surface using a skid-steer loader. A vibratory compactor was used to shake the QB into the inherent voids in the PCR skeleton. This resulted in the formation of a densely-packed layer of QB on the surface, which slowed down QB percolation, and prevented any further filling of the voids in the PCR skeleton. This is assumed to be a result of the compactive effort, which was considerably higher than that applied in the laboratory box study. To overcome this issue in the first constructed layer in the two-lift test section, the QB were uniformly intermixed with the large rocks using the teeth of an excavator bucket (See Figure 4.8).

To prevent the formation of a densely-packed thin QB lift on the surface of subsequent lifts, the QB were slowly and incrementally spread using shovels on the surface of the large rocks, in smaller increments. The construction procedure is illustrated in Figure 4.8. The QB were then vibrated into the voids of the PCR using a larger (and heavier) standard size vibratory roller, and the process was repeated several times until the full quantity of QB was added (25% by dry weight of the PCR). However, for section C1S2 constructed in a single lift, the maximum possible amount of QB that could be packed was 16.7% by the dry weight of the PCR using this approach described. A possible reason for this can be the higher moisture content of the QB used in the field construction or the more challenging single-lift percolation goal, which might have prevented the QB from percolating the full depth of the 21 in. (530 mm) single-lift layer.

The successful construction demonstrated when the QB was added in smaller increments, followed by a vibratory action, suggests that the future field practice of vibrating QB from the surface into the inherent voids of the PCR skeleton may require developing an automated technique to spread the QB uniformly and more slowly on the surface, accompanied with continuous and strong vibration.

The construction for the PCR/QB1 test sections for Cell 1 were done simultaneously for Cell 1N and Cell 1S (i.e. both paved sections and construction working platform sections). Following the construction of the PCR/QB1 aggregate layers, these sections were capped with a 3 in. (76 mm) dense-graded CA06_R, mixed and compacted at the optimum moisture content. The capping layers were constructed last for all Cell 1 test sections at the same time. Nuclear gauge dry densities measured with a back-scatter technique for the capping layer ranged between 126.0–138.0 pcf (19.8–21.7 kN/m^3), which translates to a satisfactory 97.8%–107.1% relative field compaction.

Construction of the first lift in the two-lift PCR/QB1 test section (C1S1)

QB1 placed on top of PCR (before compaction)

PCR/QB1 blends (after compaction)

Uniform spreading and incremental placement of QB1 on top of PCR lift

Final compacted surface of C1S1

Figure 4.8. Construction of PCR/QB1 sections in Cell 1.

To evaluate the quality of the constructed test sections, the stiffness of the PCR/QB1 test sections were measured using a Light Weight Deflectometer (LWD). A minimum of nine LWD drops, including three seating drops, were carried out at the two measuring points in each section; both before and after the placement of the capping layer. To ensure the uniformity of the surface, a layer of sand was placed at the locations of LWD drops. This was especially necessary on top of the PCR/QB1 layers, where the surface elevation could vary widely. The results from LWD testing on top of the measuring points for the construction platform and low volume roads test sections (i.e. Cell 1S and Cell 1N, respectively) are presented in Figure 4.9. All test sections indicated a significant increase in stiffness upon the addition of the capping layer. Before the placement of the capping layer, the sections constructed in two lifts had lower moduli compared to the sections constructed in one lift. C1S1 constructed in two lifts in Cell 1N had the lowest back-calculated modulus. As it will be discussed later

in this report, trenching results for Cell 1N indicate that this lowest modulus is largely due to the lower layer thickness for the second measuring point in this section, which resulted in a noticeably lower average modulus for this section.

| (a) | (b) |
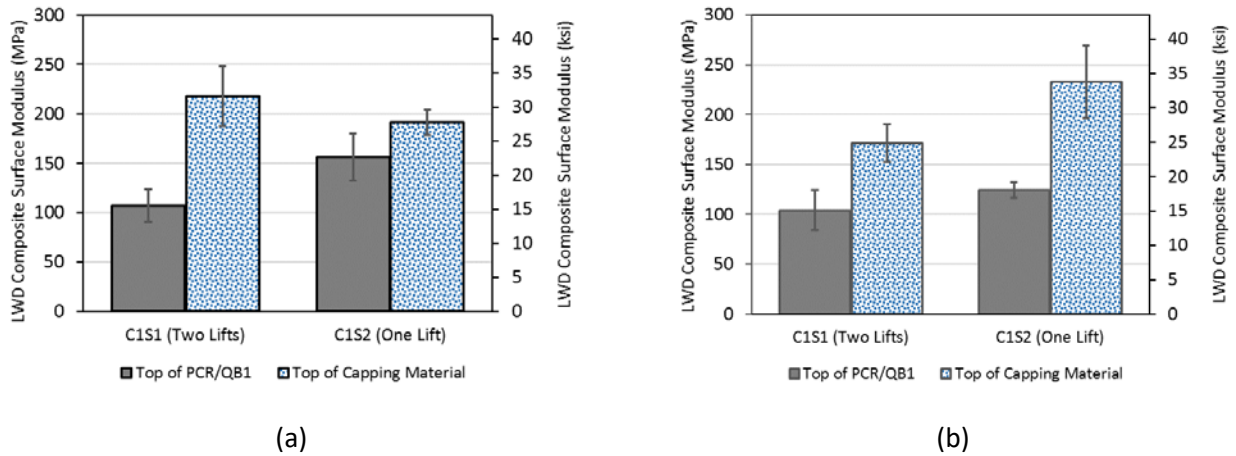
Figure 4.9. Average composite surface moduli measured by LWD for C1S1 and C1S2 for (a) Cell 1S construction platform and (b) Cell 1N low volume road sections.

4.3.2.2 Construction of CA06_15NPF and CA06_15PF aggregate layers

For the other two test sections constructed in Cell 1 with dense-graded aggregate materials (C1S3 with CA06_15PF and C1S4 with CA06_15NPF), the layers were compacted in three equal 178 mm (7 in.) lifts. Representative samples of each material were first collected and tested for their field moisture contents. Both materials had moisture contents lower than the OMC values, and more water was added in order to compact the materials at the OMC. The stockpiles were thoroughly mixed to achieve uniform moisture distributions. These sections were further overlain by a 3 in. (76 mm) dense-graded CA06_R aggregate capping layer compacted at the optimum moisture content. Figure 4.10 shows the placement of the CA06_15NPF layer and the compaction of the CA06_R capping material on top of Cell 1.

| Construction of C1S4 unbound layers | Placement of CA06_R Capping layer for Cell 1 |

Figure 4.10. Field construction activities for Cell 1 sections.

The achieved relative compaction and field moisture contents for the unbound aggregate layers in Cell 1 are given in Table 4.3. The maximum dry density was determined by laboratory testing with the standard compaction effort, and the field moisture content was calculated from the field using the nuclear density gauge measurements. As seen in Table 4.3, the relative compaction for all the test sections except for Section 3 in Cell 1N exceeded the 95% level, indicating satisfactory compaction as required by IDOT construction standards. Section 3 in Cell 1N had a relative compaction of 93.1%, and an achieved moisture content of 2.3% below the optimum.

The capping layer on top of all the test sections had relatively similar compaction levels and similar achieved moisture contents, which were near optimum. Note that the CA06_15PF and CA06_15NPF materials achieved satisfactory compaction levels despite being compacted at a considerably lower moisture content than optimum. A good explanation is the higher compactive effort in the field, compared with the standard compactive effort in the laboratory. Since most sections were compacted at moisture levels on the dry side of optimum, satisfactory compaction levels could be achieved with the higher field compactive effort.

Table 4.3. Achieved Field Densities, Moisture Contents and Relative Compaction in Cell 1 Sections

Cell 1S (Construction Working Platforms)

Section	Material	Avg. Field Density pcf (kN/m³)	MDD pcf (kN/m³)	Relative Compaction (%)	Achieved Moisture Content (%)	Optimum Moisture Conttent (%)	Difference in Moisture Content (%)
C1S3	CA06_15PF	129.9 (20.4)	135.0 (21.2)	96.6	4.4	6.5	-2.1
C1S4	CA06_15NPF	140.0 (22.0)	138.8 (21.8)	100.9	4.6	6.8	-2.2
C1S1	CA06_R Capping	135.6 (21.3)	131.8 (20.7)	102.7	4.6	5.4	-0.8
C1S2	CA06_R Capping	129.9 (20.4)	131.8 (20.7)	98.5	5.0	5.4	-0.4
C1S3	CA06_R Capping	138.1 (21.7)	131.8 (20.7)	104.7	5.4	5.4	0
C1S4	CA06_R Capping	137.5 (21.6)	131.8 (20.7)	104.2	5.5	5.4	+0.1

Cell 1N (Low Volume Roads)

Section	Material	Avg. Field Density (kN/m3)	MDD Pcf (kN/m³)	Relative Compaction (%)	Achieved Moisture Content (%)	Optimum Moisture Conttent (%)	Difference in Moisture Content (%)
C1S3	CA06_15PF	125.4 (19.7)	135.0 (21.2)	93.1	4.2	6.5	-2.3
C1S4	CA06_15NPF	135.0 (21.2)	138.8 (21.8)	97.4	4.9	6.8	-1.9
C1S1	CA06_R Capping	130.5 (20.5)	131.8 (20.7)	99.0	5.6	5.4	+0.2
C1S2	CA06_R Capping	133.0 (20.9)	131.8 (20.7)	100.6	5.3	5.4	-0.1
C1S3	CA06_R Capping	141.3 (22.2)	131.8 (20.7)	107.0	5.3	5.4	-0.1
C1S4	CA06_R Capping	135.0 (21.2)	131.8 (20.7)	102.4	5.5	5.4	+0.1

For the dense-graded aggregate subgrade test sections, a minimum of nine LWD drops including three seating drops were carried at the two measuring points in each section after each lift was constructed, as well as on top of the capping layer. The LWD back-calculated moduli are shown in Figure 4.11. All test sections showed a significant increase in stiffness upon the addition of the capping layer. The section constructed with nonplastic CA06 in Cell 1S had significantly higher modulus before the addition of capping layer. The capping layer was compacted 10 days after the construction of the CA06_15NPF and CA06_15PF layers. All four test sections had similar moduli on top of the capping layer, with an average modulus ranging from 31.0 to 37.7 ksi (214 to 260 MPa).

| (a) | (b) |
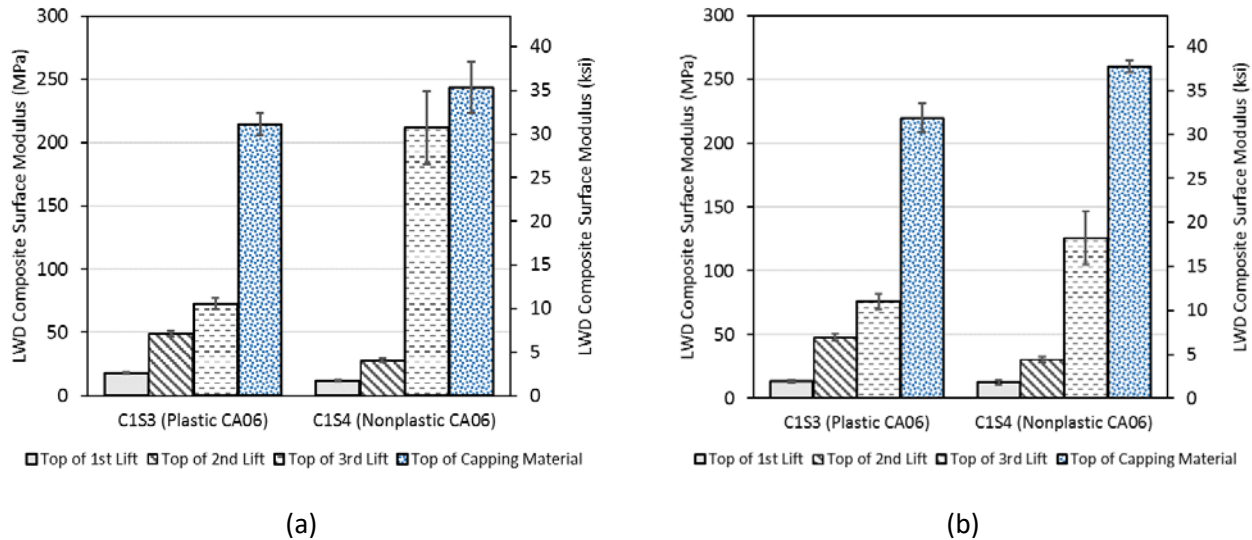
Figure 4.11. Average composite surface modulus measured by LWD for C1S3 and C1S4 for (a) Cell 1S construction platform, and (b) Cell 1N low volume road sections.

4.3.2.3 Construction of CA06_R Layers in Cell 3

Layers of CA06_R were constructed as base layers in three sections of Cell 3. For two of these sections, namely C3S2 and C3S3, CA06_R layers were constructed as a single 6 in. (152 mm) lift on top of the chemically stabilized subbase layers. For the third section, C3S4, the CA06_R for the control section was constructed in two equal 6 in. (152 mm) lifts. The CA06_R material was constructed at the optimum moisture content by adjusting the moisture content after collecting representative samples of the materials to test for field water contents.

Initially, CA06_R construction in Cell 3 resulted in some fine pockets visible on the surface at some locations, and less than desirable densities in C3S2 (i.e. relative compaction lower than 95%). Nuclear gauge density measurements also indicated that the moisture content was on the wet of optimum in some locations, with moisture contents exceeding 6.7%. Due to these issues, and the possibility of aggregate materials segregation, the whole construction was reworked by scraping the layer and bringing new material blended and compacted at the optimum moisture content. After reworking these sections, visual inspection and nuclear density measurements indicated satisfactory compaction and moisture contents achieved with better uniformity of gradation. The results for the final achieved densities and moisture contents are given in Table 4.4. and Figure 4.12. Shown also on

Figure 4.12 are the achieved dry densities before and after reconstructing the test sections, with measurements taken at two locations in each section. The back-calculated LWD moduli values for these sections are shown in Figure 4.14(b).

Fines Pockets
(Trial #1)

After Reworking Area
(Final Trial)
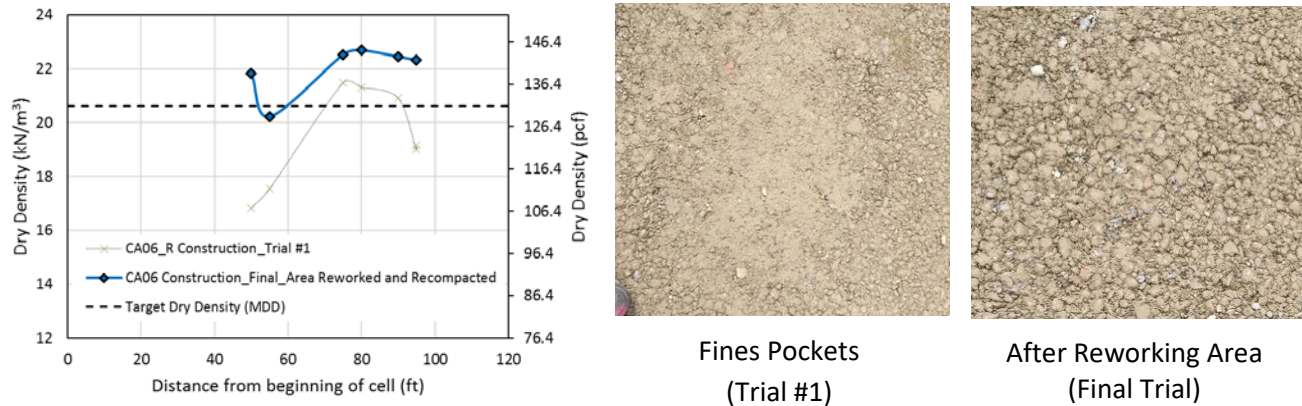
Figure 4.12. Nuclear gauge densities measured for CA06_R layer construction in Cell 3.

4.3.3 Construction of Chemically Stabilized Test Sections in Cells 2 and 3

In total, seven chemically stabilized test sections were constructed in Cells 2 and 3 to investigate the performance of pavements with stabilized QB sublayers. The chemical stabilizers used were 3% cement or 10% class 'C' fly ash by the dry weight of the QB. QB blends with FRAP and FRCA for test sections C2S1, C2S2, and C2S3 were prepared off-site in a local asphalt plant and then delivered to the construction site.

The procedure of constructing the chemically stabilized test sections was similar for all sections as outlined in Figure 4.13. As part of the quality assurance of the construction, a maximum time of two hours between mixing with the stabilizing agent on-site and compaction was enforced. Any material not compacted after two hours was discarded. The process involved the following steps:

- Stockpiles of known volume of the QB materials or QB blends with FRAP/FRCA were dry-mixed several times (at the in situ moisture contents of the stockpiles) with the bucket of a backhoe to ensure uniformity of moisture and particle size distribution.

- Moisture samples were taken to assess the in situ moisture contents of the stockpiles and to calculate the dry weights of the stockpiles accordingly.

- The stabilizing agent (cement or fly ash) was then added in the desired quantities by weight, and mixed with the QB materials or QB blends with FRAP/FRCA for uniformity using a backhoe bucket.

- Water was added, as needed, to the mixed stockpiles from a water truck to adjust the moisture content to the OMC.

- The blends were further mixed to uniformly distribute the moisture and the stabilizing agent.

- The final mixes were transferred to the construction site and placed and tilled several times using a soil tiller to ensure uniformity.

- The test sections were constructed and compacted typically in 6 in. (152 mm) lifts. Only Section 3 in Cell 2, comprising QB blended with FRAP and fly ash was tilled and compacted in three 4 in. (102 mm) lifts; since the material was tilled with a smaller sized tiller due to access constraints of a regular sized soil tiller.

Materials Stockpile	Dry-Mixing of Stockpile	
Addition of Cement		Addition of Water/ Mixing
Moving to Job Site	Placement and Tilling	Compaction

Figure 4.13. Construction of chemically stabilized test sections in Cells 2 and 3.

Table 4.4 lists a summary of the achieved relative compaction and field moisture contents for all the constructed layers in Cells 2 and 3. The field densities and moisture contents were determined using a nuclear density gauge through the help of engineers from IDOT District 5. The MDD and OMC values were determined from laboratory testing using the standard compaction effort per ASTM D698.

Except for C2S1, all other sections were compacted at moisture contents drier than optimum. However, satisfactory compaction levels exceeding 95% relative compaction were still achieved at these lower moisture contents for most test sections due to the higher compactive energy applied during construction. C2S2 had a significantly low relative compaction, while C2S4 and C3S2 (subbase layer) had lower than desired relative compaction levels of 91.9% and 92.5%, respectively. The layers

with lower compaction levels were not reworked due to the difficulty of constructing these sections. However, LWD was later used to assess the quality of the constructed layers and monitor curing of these sections. There were no issues observed in gaining strength with time.

Table 4.4. Achieved Field Densities, Moisture Contents and Relative Compaction in Cell 2 and Cell 3 Sections

Cell 2 Test Sections

Section	Material	Avg. Field Density pcf (kN/m³)	MDD pcf (kN/m³)	Relative Compaction (%)	Achieved Moisture Content (%)	Optimum Moisture Conttent (%)	Difference in Moisture Content (%)
C2S1	QB2 + FRAP + Cement	129.2 (20.3)	135.0 (21.2)	95.6	9.1	8.0	1.1
C2S2	QB2 + FRCA + Cement	113.9 (17.9)	128.6 (20.2)	88.7	7.8	9.8	-2.0
C2S3	QB2 + FRAP + Fly ash	135.0 (21.2)	136.2 (21.4)	99.4	5.6	7.5	-1.9
C2S4	QB2 + Cement	126.7 (19.9)	137.5 (21.6)	91.9	8.8	9.1	-0.3

Cell 3 Test Sections

Section	Material	Avg. Field Density pcf (kN/m³)	MDD pcf (kN/m³)	Relative Compaction (%)	Achieved Moisture Content (%)	Optimum Moisture Conttent (%)	Difference in Moisture Content (%)
C3S1	QB3 + Cement	128.0 (20.1)	129.9 (20.4)	98.4	5.3	8.4	-3.1
C3S2	QB2 + Cement Subbase	127.3 (20.0)	137.5 (21.6)	92.5	8.7	9.1	-0.4
C3S2	CA06_R Base	133.7 (21.0)	131.8 (20.7)	101.5	5.0	5.4	-0.4
C3S3	QB2 + Fly Ash Subbase	131.1 (20.6)	135.6 (21.3)	96.6	6.5	8.0	-1.5
C3S3	CA06_R Base	143.9 (22.6)	131.8 (20.7)	109.2	4.2	5.4	-1.2
C3S4	CA06_R Base	142.6 (22.4)	131.8 (20.7)	108.1	4.1	5.4	-1.3

To monitor the curing of the chemically stabilized test sections, LWD drops were done regularly on the surface of the constructed test sections in Cells 2 and 3 before the HMA paving. Each time a test was conducted, a minimum of nine LWD drops, including three seating drops, were carried out at the two measuring points in each section. The LWD back-calculated moduli are shown in Figure 4.14. All test sections showed a significant increase in stiffness with time. The highest LWD surface moduli and increases in stiffness were seen for the test sections in Cell 2, particularly the cement-stabilized test sections with QB2 and QB2 blended with FRAP/FRCA. The fly ash-treated sections had significantly lower back-calculated moduli and stiffness increases, when compared to the cement-stabilized test sections. Note that the calculated modulus is a composite surface modulus including effects of all underlying layers, which explains the noticeably lower back-calculated moduli values in C3S2 and C3S3 before the placement of the CA06_R base layer. This is because the LWD drops were conducted on top of the 6 in. (152 mm) subbase layer with higher influence from the underlying much softer subgrade when compared to the thicker 12-in. (305-mm) stabilized base layers constructed in Cell 2 test sections.
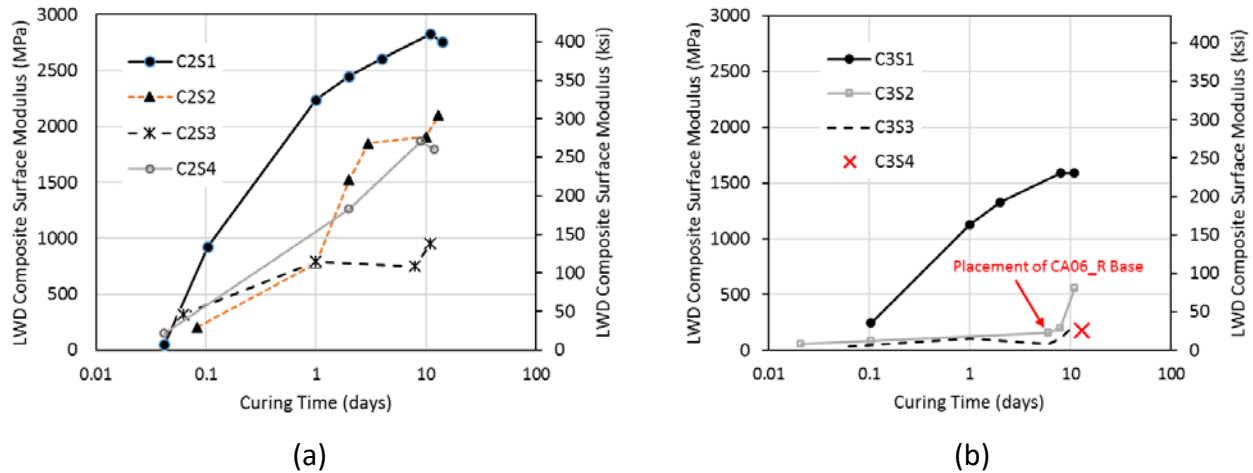
Figure 4.14. Average composite surface modulus measured by LWD for (a) Cell 2 test sections, and (b) Cell 3 test sections.

4.3.4 Hot Mix Asphalt Placement and Compaction

The HMA layer was constructed in two equal 2 in. (51 mm) lifts. The HMA used for both lifts had an asphalt binder with a Superpave performance grade of PG 64-22. Both surface course lifts had the same mix design with a 0.375 in. (9.5 mm) nominal maximum aggregate size. Note that there was no binder course with larger size aggregates. Therefore, 2 in (51 mm) thickness was selected for both lifts in order to meet the 4 in. (102 mm) total HMA thickness. Loose mixes were sampled in the asphalt plant and from the paver during construction. The two HMA lifts were compacted using the same vibratory roller compactor, and density measurements were taken with a nuclear density gauge on top of the final surface. Figure 4.15 shows three photos covering the sampling and paving activities. All test section HMA surfaces were paved on the same day. Paving was started from the west end of Cell 1, moving east towards Cell 2, and finally, Cell 3 was paved last.

Figure 4.15. Hot mix asphalt sampling and paving.

The achieved HMA centerline field densities and air voids are presented in Figure 4.16. In total, two density measurements were taken for each constructed test section, one at each measuring point. Cell 1 test sections had considerably higher densities/lower air voids compared to Cell 2 and Cell 3 sections. Specifically, C3S4 (control section) had the highest air voids of 11.9%. These air voids are based on a theoretical maximum specific gravity (G_{mm}) of 2.486 reported by the contractor. The field

cores obtained directly after construction from the wheel path at the transition zones of Cells 1, 2, and 3, and tested at ATREL had air void contents of 8.5%, 9.0%, and 10.1%, respectively. The air void contents from the tested cores were in good agreement with the trends and values calculated from the field nuclear density measurements.

Additionally, the air void contents and relative compaction reported by the contractor, through the contractor's own nuclear density gauge measurements for the constructed test sections, ranged between 7%–10% for air voids, and 90%–93% for relative compaction for Cells 1–3. The contractor's reported air void values were consistently ~2% lower than the values measured by IDOT and reported in Figure 4.16.
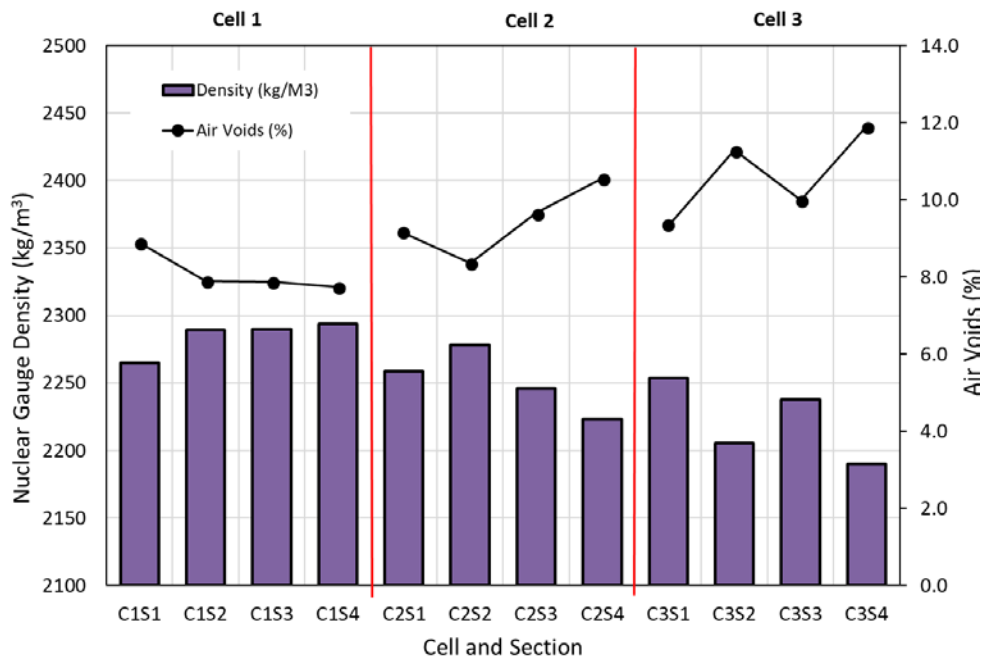
Figure 4.16. Achieved HMA densities and air void contents (%). [1000 kg/m³ = 62.4 pcf]

4.4 INSTRUMENTATION OF FULL-SCALE TEST SECTIONS

Soil pressure cells were installed on top of the subgrade in four of the test sections constructed in Cells 2 and 3; specifically under the sections C2S1, C2S4, C3S2, and C3S4. The pressure cells were installed in the wheel path on each of the transverse measurement lines in the chosen test sections. To ensure that the pressure cells lied directly under the wheel path and therefore minimized loading eccentricity, total station equipment and land surveying techniques were used to identify the locations of the pressure cells and relocate those locations after the construction of the HMA layer. In total, eight Geokon model '3500' soil pressure cells, with a standard range of 58 psi (400 kPa) and a 9 in. (230 mm) diameter were installed. The locations of the installed soil pressure cells, and installation photos are highlighted in Figure 4.17. Data from soil pressure cells provided the levels of wheel load deviator stresses applied on the subgrade and helped to compare the performance trends of the instrumented test sections.
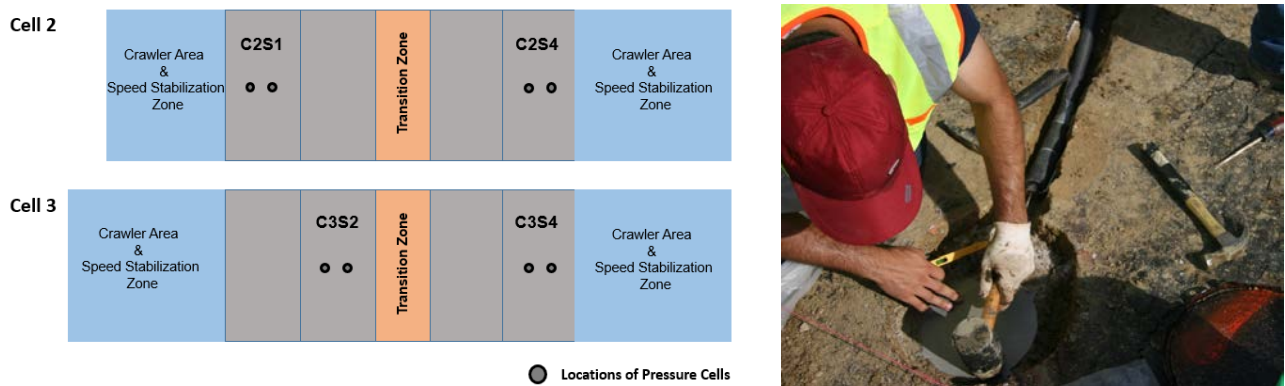
Figure 4.17. Soil pressure cell locations in Cell 2 and Cell 3 sections and installation photo.

4.5 FALLING WEIGHT DEFLECTOMETER TESTING BEFORE TRAFFICKING

Falling Weight Deflectometer (FWD) testing was carried out on all of the construction working platforms and flexible pavement test sections after field construction was completed. Additional FWD testing was also conducted for the test sections in Cells 2 and 3 before trafficking to assess the curing of the chemically stabilized test sections. The tests were conducted by dropping three different load levels at each measuring point to induce variable stress states. The deflection basins were normalized to a standard 9-kip (40-kN) equivalent single-axle load applying a uniform pressure of 80 psi (551 kPa) over a 12 in. (305 mm) diameter circular loading area.

After trafficking was completed for each test Cell, additional FWD drops were carried on all flexible pavement test sections. The results and interpretations of FWD testing after construction, before and after trafficking will be discussed in detail in Chapter 6 (Section 6.2.1).

CHAPTER 5: PERFORMANCE MONITORING WITH ACCELERATED PAVEMENT TESTING

5.1 INTRODUCTION

Following the construction of the three test Cells at the University of Illinois ATREL facility in Rantoul, the constructed test sections were monitored for performance through accelerated pavement testing (APT). Heavy vehicle loads were applied using the Accelerated Transportation Loading Assembly (ATLAS) shown in Figure 5.1. Important features of the ATLAS equipment include:

(1) 124 ft. (37.8 m) long, 12 ft. (3.65 m) high, and 12 ft. (3.65 m) wide.

(2) 85 ft. (25.9 m) loading length with approximately 65 ft. (19.8 m) of constant velocity loading of the wheel.

(3) ATLAS weighs 175 kips (780 kN) and is mounted on four crawler tracks.

(4) The ATLAS wheel carriage assembly can accommodate a single tire, dual-wheel tire, aircraft tire, or a single-axle rail bogey.

(5) The load level can vary between 0 and 80 kips (355.6 kN).

(6) The wheel carriage can wander up to 3 ft. (0.9 m) laterally.

(7) The maximum speed of the wheel is 10 mph (16 km/h).

(8) Aluminum panels can be attached on both sides and heaters can be distributed inside the panels to control and maintain constant temperatures. Temperature control is divided into three zones with six heaters that can be controlled individually.

Accelerated Transportation Loading Assembly (ATLAS) at ICT

Super-Single Tire (455/55R22.5)   Insulation Panels   Heaters for Temp. Control

Figure 5.1. ATLAS accelerated pavement tester at ICT, showing some features.

5.2 APT LOADING PARAMETERS AND DATA COLLECTION

Each Cell, comprising four test sections, marked one location for ATLAS. Accordingly, Cell 1S, Cell 1N, Cell 2 and Cell 3 were trafficked separately. The trafficking of Cell 1S with construction platform test sections was completed first, followed by Cell 1N, Cell 2, and finally Cell 3. The details of the test sections in these four cells were previously discussed in Section 4.2 (see Figure 4.2, Table 4.1, and Table 4.2).

A super-single tire (455/55R22.5), shown in Figure 5.1, was used to traffic the test sections. The first number (455) refers to the tire width from wall to wall in mm, the second number (55) corresponds to the side wall height expressed as a percentage of tire width, and the third number (22.5) is the rim diameter in inches.

For the purposes of this research, a constant unidirectional wheel load of 10 kip (44.5 kN), a tire pressure of 110 psi (760 kPa), and a constant speed of 5 mph (8 km/h) were assigned to load the constructed sections, and to evaluate their rutting potential. The same loading parameters were used to test all flexible pavements and construction working platforms test sections. Once the Cell 2 and Cell 3 sections were done receiving 100,000 wheel passes at the above listed standard load/pressure, the wheel load was increased to 14 kips (62.3 kN) and the tire pressure was increased to 125 psi (862 kPa), and additional 35,000 passes were applied at these increased load/pressure levels.

Performance monitoring was conducted by periodic surface profile measurements after a certain number of passes. For each measuring point, the non-trafficked profile measurements, i.e. at zero pass, was taken as the reference. Measurements of deflections at the wheel path was taken on more frequent occasions for the initial (e.g. 1, 10, 100, 250, 500, 750, and 1,000) passes, and then less frequently (e.g. every 2,000 passes for construction platforms, and every 5,000 passes for HMA-paved sections). On occasions heavy rain occurred, especially for the construction platform sections, rut measurements were collected more frequently after each occasion. Trafficking was continued until a certain threshold was achieved or a sufficient number of passes were applied. The wheel path rut threshold was selected to be 3 in. (76 mm) for the construction platforms, while that for the HMA-paved sections was selected to be 0.5 in (12.5 mm).

The transverse surface rut profile measurements for the construction working platforms were taken using a customized surface rut measurement device as shown in Figure 5.2(a). The figure consists of a hollow perforated channel with holes at an interval of 2 in. (50.8 mm) and calipers that measure depths to the nearest 0.4 mils (0.01 mm). Transverse rut measurements (orthogonal to the travel direction) were taken at the two measuring points in each test section, and up to a lateral distance of 30 in. (760 mm) on each side of the centerline of the wheel path to capture any possible heaving of materials on the sides of the wheel path. The rut depth was reported as the average rutting of the centermost 11.8 in. (300 mm) of the wheel path.

The transverse surface rut profile measurements for the HMA-paved test sections were measured using an automated laser profiler as shown in Figure 5.2(b). Transverse rut measurements at the two measuring points in each test section were taken up to a distance of 16 in. (405 mm) on each side of the centerline of the wheel path. At each measuring point, a total of six 31.9 in. (810 mm) lateral

scans were performed at 0.2 in. (5 mm) spacing, and the rut depth was reported as the average rutting of the centermost 11.8 in (300 mm) of the wheel path from the six measurements.

| (a) Customized Rut Depth Measuring Device | (b) Automated Laser Profiler |

Figure 5.2. Rut measurements for construction platforms and flexible pavement test sections.

5.3 PERFORMANCES OF CONSTRUCTION PLATFORM TEST SECTIONS (CELL 1S)

Rutting is the primary mode of failure in constructed unbound aggregate layers. Thus, the performance of aggregate subgrade materials was assessed through measurements of the permanent deformation accumulation in the construction working platforms. This section presents analyses and comparisons of rut accumulations in the construction platform test sections.

Figure 5.3 presents the average accumulations of permanent deformation with increasing number of passes in Cell 1S test sections, and the individual rut accumulations at each measuring point. The horizontal dashed lines indicate the 3 in. (76 mm) threshold. Additional details of the collected rut data are presented in Appendix B. At each measurement point, the wheel path deflection was calculated as the average deflection at thirteen points along the width of the wheel path. Except for Cell 1S Section 3 constructed with CA06 having 15% plastic fines, all other sections showed good performance up to a total of 20,000-wheel loading passes. On average, section 3 showed consistently higher permanent deformation trends than the other three sections, while the similar Cell 1S Section 4 with 15% nonplastic fines had consistently the lowest permanent deformation accumulations; clearly contrasting the drastic effect of the plasticity of fines on construction platform performance.

Additionally, Cell 1S Section 1 constructed with PCR/QB1 in two equal lifts showed higher rut accumulations than Cell 1S Section 2, which was constructed in a single lift. The East measuring point is section 1 constructed in two lifts and it had considerably higher rutting, which upon trenching also showed a crack propagating the full depth of the capping layer and half the depth of the aggregate subgrade layer, i.e. the second lift (see Figure 5.4). One possible explanation for the crack is an internal shear failure in the aggregate subgrade layer, which can be attributed to the construction procedure that left excess QB on the surface between the two lifts, possibly creating a weak shear plane due to loss of contact between the large PCR aggregates. The differences in performance trends of the two sections can be considered within the acceptable tolerance of construction variability.
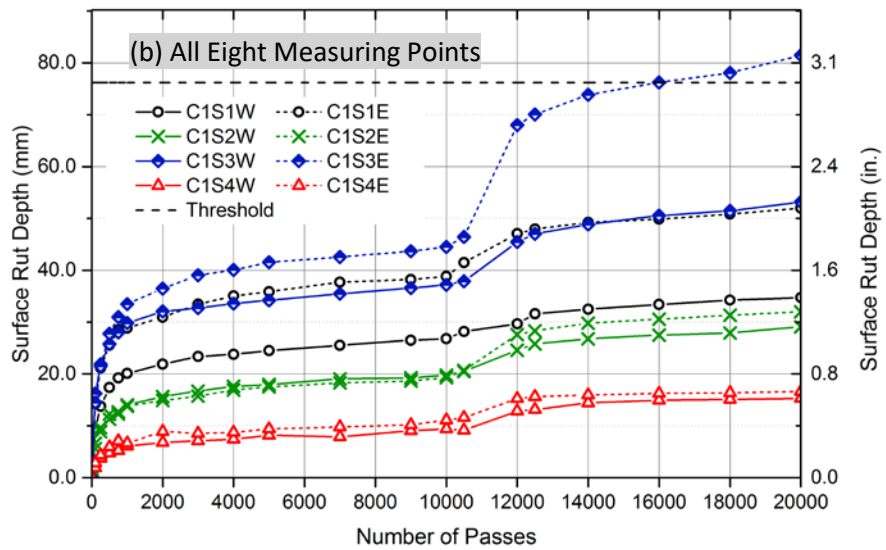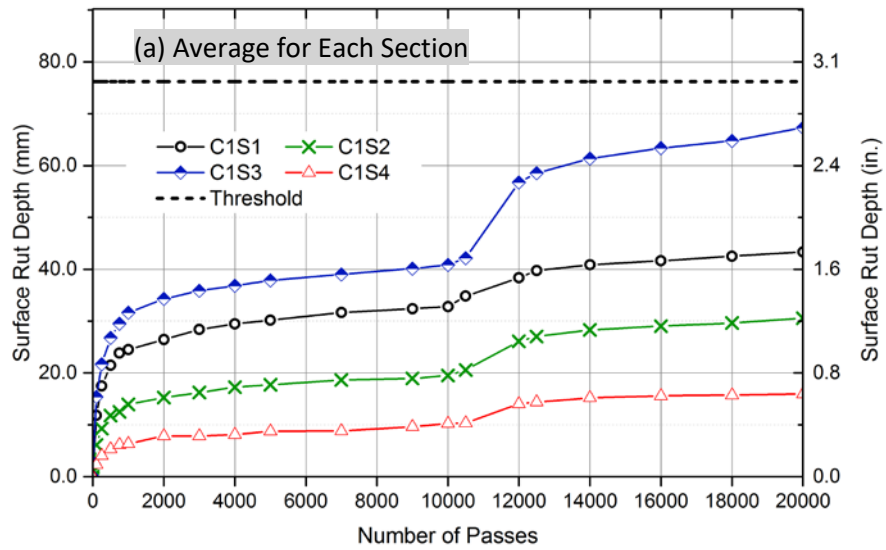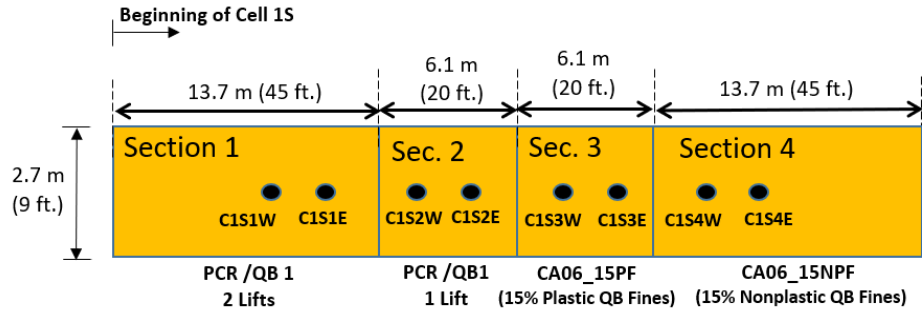
Figure 5.3. Wheel path maximum rut progression in Cell 1S test sections - construction platforms.

Compared to other test sections, Cell 1S Section 3 constructed with 15% plastic fines CA06 showed the most severe cracking, which started to appear on the sides of the wheel path after only 100 passes, indicating possible shear failure in the aggregate subgrade material. The East measuring point in section 3 (C1S3E) had more severe cracks and accumulated significantly higher permanent deformations. Upon trenching, it was discovered that the section at this measuring point was constructed 2.5 in. (63 mm) less than the target layer thickness, which clearly affected performance. The cracks observed in Cell 1S Section 3 are shown in Figure 5.4 after 9,000-wheel passes.

Further, an incident of heavy rain was reported between passes 10,000 and 12,500, for which all test sections showed a steeper increase in the rut accumulation. This was particularly true for Cell 1S Section 3 where the plastic fines showed the steepest increase in rutting with rain, while the other three sections had comparable increases in rutting rate. Several other incidents of rain were encountered during the trafficking of Cell 1S, and heavier rain (i.e. increased moisture content in the aggregate subgrade layers) led to more a rapid progression in rut accumulation of the construction working platforms.

| Cracking in C1S1E (PCR/QB1 – 2 Lifts) | Plan view for cracking in C1S3 (CA06_15PF) |

Figure 5.4. Visible cracks in Cell 1S - sections 1E and 3E/W.

5.4 PERFORMANCES OF FLEXIBLE PAVEMENTS TEST SECTIONS

This section discusses the performance trends of the flexible pavement test sections constructed in Cells 1N, 2 and 3. Surface rut profiles were periodically measured with the automated laser profiler in all the three cells. Further, Cells 2 and 3 were instrumented with pressure cells on top of the subgrade in four of the sections, the results of subgrade pressures measured are also reported and discussed in this section.

5.4.1 Performance of Cell 1N - Unbound Applications of QB

Cell 1N studied low volume road applications of QB as a filler material in the voids of large aggregate subgrade rocks and as a plastic/nonplastic fine material in dense-graded aggregate subgrade/CA06 layers. Flexible pavement test section performances in Cell 1N were monitored up to 90,000 passes. Selected cross sections in Cell 1N are shown in Figure 5.5 to highlight certain construction issues (see discussion below). The wheel path rut accumulations for Cell 1N are presented in Figure 5.6.

As shown in Figure 5.6, none of the test sections accumulated rutting greater than the 0.5 in. (12.5 mm) threshold (horizontal dashed line in the figure), which was decided earlier to end trafficking. However, testing was stopped after 90,000 wheel passes since all test sections showed, on average, comparable results and had a low rate of rutting after 60,000 passes. The low rutting rate after 60,000 passes is highly attributed to the stiffening of the HMA layer due to the decrease in air temperatures in October/ November. More details on the rutting data are presented in Appendix B.

Figure 5.6 indicates higher discrepancies in rutting trends from the two measuring points for Cell 1N Sections 1 and 4, which can both be attributed to construction variability. For section 1 constructed in 2 lifts, trenching showed that the East point, C1S1E, which accumulated the highest rutting was short in aggregate subgrade thickness and had lower QB content packed underneath the wheel path (see Figure 5.5), while the C1S1W was constructed more uniformly with the proper aggregate subgrade thickness. Additionally, C1S4W showed the second highest rut accumulation and indicated some segregation in materials, where the gradation under the wheel path was finer than anticipated (see Figure 5.5), which is visible for comparison with other cross sections for section 4 in Cell 1S and with C1S4E in Cell 1N. The analysis of the full trenching data is discussed in Chapter 6. If the two measuring points with construction issues were eliminated from the comparison, the rutting accumulation trends for Cell 1N and Cell 1S would follow the same order for the test sections.

| C1S1E – PCR/QB1 in 2 lifts | C1S4W – CA06_15NPF | C1S4E – CA06_15NPF |

Figure 5.5. Cross sections of some measuring points in Cell 1N test sections.

The average rutting results for sections in Cell 1N show that section 3 with 15% plastic fines accumulated the highest rutting among all the paved test sections. This was also the case for unpaved sections in Cell 1S, which indicate the detrimental effect of plastic fines on performance, especially

when exposed to moisture. The presence of HMA cover on top of plastic fines, however, reduced the effect of plastic fines due to significantly lower load levels experienced by these aggregate layers.
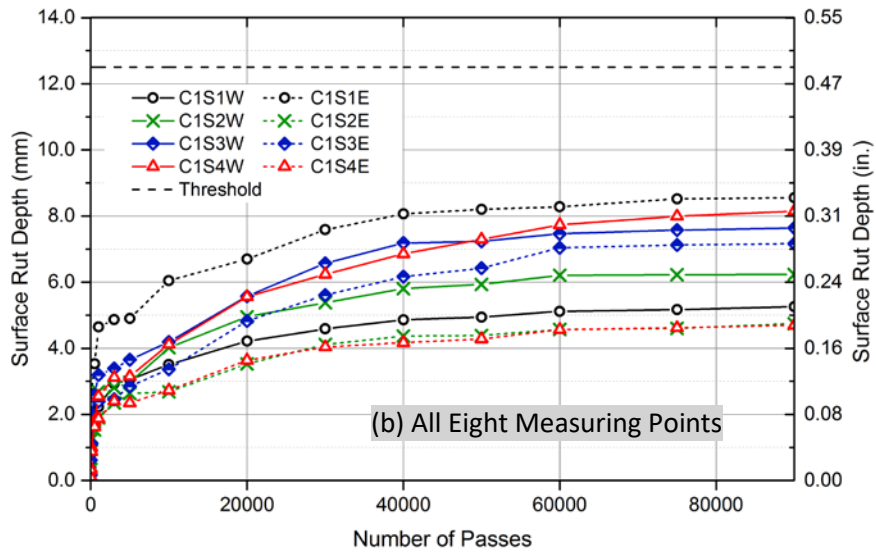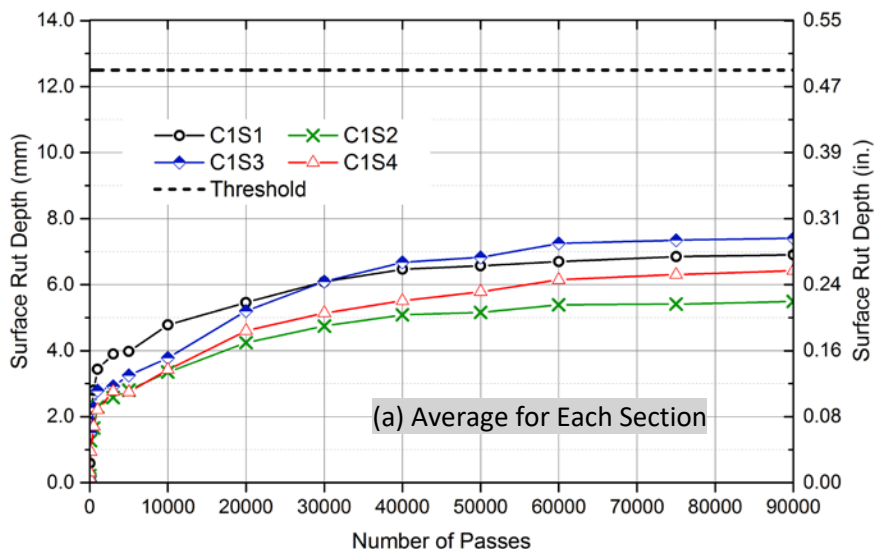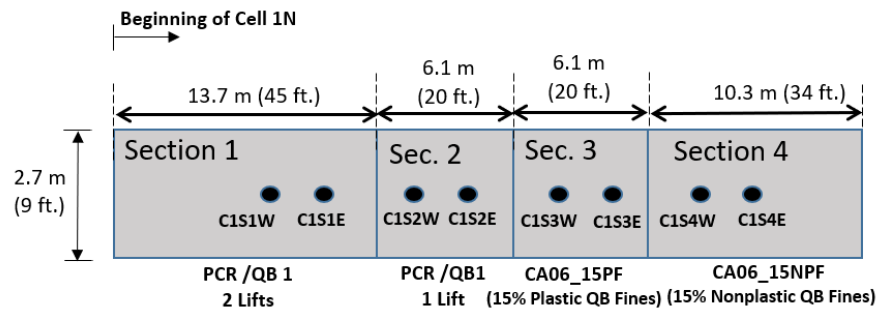
Figure 5.6. Wheel path maximum rut progression in Cell 1N test sections - flexible pavements.

5.4.2 Performance of Cell 2 – Chemically Stabilized Base Course Applications of QB

Cell 2 test sections were constructed to study flexible pavement applications of chemically stabilized QB and QB blends with FRAP/FRCA used as base materials. The performance trends of the flexible pavement test sections in Cell 2 were monitored up to 135,000 passes. The results for the wheel path maximum rut accumulations for Cell 2 test sections are presented in Figure 5.7.

Initially, 100,000-wheel passes were applied at a load of 10 kip (44.5 kN), a tire pressure of 110 psi (760 kPa), and a constant speed of 5 mph (8 km/h). Two of the test sections (C2S1 and C2S2) studying cement-stabilized blends of 70% QB2 with 30% FRAP/FRCA had exceptionally good performance and accumulated less than 80 mils (2 mm) of rutting at 100,000 passes. Thus, it was decided to run an additional 35,000 passes at the increased load level of 14 kip (62.3 kN) and an increased pressure level of 125 psi (862 kPa). The tire pressure was therefore increased to ensure that the loading mechanism does not change the pattern of stress distribution in the HMA layers due to the increased load level. The Equivalent Single-Axle Loads (ESALs) for each wheel pass at the original and increased load levels are calculated using the AASHTO equivalency factors using Equations 5.1–5.3, which are based on the results of AASHO road tests (Huang, 2004). The results are tabulated in Table 5.1. Note that these values somewhat underestimate the ESALs from one ATLAS pass, which may induce more damage since the speed of ATLAS (5 mph or 8 km/h) is significantly lower than typical highway speeds.

$$log \left(\frac{W_{tx}}{W_{t18}} \right) = 4.79 \log(18+1) - 4.79 \log(L_x + L_2) + 4.33 \log L_2 + \frac{G_t}{B_x} - \frac{G_t}{B_{18}} \tag{5.1}$$

$$G_t = \log \left(\frac{4.2 - p_t}{4.2 - 1.5} \right) \tag{5.2}$$

$$B_x = 0.4 + \frac{0.081(L_x + L_2)^{3.23}}{(SN + 1)^{5.19}(L_2)^{3.23}} \tag{5.3}$$

where

W_{tx} is the number of x-axle load applications at the end at time t;

W_{t18} is the number of 18-kip (80-kN) single-axle load applications to time t;

L_x is the load in kips on one single-axle, one set of tandem axles, or one set of tridem axles;

L_2 is the axle code (1 for single-axle, *2* for tandem axles, and *3* for tridem axles);

SN is the structural number; and

p_t is the terminal serviceability.

Table 5.1. Approximate Conversions of Two ATLAS Load Level Passes to ESALs

Load Level	Inputs						Calculations		
	W_{18}	L_x	L_2	SN	P_t	G_t	B_{18}	B_x	ESALs (W_{tx})
10 kip (44.5 kN) Load	1	20	1	5	2.5	-0.2009	0.5001	0.5382	1.50
14 kip (62.3 kN) Load	1	28	1	5	2.5	-0.2009	0.5001	0.7921	5.40
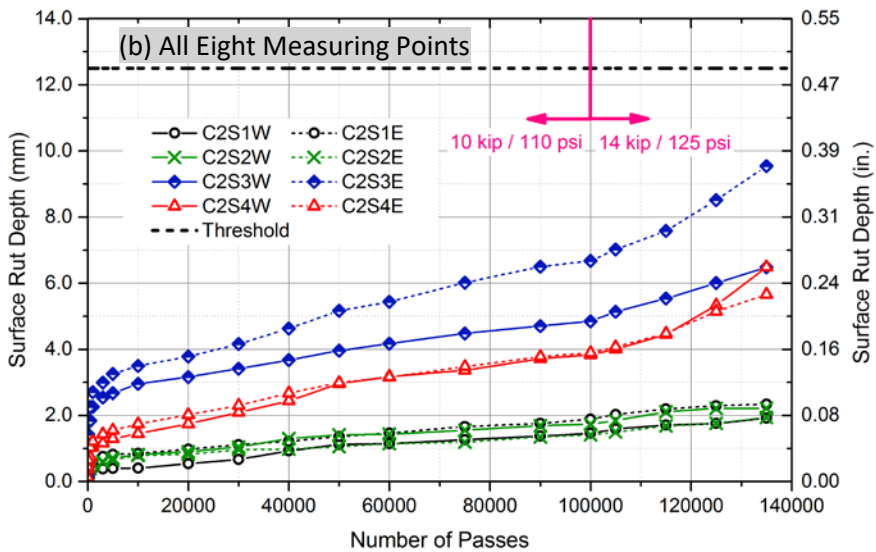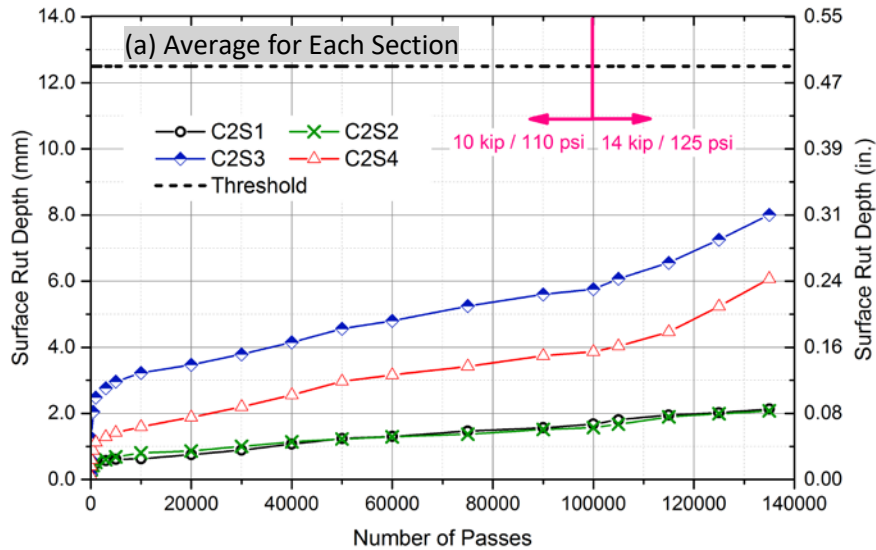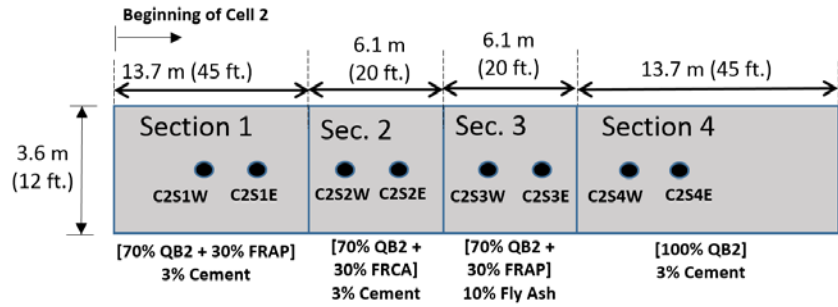
Figure 5.7. Wheel path maximum rut progression in Cell 2 test sections - flexible pavements.

As shown in Figure 5.7, satisfactory rutting accumulation was achieved for all the Cell 2 test sections utilizing QB applications, even at the increased load level. The C2S3 test section, having the blend of 70% QB2, 30% FRAP by weight, and stabilized with 10% class 'C' fly ash had significantly higher rut accumulation than the equivalent C2S1 section stabilized with 3% cement, which indicates the better performance of sections stabilized with cement. Additionally, sections with a coarse fraction of recycled FRAP/FRCA aggregates accumulated significantly lower rutting compared to C2S4 with cement-stabilized QB2 fines only. The low rutting accumulation under heavy loading by the APT in these test sections indicate the potential use of this application to sustain higher traffic levels, such as medium volume roads. Sections in Cell 2 also showed low variability in rut accumulation between the two measuring points in each section, despite the construction variability in HMA thicknesses in some sections. More details of the rutting data from Cell 2 test sections are presented in Appendix B.

Figure 5.8 shows the wheel load deviator stresses measured on top of the subgrade by the soil pressure cells in the instrumented test sections in Cell 2 (C2S1 and C2S4). Both test sections showed noticeably low vertical subgrade pressures not exceeding 2.5 psi (17.5 kPa) for the 10-kip (44.5-kN) load level or 5 psi (35.0 kPa) for the increased 14-kip (62.3-kN) load level. The measured pressures increased 1.5 to 2 times when the load was increased in both test sections. The pressures on top of the subgrade are also lower for C2S1 with QB/FRAP and cement blends when compared to C2S4 with QB and cement only. This observation is in agreement with the increase in moduli values and rutting trends for the two sections indicating the positive effect of having recycled coarse aggregate materials in the mix on load distribution and rutting performance. The results, shown as the average values from two pressure cells in each section, were taken after a certain number of ATLAS passes. The measurements were consistent throughout the testing period.
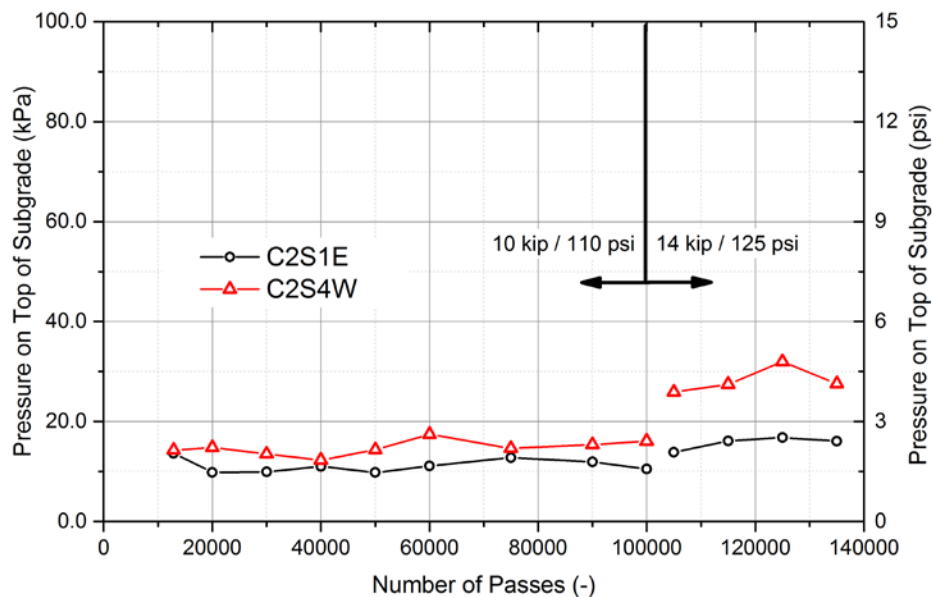
Figure 5.8. Average pressures on top of subgrade from the two instrumented sections in Cell 2.

5.4.3 Performance of Cell 3 – Chemically Stabilized Base/Subbase Applications of QB

Flexible pavement applications of chemically stabilized QB as base and subbase materials were investigated in Cell 3. Note that the last section in Cell 3 (C3S4) is a control section constructed with CA06_R base material without any QB or stabilization. Similar to Cell 2, the performance trends of the flexible pavement test sections in Cell 3 were monitored up to 135,000 passes, with the first 100,000-wheel passes applied at a load of 10 kip (44.5 kN), and a tire pressure of 110 psi (760 kPa). The latter 35,000 passes were applied at the increased load level of 14 kip (62.3 kN) and increased tire pressure of 125 psi (862 kPa).

Since Cells 2 and 3 have comparable applications of QB as chemically stabilized materials in base/subbase layers, it was imperative that both Cells were constructed similarly and tested at similar load levels and climatic conditions. Both Cells were constructed on top of an engineered CBR = 6% subgrade soil, and the nominal design thicknesses for subsurface and HMA layers were similar. The trafficking of Cell 3 test sections was running into winter, and temperatures during the day and night were dropping significantly. Therefore, in order to maintain similar average surface temperatures maintained for Cells 2 and 3, it was necessary that Cell 3 test sections be covered with ATLAS panels, and heaters set inside to maintain the HMA surface temperature at 75 °F (24 °C). This was done after 85,000 passes. This temperature was decided upon based on the average surface temperature for Cell 2 trafficking, which was calculated as 74.8 °F (23.7 °C). Due to the shading provided by ATLAS, the surface temperatures were measured to be no more than 7°F (4 °C) higher than air temperature at the wheel path. The installation of heat control panels, and heaters are shown in Figure 5.9.

| Panel Installation | Heaters on Pavement | Temperature Control – 3 Zones |

Figure 5.9. Installation of heaters and insulation panels on Cell 3 sections for temperature control.

The results for the wheel path maximum rut accumulations for Cell 3 test sections are presented in Figure 5.10. For section 4 with CA06_R base, only the west measuring point (C3S4W) was considered for the average rutting progression. The other east measuring point (C3S4E) was omitted due to the influence of the transition zone, which was paved last with less than desired HMA thickness (2.75 in. or 70 mm), had more permeable HMA with relatively low density/high porosity, and showed premature transverse fatigue and longitudinal wheel path cracking that is not typical for the base layers constructed with CA06 type of materials. With early cracking, the transition zone and C3S4E were exposed to higher levels of moisture that caused eventual pumping of fines from the CA06 material through the cracks and resulted in severe cracking and rutting as the loading progressed. Therefore, in order to have more representative data from this section, only C3S4W results are included in the average and discussion herein. The individual rut progression of C3S4E is shown in Figure 5.10(b). More details of the Cell 3 test section rutting data are presented in Appendix B.

Figure 5.10 also shows additional performance data from a previous APT study labelled as "Previous Study R27-124" for comparison with the control section. The test section from the previous R27-124 study was constructed on an engineered subgrade with CBR of 3%, with an aggregate subgrade thickness conforming to CS02 gradation and having a thickness of 9 in. (229 mm), overlain by a 3 in. (76 mm) of CA06_R material (similar to the one for C3S4) and HMA surface thickness of 4.3–4.9 in. (109–124 mm). More details about this test section can be found in the final report from the R27-124 study (Kazmee and Tutumluer, 2015).

As shown in Figure 5.10, C3S1 constructed with cement-stabilized QB2 material showed, on average, the least rutting, followed by C3S2 with a cement-stabilized QB2 subbase and a CA06_R base. The wheel path maximum rutting progression trends for C3S4 are only shown up to 40,000 passes due to the progression of fatigue to the surface resulting in increased moisture contents in the base and overall reduction in structural capacity from that of originally constructed cross-section. As a result, the rutting accompanied by cracking was more severe in the control section with further trafficking. It is also important that the structural capacity of the control section was originally weaker than the sections constructed with same base layer thickness and higher modulus stabilized materials.

Rutting rates increased considerably in all test sections when the load level was increased. In particular, C3S3 constructed with a fly ash-stabilized QB2 subbase and a CA06_R base showed significant increases in rutting rate at the increased load level and surpassed the threshold of 0.5 in. (12.5 mm) after 135,000-wheel passes. Comparisons of rutting progressions of C3S2 and C3S3 indicate a big discrepancy in performance trends between the fly ash and cement-stabilized QB sections, which was also clearly seen from sections in Cell 2.

Comparing the results of the stabilized test sections of C3S4 with a similar section from the R27-124 study (Kazmee and Tutumluer, 2015), these unbound aggregate sections accumulated higher rutting than the stabilized sections in Cells 2 and 3. Note that the section highlighted in Figure 5.10 from Kazmee and Tutumluer's R27-124 study (Kazmee and Tutumluer, 2015) was constructed on a significantly weaker CBR 3% subgrade soil, but had a higher HMA thickness than C3S4W, which had a constructed HMA thickness of only 2.75 in. (70 mm).
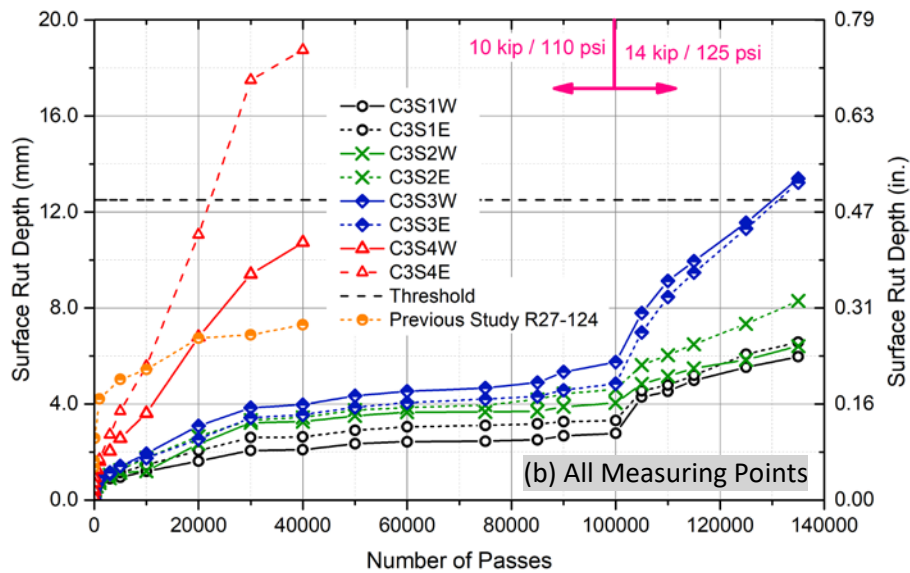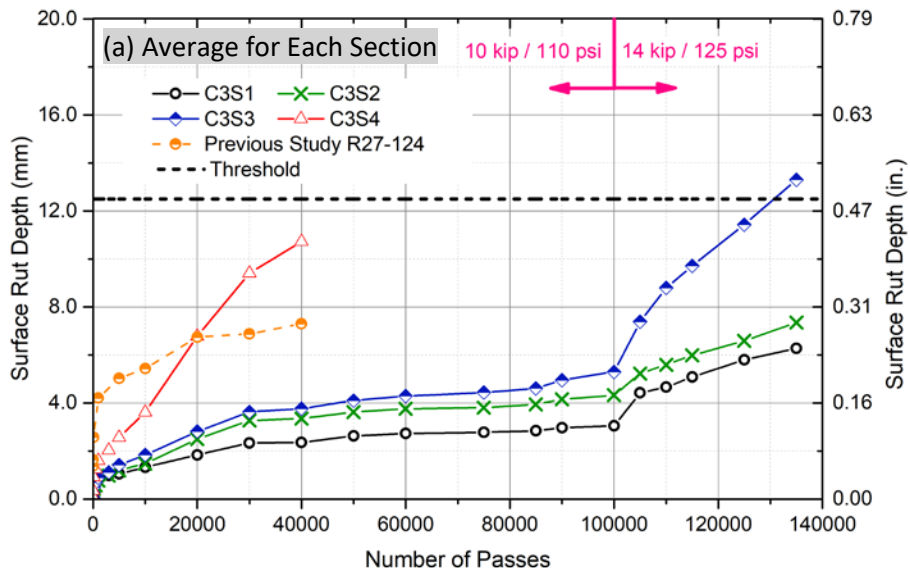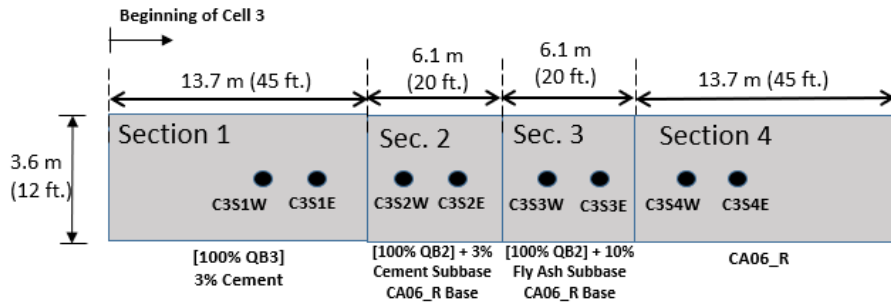
Figure 5.10. Wheel path maximum rutting progression in Cell 3 test sections - flexible pavements.

Figure 5.11 shows the wheel load deviator stresses measured on top of the subgrade by soil pressure cells instrumented in two test sections in Cell 3 (C3S2 and C3S4). C3S2, which has a cement-treated QB subbase and a CA06_R unbound aggregate base had relatively low vertical subgrade pressure not exceeding, on average, 2.5 psi (17.5 kPa) for the 10-kip (44.5-kN) load level or 5 psi (35.0 kPa) for the increased 62.3-kN (14-kip) load level. C3S4, however, had subgrade pressures that were 3–5 times higher than those measured for C3S2 and for the chemically stabilized sections in Cell 2. The measured trends for pressures on top of the subgrade are also matching with the rutting performance trends for the two sections. This finding clearly indicates that having a stiffer chemically stabilized base/subbase can significantly reduce the pressure on top of the subgrade and therefore protect the subgrade by minimizing permanent deformation accumulation in this weakest pavement layer.
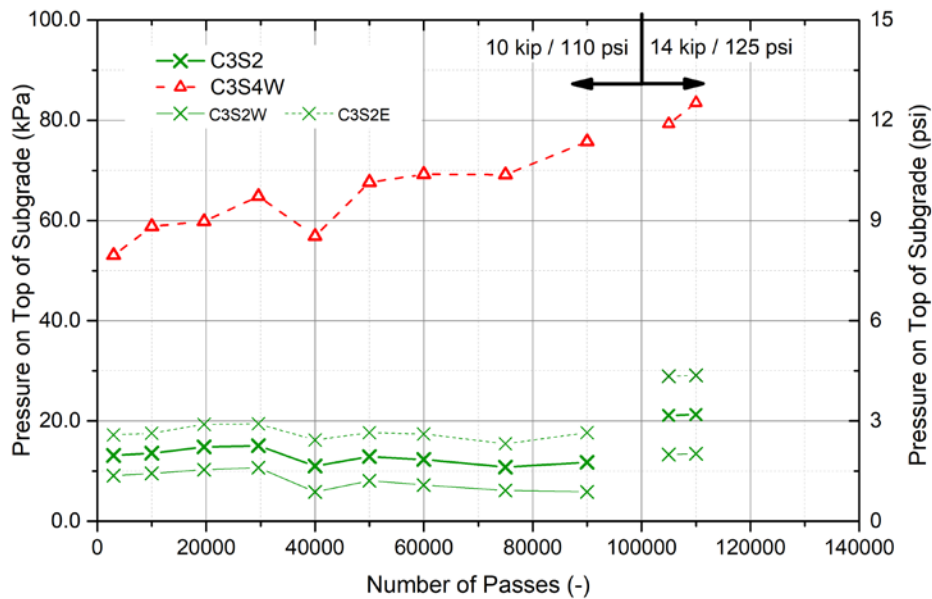
Figure 5.11. Average pressures on top of subgrade from the two instrumented sections in Cell 3.

5.5 SUMMARY

This chapter provided a summary of the performance records of the constructed working platform and flexible pavement test sections. This includes the rutting progression in all test sections and the measured top of the subgrade wheel load deviator stresses for sections instrumented with soil pressure cells in Cells 2 and 3. The constructed test sections were loaded using the ATLAS accelerated pavement tester. A summary of the test cell loading levels and the number of passes at each load level is given in Table 5.2.

Performance monitoring with accelerated pavement testing showed quite satisfactory results of QB applications for each of the construction platform and flexible pavement test sections. All construction platform sections in Cell 1S accumulated less than 3 in. (76 mm) of rutting for up to 20,000-wheel passes; while all paved sections in Cell 1N accumulated less than 0.5 in. (12.5 mm) of

rutting after 90,000 passes. Section 3 with 15% plastic fines accumulated the most rutting for both paved and unpaved sections, indicating the detrimental effect of plastic fines on performance.

Chemically stabilized sections in Cells 2 and 3 accumulated relatively low rutting after 135,000 wheel passes at the two load levels. Cement-stabilized test sections outperformed those stabilized with class C fly ash. The measured wheel load deviator stresses on top of the subgrade, recorded for three cement-stabilized test sections in Cells 2 and 3 indicated relatively low subgrade pressures of around 2 psi (14 kPa). These subgrade pressures were considerably lower (3–5 times lower) than those recorded for the conventional flexible pavement test section in Cell 3 (C3S4).

Table 5.2. Summary of Accelerated Pavement Testing Parameters

Cell	No. of ATLAS Passes Load: 10 kip (44.5 kN) Pressure 110 psi (760 kPa)	No. of Additional ATLAS Passes Load: 14 kip (62.3 kN) Pressure 125 psi (862 kPa)	Total Number of ATLAS Passes
Cell 1 South	20,000	-	20,000
Cell 1 North	90,000	-	90,000
Cell 2	100,000	35,000	135,000
Cell 3	100,000	35,000	135,000

The next chapter provides a summary of tests conducted after the APT, and an interpretation of the test section performance trends in light of the different datasets collected during the stages of construction, trafficking, and forensic analysis.

CHAPTER 6: FULL-SCALE TEST STUDY RESULTS AND INTERPRETATIONS

6.1 INTRODUCTION

Chapter 5 presented the results from the accelerated pavement testing of the Cells 1S, 1N, 2, and 3 constructed in full-scale to study applications of QB materials in aggregate subgrade, subbase, and base layers. This Chapter presents further details from the field testing conducted before/after the APT study and forensic analysis. The overall goal to collect more data and better understand the observed performance trends of the various QB applications and properly interpret the results.

6.2 FORENSIC ANALYSIS

This section presents testing that was conducted after APT with the ATLAS to better understand and assess the performance trends of the test sections constructed in all full-scale pavement test Cells. The tests that were conducted are: (1) FWD testing to track changes in deflections before and after testing; (2) HMA coring at the measuring points to obtain accurate wheel path HMA thicknesses for each test section; (3) Dynamic Cone Penetrometer (DCP) testing of the aggregate subgrade/subbase/base to assess the strength profiles of the pavement foundation/substructure layers with QB applications; (4) Flooded pavement tests for the aggregate subgrade/QB (i.e. PCR/QB) test sections to assess the effect of flooding on FWD deflections; and (5) Trenching of the test sections to determine the as-constructed layer thicknesses and assess uniformity of the pavement test section construction. A summary overview of the constructed test sections is shown in Figure 6.1. Detailed discussions on the findings of the conducted tests are presented in Sections 6.2.1 to 6.2.5.
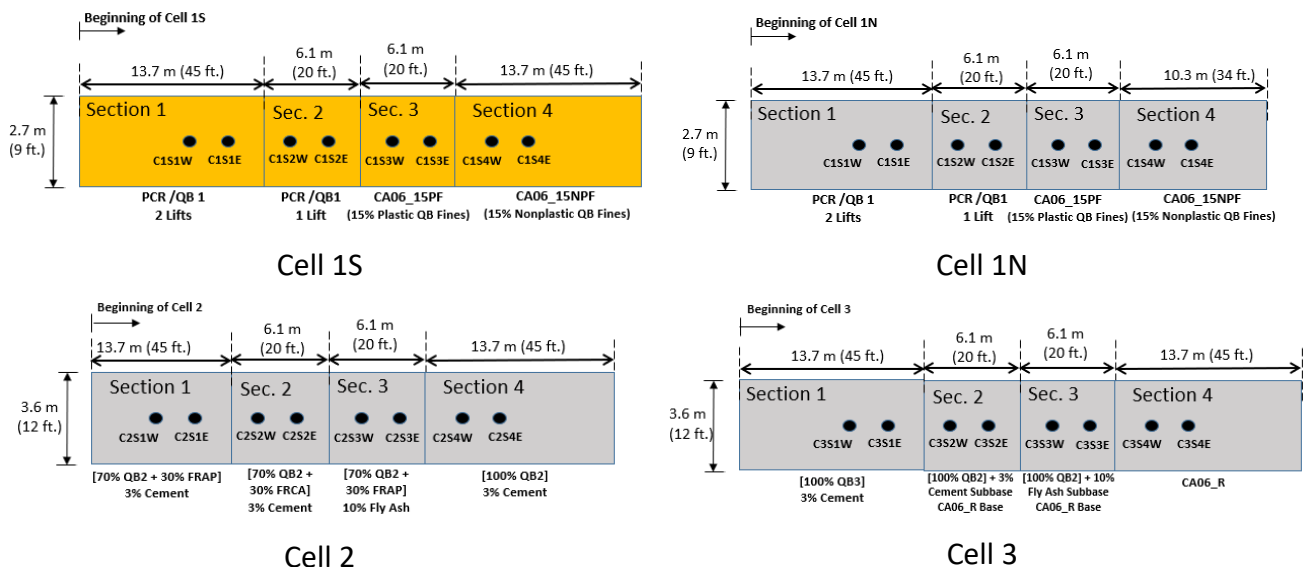
Figure 6.1. Summary overview of the constructed test sections in Cells 1S, 1N, 2, and 3.

6.2.1 Falling Weight Deflectometer Test Results and Interpretations

Falling Weight Deflectometer (FWD) testing was carried out on all of the construction working platforms and flexible pavement test sections. For Cell 1S construction platform test sections, one set of FWD tests was performed for all measuring points in September 2016, before trafficking with the ATLAS. For Cell 1N with flexible pavement test sections, FWD tests were conducted before and after trafficking to compare results. For Cells 2 and 3 studying chemically stabilized applications of QB, three sets of FWD tests were conducted for each measuring point; one after construction and two others before and after trafficking, respectively. It was imperative to monitor the curing of the test sections and detect any possible layer material property deteriorations due to freeze-thaw cycles in winter seasons, since the test sections in Cells 2 and 3 were constructed in 2016.

FWD tests were conducted by dropping three different load levels at each measuring point to induce variable stress states in pavement layers, and detect the surface deflections from seven geophones set 12 in. (305 mm) apart, including a center geophone directly under the load drop location. The complete data covering all deflection basins from the conducted tests are presented in Appendix C, which also presents the deflection basins from the three drops normalized to a standard 9-kip (40-kN) equivalent single-axle load, applying a uniform pressure of 80 psi (551 kPa) over a circular area with a radius of 6 in. (152 mm).

Figure 6.2 shows the maximum FWD deflections from the load dropped center geophone (D_o) for the test sections in Cell 1S having aggregate subgrade construction platform applications of QB. It is interesting to note that the trend for center deflections closely follows the trend of surface rutting progression (see Figure 5.3). For each test section, the progression of rutting and FWD deflections at the two measuring points are matching for all sections, where higher FWD deflections were recorded at the point, typically greater maximum ruts were accumulated in the wheel path. Additionally, except for section 3 with plastic fines CA06, the trends of FWD deflection and rutting accumulation are matching.
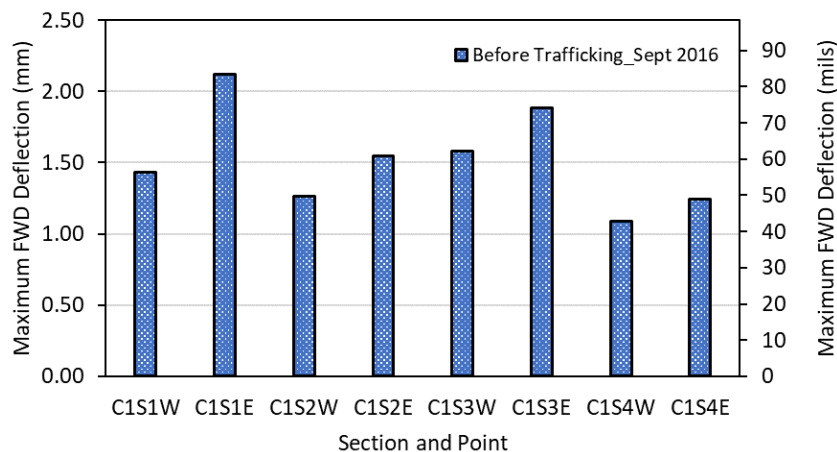
Figure 6.2. Maximum FWD deflections (D0) for Cell 1S test sections (construction platforms).

Figure 6.3 presents the maximum FWD deflections from the center sensor (D_o) for the flexible pavement test sections in Cells 1N, 2 and 3. The temperatures indicated in the figure are HMA surface

temperatures measured during FWD testing. Similar to the construction platform test sections, the trends in FWD deflections for Cell 1N test sections closely follow the rutting progression trends for all test sections and all measuring points (see Figure 5.6). For all test sections in Cell 1N, lower FWD deflections were measured after trafficking, likely due to the densification of HMA and aggregate subgrade layers with loading, especially considering that no clear damage was detected in these test sections.

Figure 6.3 also shows that the lowest FWD deflections measured in Cell 2 were for C2S1 and C2S2, constructed with blends of QB2 and FRAP/FRCA and stabilized with cement. These two sections had the best performance of all test sections, and also had the least recorded FWD deflections. The trend of FWD deflections for Cell 2 also closely follows the rutting progression (see Figure 5.7). For Cell 3, the trends of rutting accumulation (see Figure 5.10) and those of FWD deflections again closely match, except for Cell 2 Sections 1 and 2, which had similar rutting progression performances.

Note that for Cells 2 and 3, the measured FWD deflections were lower after trafficking when compared to the deflections recorded before trafficking. The exception to this general trend are points in Cell 2 Section 4 and Cell 3 Section 1 having cement-stabilized QB bases, where the FWD deflections were higher after trafficking. One possible explanation is the cracking of the base sections after construction. This is well supported by the higher FWD deflections and the higher LWD deflections that were recorded from the last measurements for these two sections before HMA paving (see Figure 4.14).

6.2.2 Hot Mix Asphalt Coring

The HMA pavement surface layers were cored in the center of the ATLAS wheel path to obtain accurate HMA thicknesses at the measuring points where the rutting data and other construction quality properties were measured. Additional cores were taken from the north and south sides of the wheel path measuring points. The data for HMA cores at the center of the wheel path are summarized in Figure 6.4. Images of cores extracted from the wheel path are presented in Appendix D. Note that the target HMA thickness was 4 in. (102 mm) for all test sections. As shown in Figure 6.4, the cored HMA thicknesses varied greatly from 2.75 to 4.7 in. (70 to 120 mm) in the different pavement test sections.

Note that the lowest HMA thickness was measured for the C3S4 control section with the unbound aggregate CA06_R base course, and the second lowest was measured for the C2S1E with cement-stabilized QB/FRAP, which was the best performing section. The poor performance of the control section (C3S4) can thus be highly attributed to the low HMA thickness and density. The extreme low density allowed high amount of water penetration through the HMA and higher water table; while the low HMA thickness led to premature cracking, thus pumping fines under the ATLAS loading and rapidly increasing damage potential. Note that for sections with chemically stabilized base/subbase applications of QB, particularly the ones stabilized with cement, the sections generally showed good performance despite the variability in HMA thicknesses (in the same section and in different sections). This can be partly attributed to the significantly higher stiffness's of the stabilized base materials which better distribute wheel load to protect pavement foundation.
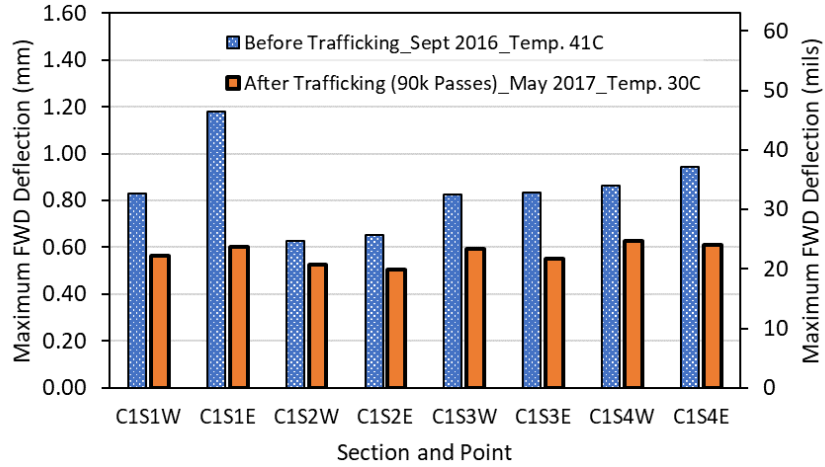
Cell 1N
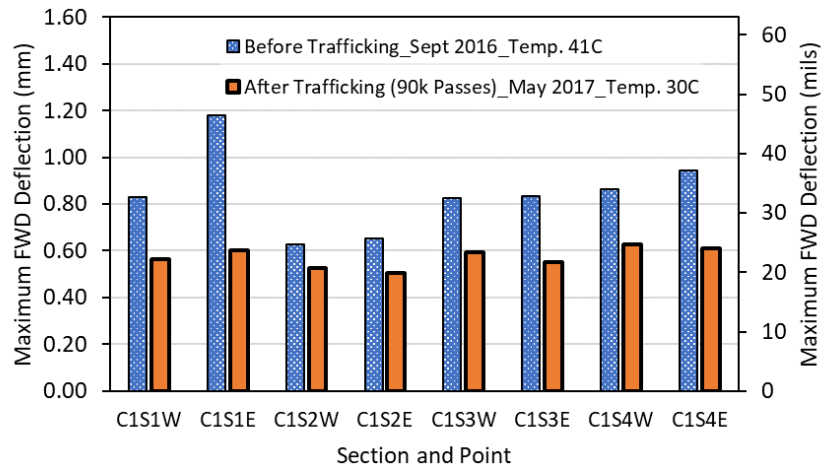
Cell 2
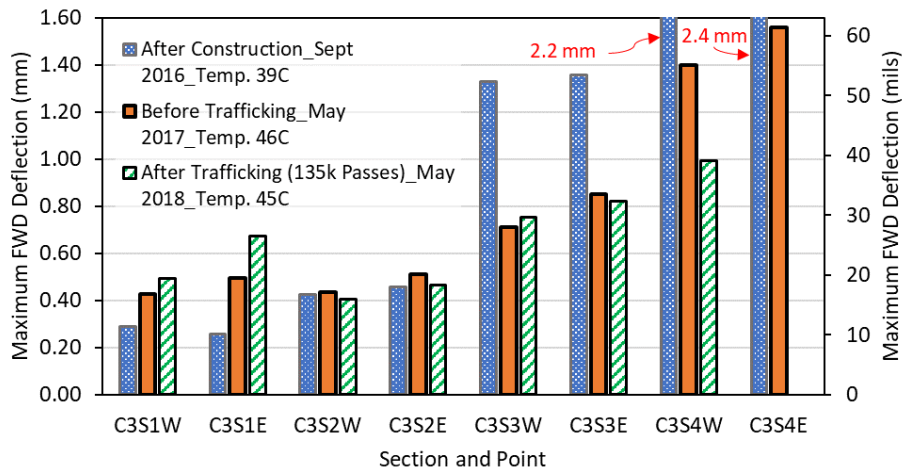
Cell 3

Figure 6.3. Maximum FWD deflections (D0) for Cells 1N, 2, and 3 flexible pavement test sections.
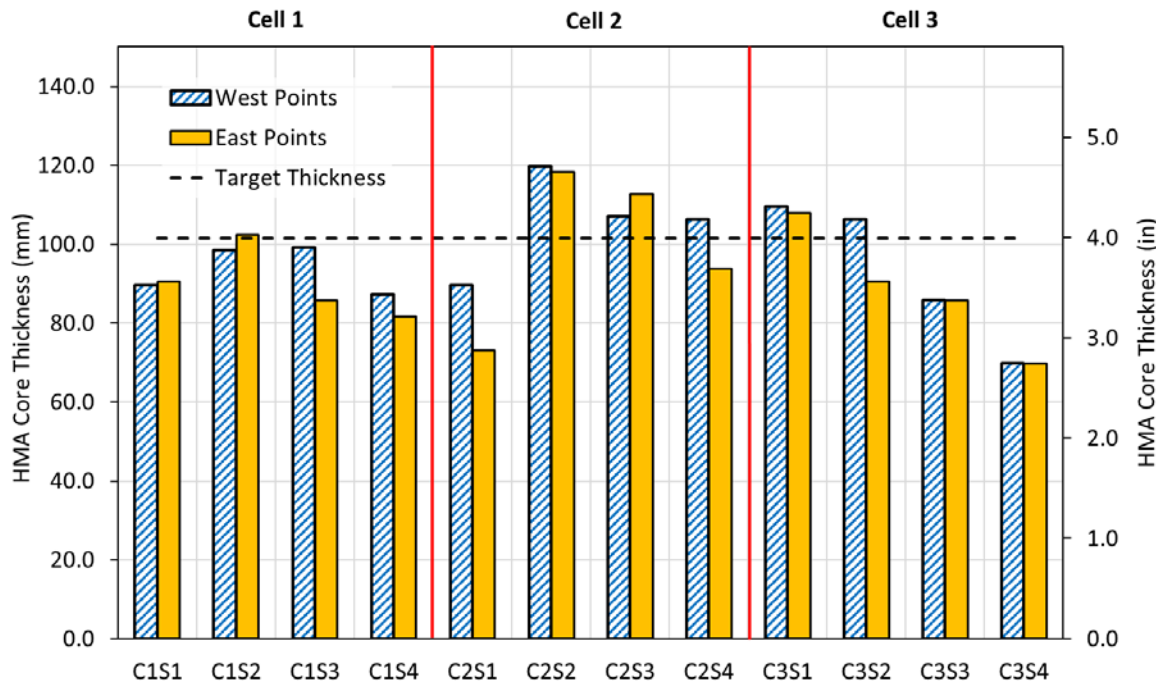
Figure 6.4. HMA Core Thicknesses of Flexible Pavement Test Sections in Cells 1N, 2 and 3.

6.2.3 Subsurface Layer DCP Profiling

Following HMA coring, Dynamic Cone Penetrometer (DCP) testing was conducted into the underlying base, subbase, and subgrade layers of all test sections in Cells 1N, 2, and 3. The DCP tests were conducted directly in the center of the wheel path at the measuring points through the holes of the cored HMA. Note that only one test was conducted in each section at one of the measuring points due to the difficulty and time required for these tests, especially for the stabilized sections where the number of drops to penetrate the full depth was noticeably high [e.g. it took 852 DCP hammer drops for penetrating 12.25 in. (311 mm) into the C2S1 cement-stabilized QB/FRAP blends, i.e. 70 DCP drops per 1 in. (25 mm) of penetration].

All DCP tests were conducted in dry weather conditions after several days/few weeks of no rain. The results for all test sections are summarized in Figure 6.5, which shows the number of DCP drops normalized for 1 in. (25 mm) of penetration. Higher numbers correlate with higher shear strength characteristics of the stiffer subsurface layers since DCP results produce shear strength profiles.

Figure 6.5 also shows the surface rut accumulations after 40,000 ATLAS passes at the measuring points tested with DCP. For Cells 2 and 3 in particular, the strength profiles of the subsurface pavement base/subbase layers were found to correlate well with performance trends, where sections accumulating the least rutting had the highest number of DCP drops per 1 in. (25 mm). In particular, C2S1 and C2S2 with blends of QB with FRAP/FRCA accumulated the least rutting, and had the strongest DCP profiles. The rutting performance trends and DCP profile correlations were less clear

for the unbound sections in Cell 1N, which might indicate that the thickness of HMA layers and the relatively weaker aggregate subgrade had greater control on performance, when compared to chemically stabilized test sections.
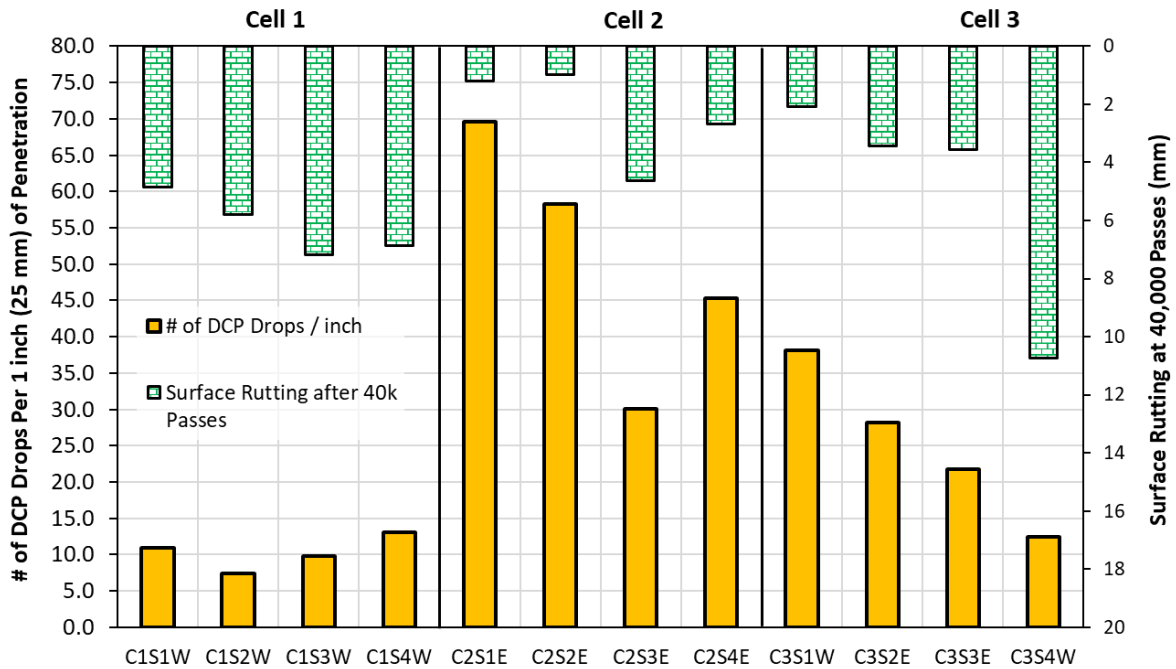
Figure 6.5. DCP penetrations into base, subbase, and subgrade layers in Cells 1N, 2, and 3.

6.2.4 Flooded Tests for Aggregate Subgrade/QB Test Sections

For the QB applications in Cell 1 that involved using QB as a filler material in the voids of large aggregate subgrade materials (C1S1 and C1S2), an investigation of the effect of moisture on performance was pursued by attempting to flood the aggregate subgrade layers, and study the influence of flooding/saturation on the measured FWD deflections at the same locations before and after flooding. The goal of the flooding study was to evaluate the saturated worst case scenarios on the retention of QB fines in the voids and how to achieve the stability of the large rock skeleton for the structural loading carrying ability in the PCR/QB designs of constructed aggregate subgrade layers.

Raising the water table level was achieved in the flooded test sections, with PCR/QB constructed in one lift and two lifts, by using hoses to apply water from the surface of the pavements. Simple calculations of the volumes of the constructed test sections and the known flow rate from the hoses indicated that the sections needed one day to flood. The sump pump that was used to store and divert the water from the test sections (see Figure 4.2) was shut off to increase water retention in the sections. The water was applied for ten continuous days, and the highest recorded water elevation was 17.5 in. (445 mm) from the surface, indicating partial flooding of the aggregate subgrade layers in both sections. The water level was monitored by drilling holes in the pavement and monitoring the water level. At the end of the experiment, these holes were used to obtain samples of the subgrade

and test them for moisture content, which ranged between 14.4% and 16.8% for the different samples.

The results of FWD deflections before and after this ''partial'' flooding of the PCR/QB aggregate subgrade layers in Cell 1S are shown in Figure 6.6, which shows that the center FWD deflections increased only slightly in three of the four locations, particularly for the two locations in Section 2 that was constructed in one lift (possibly due to little downward QB migration). The little change in the FWD deflections before and after flooding and the inspection of the pavement cross sections after digging trenches in these test sections indicated that a good QB retention in the voids of the large rocks was maintained and the PCR/QB construction technique was successful.

Note that the results shown here are preliminary results since only FWD tests were conducted, and since the test sections were partially flooded. In order to better investigate the effect of flooding on performance, it is recommended to expose these sections to real dynamic loading from heavy moving wheel loads. However, the preliminary results indicate promising results and that the construction method for these test sections was proper.
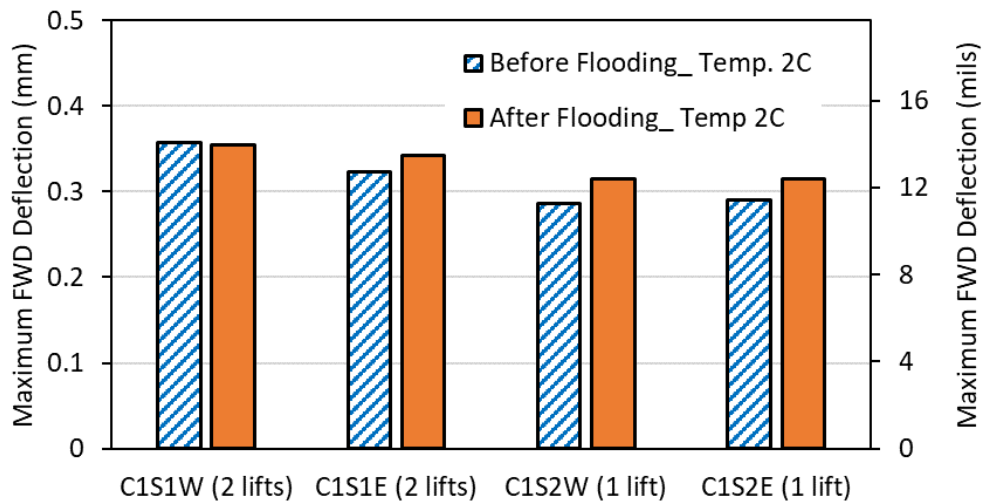
Figure 6.6. Maximum FWD deflections (D0) for Cell 1S aggregate subgrade/QB sections before and after flooding.

6.2.5 Trenching

After the completion of the field experiment, 5 ft. (1.5 m) wide trenches were excavated along the width of the cross-section for the visual examination of the rutting patterns in all of the construction platform and flexible pavement test sections. The trenches were necessary to measure the actual as-constructed layer thicknesses for each test section. The trenches were dug in a manner that the two faces of the trench exposed the cross sections of the West and East measuring points in each test section. The trenches were dug with the backward bucket of a backhoe loader. The chemically stabilized test sections were more difficult to excavate, and it took 6–8 times more time to dig a trench in a stabilized test section.

The photos taken for the cross sections of the full-scale test sections in Cell 1S and Cell 1N are shown in Figure 6.7 and Figure 6.8, respectively. In these figures, the red lines indicate the interface between the engineered in situ subgrade and the constructed aggregate layers. A summary of the as-constructed thicknesses of all layers is given in Figure 6.9 and Figure 6.10 for Cell 1S and Cell 1N, respectively. For Cell 1 test sections, no subgrade failure was visible in any section. For Cell 1S test sections, intended to study construction platform applications of QB, the accumulated surface rut was mostly due to the permanent deformations in the capping layer and the underlying aggregate subgrade materials. For Cell 1N test sections, on the other hand, only little surface rutting accumulated in general. These little surface ruts appeared to come mostly from the HMA layer with little or no contribution from the underlying capping and aggregate subgrade layers.

The photos taken for the cross sections of full-scale test sections in Cell 2 and Cell 3 are shown in Figure 6.11 and Figure 6.12, respectively. In these figures, the circled materials are big chunks of stabilized materials recovered from the trenches. A summary of the as-constructed thicknesses of all layers is given in Figure 6.13 and Figure 6.14 for Cell 2 and Cell 3, respectively. For both Cells, no subgrade failure was visible in any test section. For the chemically stabilized base course sections in Cell 2, and the first section in Cell 3 (C3S1), the little accumulated rutting was mostly coming from the HMA layer. For the other three sections in Cell 3 having a CA06_R base, the accumulated surface rutting appeared to be due to permanent deformations in both HMA and CA06_R layers.

From the trenching and coring results of Cell 1 test sections, the following observations can be made (see Figure 6.7 through Figure 6.10):

- For sections intended to study applications of QB for filling the voids of large aggregate subgrade materials, a uniform mixing between the PCR and QB was generally observed. QB percolated the full depth of the aggregate subgrade layer in both the one-lift and two-lift construction experiences in this research study. The QB that occupied the voids apparently survived APT loading, flooding and trenching. In particular, trenching photos for C1S1E in Cell 1S showed a crack starting from the surface and extending into mid-depth of the aggregate subgrade layer, possibly indicating an internal shear failure in the aggregate subgrade layer. Additionally, C1S1E in Cell 1N had little QB fines in the voids of the large aggregate subgrade rocks, and was constructed short on thickness, which justifies the poor performance at this measuring point compared to the other point, C1S1W, in the same section (see Figure 6.8 and Figure 6.10).

- A visual inspection of the trench photos for section C1S4W in Cell 1N, constructed with CA06_15NPF aggregates, indicates that this measuring point possibly had a higher fines content than the desired 15% fines due to materials segregation. This observation possibly explains the higher rutting accumulation at this measuring point despite the proper thicknesses and densities. The higher fines content were detected by comparing trenching photos with those taken for measuring points C1S4E and C1S4W from Cell 1S, and with C1S4E from Cell 1N, constructed with the same materials.

- Inspection of the trench photos did not indicate a major subgrade failure in any of the test sections. The surface rut accumulations were mostly coming from the HMA layer, and/or the aggregate subgrade and capping layers. Note that no surface cracking was observed at any of Cell 1N test sections.

C1S1W – PCR/QB1 in 2 Lifts

C1S1E – PCR/QB1 in 2 Lifts

C1S2W – PCR/QB1 in 1 Lift

C1S2E – PCR/QB1 in 1 Lift

C1S3W – CA06_15PF

C1S3E – CA06_15PF

C1S4W – CA06_15NPF

C1S4E – CA06_15NPF

Figure 6.7. Trenches exposing the cross sections of test sections in Cell 1S.

C1S1W – PCR/QB1 in 2 Lifts

C1S1E – PCR/QB1 in 2 Lifts

C1S2W – PCR/QB1 in 1 Lift

C1S2E – PCR/QB1 in 1 Lift

C1S3W – CA06_15PF

C1S3E – CA06_15PF

C1S4W – CA06_15NPF

C1S4E – CA06_15NPF

Figure 6.8. Trenches exposing the cross sections of test sections in Cell 1N.
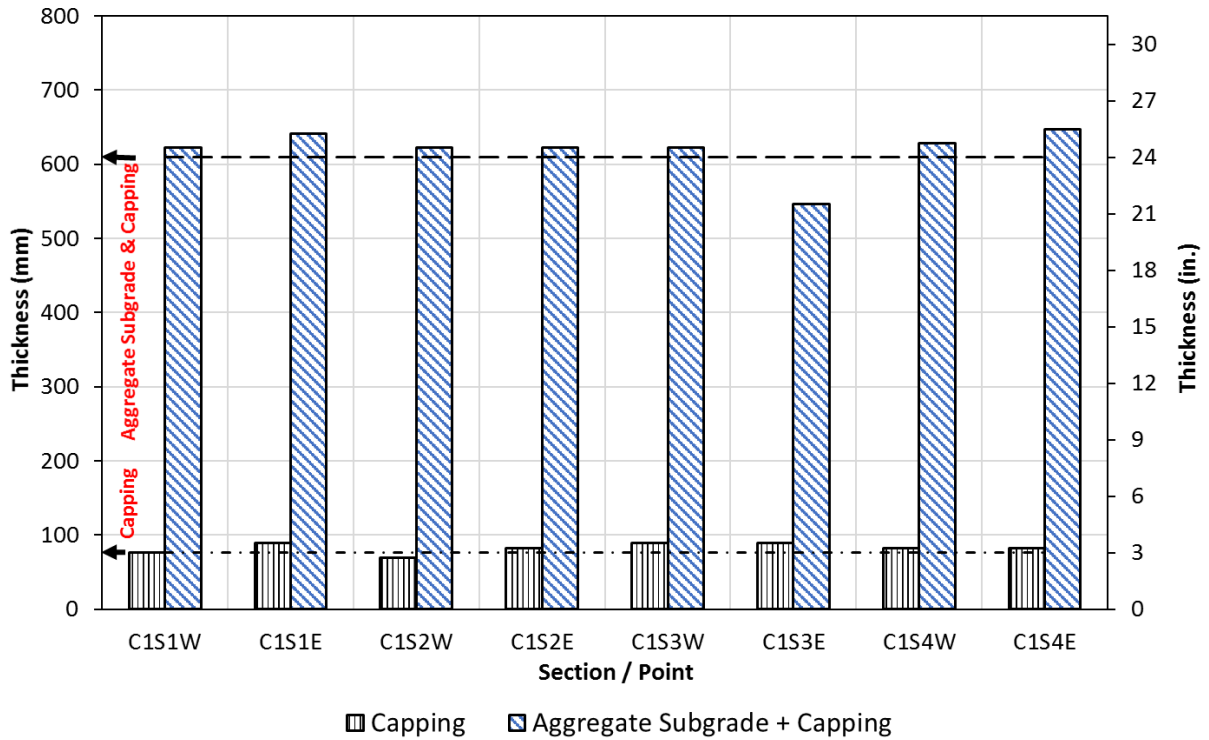
Figure 6.9. As-constructed layer thicknesses of Cell 1S test sections.
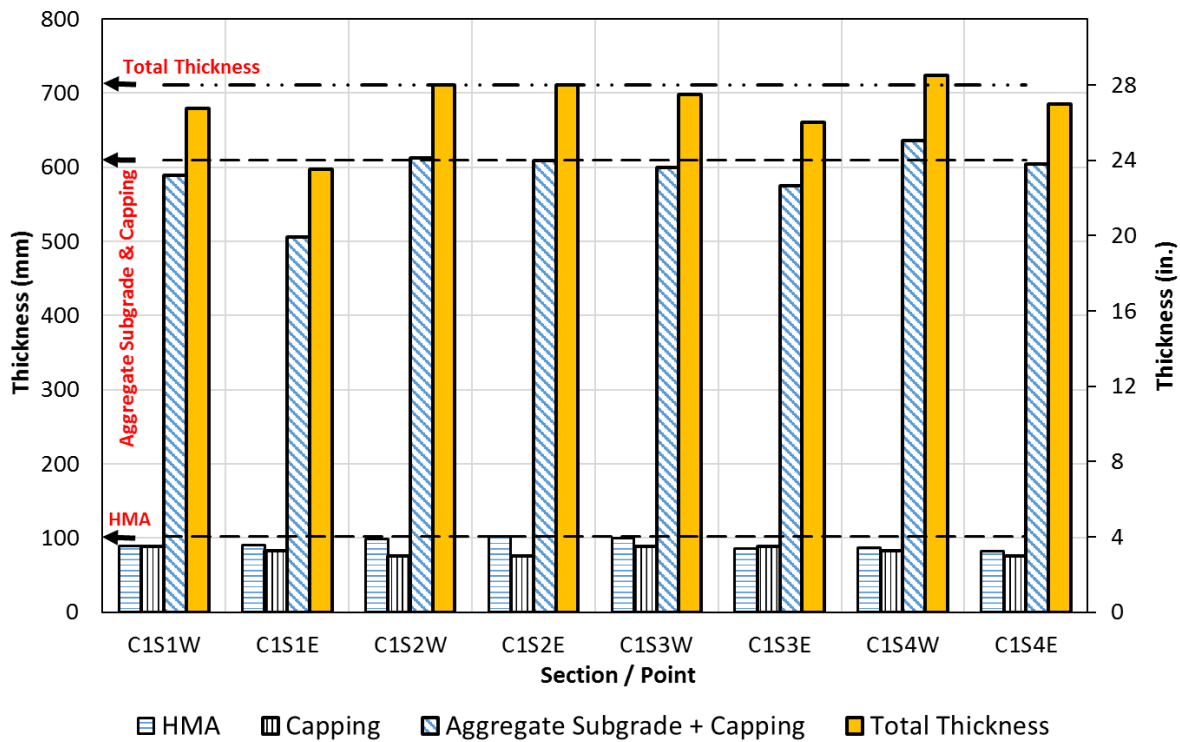
Figure 6.10. As-constructed layer thicknesses of Cell 1N test sections.

C2S1W – QB2 + FRAP + Cement

C2S1E – QB2 + FRAP + Cement

C2S2W – QB2 + FRCA + Cement

C2S2E – QB2 + FRCA + Cement

C2S3W – QB2 + FRAP + Fly Ash

C223E – QB2 + FRAP + Fly Ash

C2S4W – QB2 + Cement

C2S4E – QB2 + Cement

Figure 6.11. Trenches exposing the cross sections of test sections in Cell 2.

C3S1W – QB3 + Cement
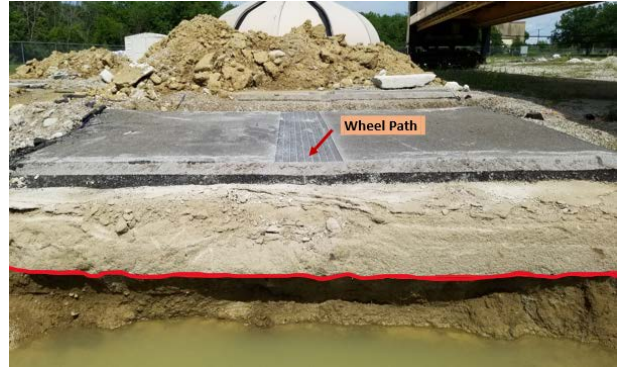
C3S1E – QB3 + Cement

C3S2W – QB2 + Cement Subbase & CA06_R Base
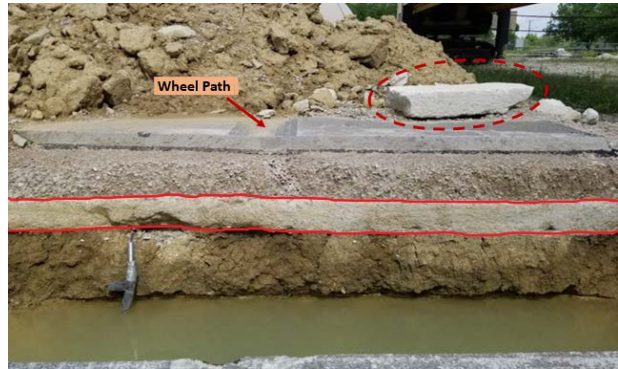
C3S2E – QB2 + Cement Subbase & CA06_R Base

C3S3W – QB2 + Fly Ash Subbase & CA06_R Base

C323E – QB2 + Fly Ash Subbase & CA06_R Base

C3S4W – CA06_R

C3S4E – CA06_R

Figure 6.12. Trenches exposing the cross sections of test sections in Cell 3.
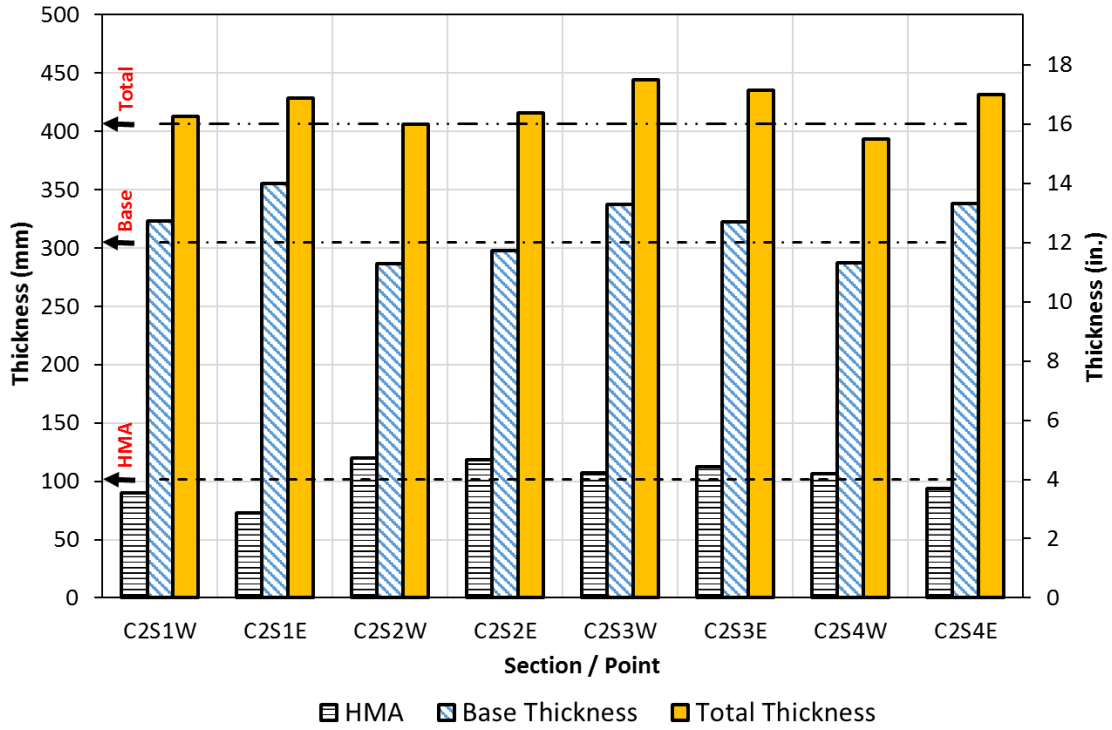
Figure 6.13. As-constructed layer thicknesses of Cell 2 test sections.
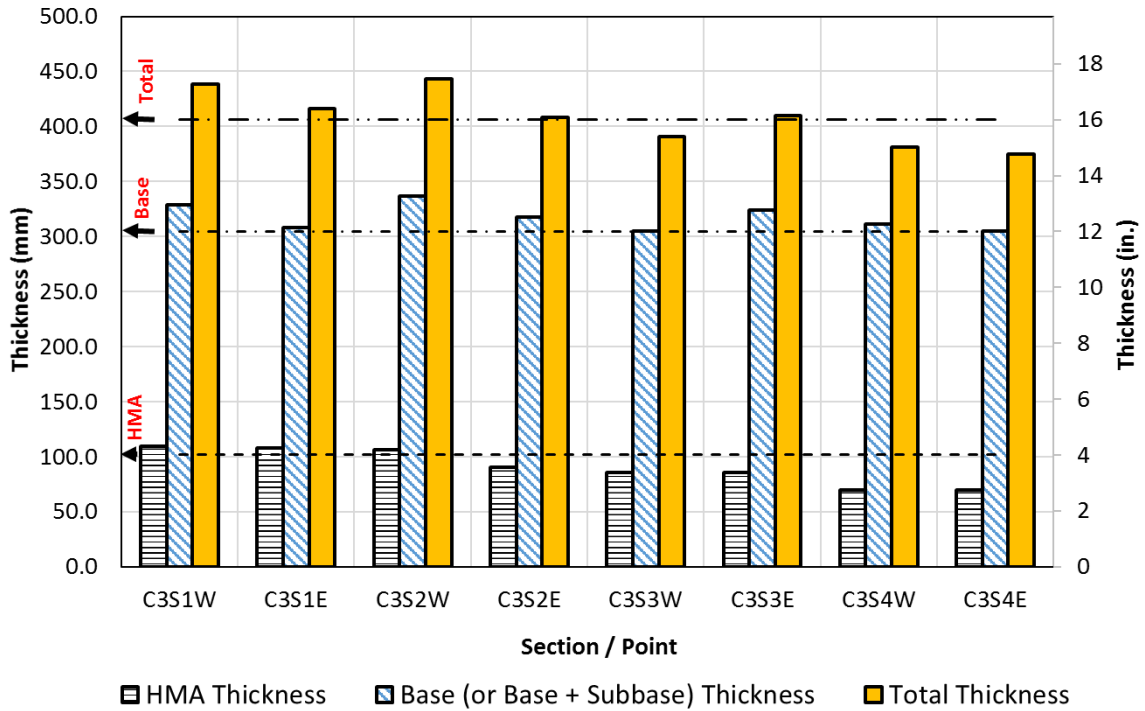
Figure 6.14. As-constructed layer thicknesses of Cell 3 test sections.

From the trenching and coring results of Cell 2 and Cell 3 test sections, the following observations can be made (see Figure 6.11 through Figure 6.14):

- Inspection of the trench photos did not indicate a major subgrade failure in any of the test sections, including the control section in Cell 3. The surface rut accumulations were mostly coming from the HMA layer in the chemically stabilized test sections, and the HMA/CA06_R layers in sections C3S2, C3S3, and C3S4 in Cell 3 with a CA06_R unbound aggregate base. The stabilized QB layers had very little rutting. No HMA cracking was observed at any of the chemically stabilized test sections in Cells 2 and 3.

- The as-constructed thicknesses of the stabilized base layers in Cell 2 ranged from 11.3–14 in. (287–356 mm) when compared to the target 12 in. (305 mm). In particular, C2S1E was constructed with largest base course thickness of 14 in. (356 mm), which counterbalanced the low HMA thickness at this point of 2.9 in. (73 mm). The as-constructed thicknesses of base or (base + subbase) layers in Cell 3 ranged from 12–13.3 in. (305–337 mm).

- For the cement-stabilized test sections, large blocks of stabilized layers were excavated and recovered during trenching. Some of these are highlighted in Figure 6.11 and Figure 6.12**.**

6.2.6 Cube Unconfined Strength Tests for Stabilized Test Sections

Following trenching of the test sections, some of the stabilized materials were recovered in intact pieces that were large enough to extract laboratory samples for Unconfined Compressive Strength (UCS) testing. Earlier on, attempts to extract and test cores of the stabilized base/subbase layers from the wheel path were not successful as the materials eroded with the presence of water from the coring process. In another attempt, a dry coring technique was employed to extract cylinders from the stabilized base and subbase layers for UCS testing. However, the lightly cemented layers eroded under the drilling action, producing fine fragments that clogged the coring bit; creating high friction and preventing the recovery of fully intact cores.

Test cubes, 3 in. (76 mm) in size, were successfully saw-cut in the laboratory from the recovered intact blocks cut using a dry-sawing process. The size of the test cubes were 4 times the nominal maximum aggregate size (NMAS) for the FRAP course aggregate particles used in C2S1 and C2S3 test sections (NMAS of FRAP was 0.75 in. or 19 mm), thus conforming with ASTM recommendations for sample size. For C2S2 with QB/FRCA blends, 96% of the material blend was smaller than ¾ in. (19 mm) in accordance with the combined QB/FRCA gradation.

Three test cubes were prepared and tested for each stabilized test section in Cell 2, as well as for stabilized QB3 base in C3S1 and the stabilized subbase layers in C3S2 and C3S3. Prior to testing, the cubes were capped using a sulfuric compound to ensure more uniform loading and then tested for unconfined compressive strength at a rate of 0.04 in./minute (1 mm/minute). Figure 6.15 summarizes the UCS results for the different mechanically stabilized QB combinations, while Figure 6.16 demonstrates the procedure for cutting and testing the test cubes.

Figure 6.15 compares the achieved field UCS of the tested cubes. Since only three cubes were tested for each test section, which is insufficient for conducting statistical analyses, the minimum, average, and maximum cube strengths are shown. Also shown in Figure 6.15 are the UCS for the laboratory test cylinders, which were previously presented in Figure 3.4. Note that for concrete specimens, it is generally agreed that cube strengths are 18-30% higher than cylinders with a 2:1 aspect ratio of height: diameter (Townsend et al., 1977; Kumavat and Patel, 2014).

On average, the highest UCS was achieved for the QB2 with 3% cement combination (C2S4 and C3S2), which was significantly higher than the USCS for laboratory cylinders, followed by cement-stabilized QB/FRCA and QB/FRAP (C2S2 and C2S1), respectively. The lowest strength was achieved for the fly ash-stabilized QB2/FRAP combination, which was the only combination that achieved a lower average UCS than the laboratory cylinders. Note that the reported strength values for the field cubes can be considered to represent the UCS for the recovered intact blocks. The cubes were visually inspected to ensure no cracks or fractures were visible prior to testing, but the presence of internal cracks resulting from trenching and handling might contribute to lower strength. Generally, the strength values of these cubes are expected to be on the higher end since they were extracted from the intact blocks recovered after trenching, while the weaker parts of the stabilized pavement layers would not be found intact.
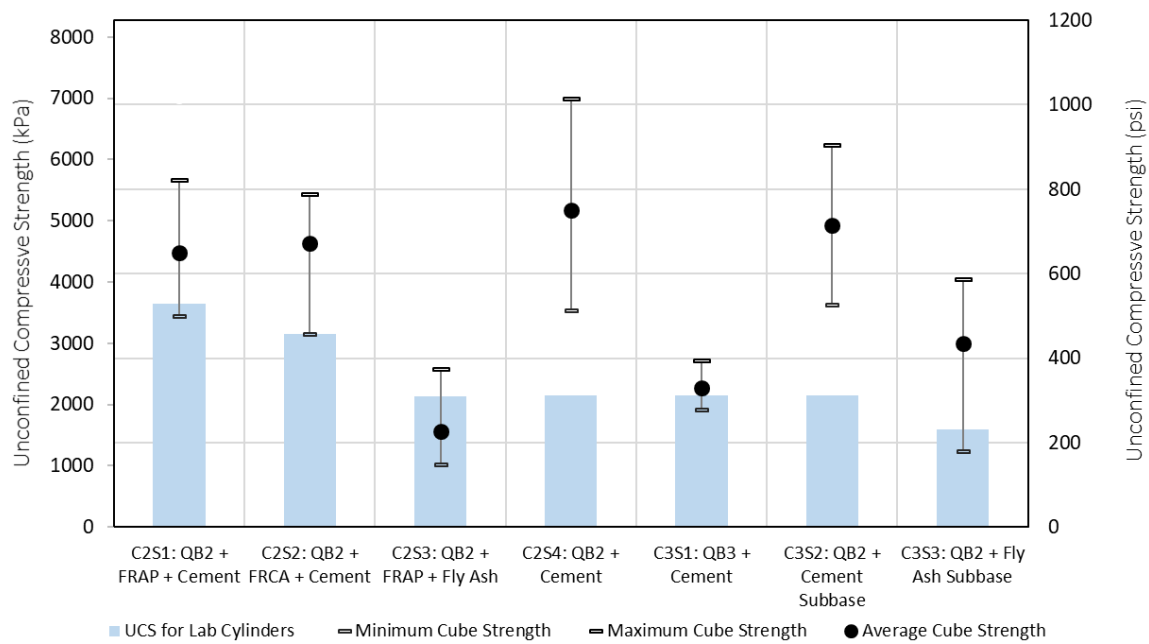
Figure 6. 15 Unconfined compressive strength (UCS) values of the cement ad fly ash stabilized QB and aggregate material combinations retrieved from the field test sections.

Saw-cutting cubes for strength testing

Saw-cut cubes from different sections

Capped cubes prepared for UCS testing
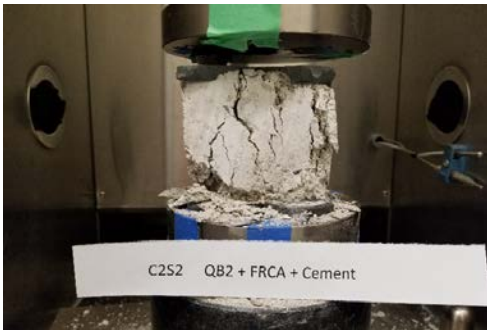
UCS testing of a cube

Strength cubes after UCS testing

Figure 6. 16 Preparation and testing of the field cubes

6.3 INTERPRETATION OF TEST RESULTS

The complete sets of detailed rutting progression results for Cells 1S, 1N, 2, and 3 were presented in Chapter 5 and Appendix B. Comparisons of maximum wheel path rutting progressions of test sections in Cell 2 and Cell 3, intended to study chemically stabilized layer applications of QB, are made in Figure 6.17. Overall, for the stabilized sections, the two sections chemically stabilized with 10% class 'C' fly ash (C2S3 and C3S3) consistently accumulated higher rut amounts and also showed higher

rates of rutting progression at the increased load level when compared to the other test sections chemically stabilized with 3% Portland cement. For the two sections, intended to study the effect of QB source, i.e. C2S4 with cement-stabilized QB2 base and C3S1 with cement-stabilized QB3 base, the trends of rutting progression were similar, indicating little effect of the source of QB on performance. Further, satisfactory rut performance was achieved for C3S2 inverted test section with a cement-stabilized QB subbase. The best performances with the lowest rut amounts were obtained for C2S1 and C2S2 having stabilized base courses of the QB blends with FRAP/FRCA, and the highest rutting accumulation was observed for C3S4 with an unbound aggregate CA06_R base.

A comparison of the measured wheel load deviator stresses on top of the subgrade for all the test sections instrumented with soil pressure cells in Cells 2 and 3 is presented in Figure 6.18. It shows that the stiffer chemically stabilized test sections (C2S1, C2S4, and C3S2) consistently recorded lower pressure on top of the subgrade when compared to the C3S4 control section, both at the original and increased ATLAS load levels. Clearly, the stiffer stabilized base materials are changing the mechanism of stress distribution in the pavement structure, allocating a higher share of the load to the stiffer base/subbase layers, and thus reducing subgrade pressures and subgrade rutting potential.
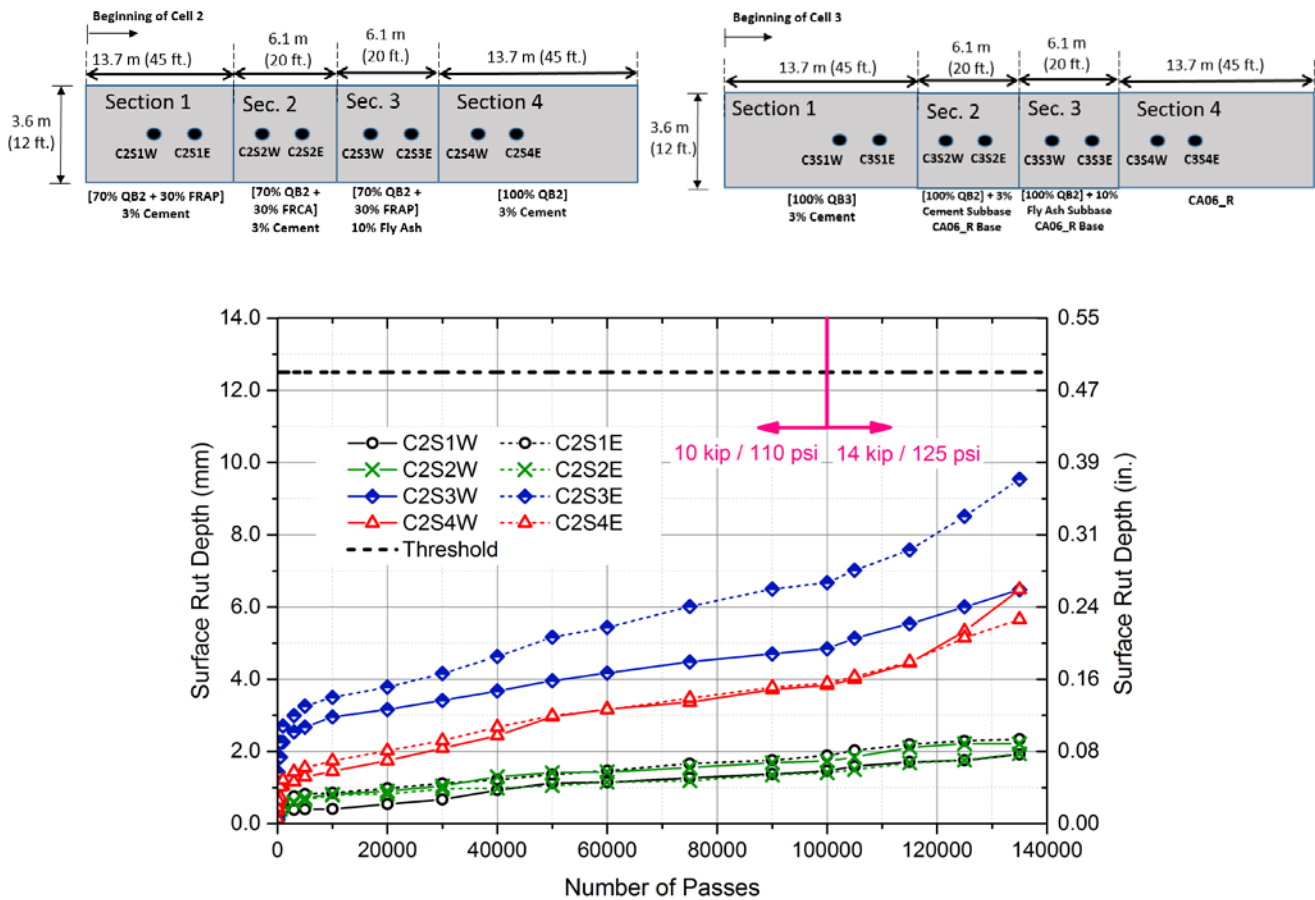
Figure 6.17. Comparisons of maximum wheel path rutting progressions in Cell 2 and Cell 3 test sections.
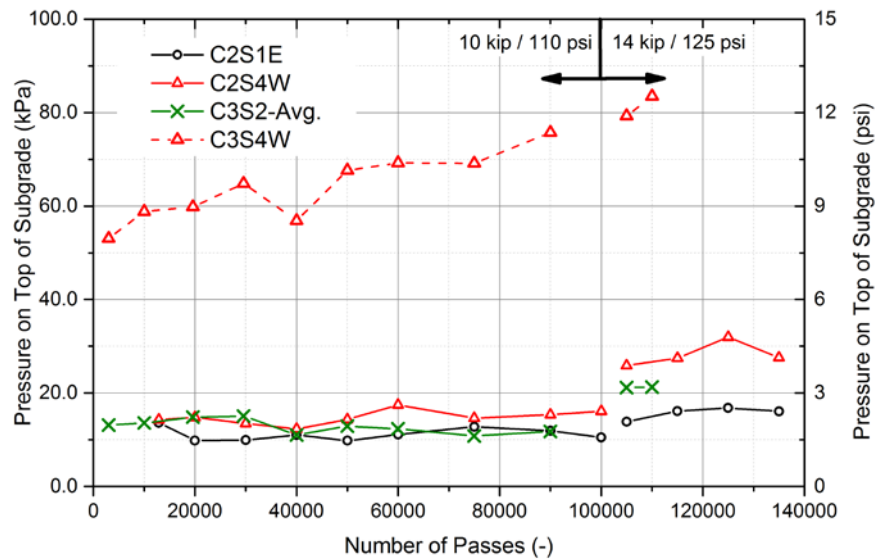
Figure 6.18. Comparisons of measured subgrade pressures in Cell 2 and Cell 3 test sections.

Figure 6.19 compares the wheel path average rutting progressions for C1S1 and C1S2 construction platform test sections built with QB filling the voids of large aggregate subgrade rocks (in 2-lifts and 1-lift, respectively) to the average rutting of a previous study in which a test section was constructed and tested with the same large rocks, same capping materials, same layer thicknesses, as well as a similar subgrade strength of CBR = 1% by Kazmee and Tutumluer in the previous R27-124 study (Kazmee and Tutumluer, 2015). This test section was loaded up to 4,000 load passes with the same wheel type and load levels as the current study. It can be seen that up to 4,000 passes, the construction platform with "PCR aggregates only" (with no QB filling the voids) had accumulated significantly higher rutting levels; indicating that the packing of QB in the voids has indeed increased the stability of the rockfill layers in the current study and reduced their wide variations in rutting performance as reported in the aforementioned study (Kazmee and Tutumluer, 2015).

Measurements of groundwater height were also taken after trenching by inspecting the water table levels in the excavated trenches. The measurements, reported in Figure 6.20, are for water table depths measured from the surface of the HMA after one week of trenching and with no rain event encountered. Note that the highest water table level was measured for the C3S4 control section (43 in. or 1.09 m from the surface of HMA), and the lowest water table level was reported for C1S4 (57.5 in. or 1.46 m). For all pavement test sections, wheel path rutting performance trends and rutting progression with number of passes correlate well with the heights of water table levels in the different sections. Note that the water table levels were relatively high in the subgrade, but this level could have been higher during/after rain events when the test sections were trafficked. Additionally, the nature of the silty subgrade soil at the test site could have allowed for significant capillary action of water movement towards the top of the subgrade, which could have resulted in higher moisture content conditions than the constructed near optimum moisture levels in the sections during testing. Therefore, the height of the water table could have influenced performance.
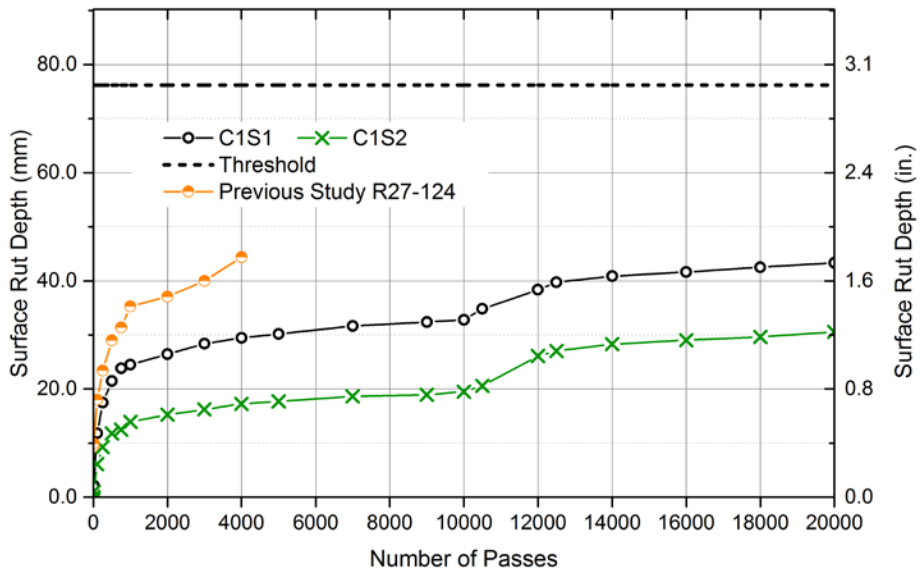
Figure 6.19. Comparisons of wheel path average rutting progressions for aggregate subgrade with and without QB.
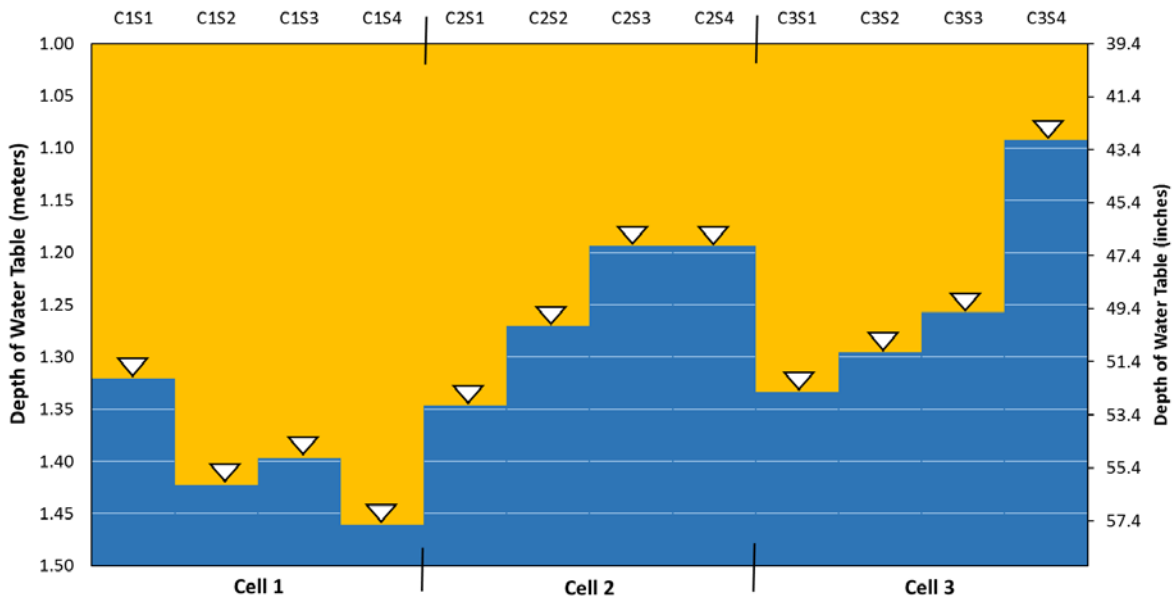
Figure 6.20. Depth of water table levels from the surface for all full-scale pavement test sections.

CHAPTER 7: SUMMARY AND CONCLUSIONS

7.1 INTRODUCTION

This research project focused on evaluating new sustainable applications of Quarry By-products (QB) or QB mixed with other marginal, virgin, or recycled aggregate materials in pavements; both as unbound and chemically stabilized pavement layers. In total, sixteen full-scale pavement test sections were constructed to evaluate the use of QB in base, subbase, and aggregate subgrade applications. The chemically stabilized test sections utilizing QB were stabilized with 3% cement or 10 % Class 'C' fly ash, by dry weight, and were constructed over a subgrade having an engineered unsoaked California bearing ratio (CBR) of 6% to study their effectiveness in low to medium volume flexible pavements. The unbound applications of QB investigated the use of QB to fill the voids between large aggregate subgrade rocks commonly used for rockfill applications on top of very soft subgrade soils, as well as using dense-graded aggregate subgrade layers with higher fines content up to 15% passing No. 200 sieve for soft subgrade remediation. These unbound test sections were constructed over a CBR=1% subgrade soil to investigate their effectiveness in both construction platforms and low volume road applications.

All the field test sections were then evaluated in rutting and fatigue by Accelerated Pavement Testing (APT). Following APT, forensic analysis tests were conducted to further evaluate the performance of the test sections. These tests included Falling Weight Deflectometer (FWD) tests before and after trafficking, hot mix asphalt coring, Dynamic Cone Penetrometer (DCP) testing and strength profiling with depth of subsurface layers, and trenching to expose the cross sections of the constructed test sections. In general, results from APT and forensic analysis, which were thoroughly presented in this report, indicated that quite satisfactory results were obtained for field rutting performance trends. Pavement testing and evaluations indicated that the selected QB applications can be successfully incorporated in standard pavement construction and rehabilitation practices.

7.2 SUMMARY OF FINDINGS FROM CELL 1

Two categories of applications were selected and tested for field performance in Cell 1, both for construction platform and low volume flexible pavement applications with hot mix asphalt (HMA) surfacing. The categories are: (1) QB used as a filler material in the voids of large, unconventional, uniformly graded 'aggregate subgrade' materials to improve strength and reduce potential settlement that could result from stability concerns due to the presence of large voids in the granular matrix; and (2) The construction of commonly used dense-graded aggregate base/subbase materials with the use of higher fines content, i.e., 15% passing the No. 200 sieve (or smaller than 0.075 mm), on top of a very weak (CBR $\leq$ 1) subgrade.

The conducted field investigation involved constructing eight different test sections (four construction platforms and four low volume road sections), and monitoring their performance through accelerated pavement testing. A laboratory packing study suggested that the optimum quantity of QB to be mixed with the large primary crusher run (PCR) aggregates by shaking them into the voids using vibratory action was 25% QB by the weight of the PCR, considering more likely wet

conditions of QB in the field. The study also concluded that the moisture content of the QB is one of the main factors governing the quantity of QB that can be packed in the voids.

Field construction of PCR/QB sections successfully incorporated 25% QB by weight for sections constructed in two lifts. However, for the full-scale test sections constructed in a single lift of PCR aggregate, only 16.7% QB could be packed. Quality control (QC) testing was accomplished using a lightweight deflectometer (LWD) on top of the capping layers of all test sections and a falling weight deflectometer (FWD) on top of the final surface courses. The composite surface modulus back-calculated from LWD deflections relatively showed similar modulus values for all test sections. FWD deflections showed significantly lower deflections for the HMA-paved test sections, with Section 1 constructed with PCR/QB in two lifts giving the highest deflections at one of the measuring points.

Performance monitoring with accelerated pavement testing showed quite satisfactory results of QB applications for each of the construction platform and flexible pavement test sections. All construction platform sections in Cell 1S accumulated less than 3 in. (76 mm) of rutting for up to 20,000-wheel passes; while all paved sections in Cell 1N accumulated less than 0.5 in. or 12.5 mm of rutting after 90,000 passes. Section 3 with 15% plastic fines accumulated the most rutting for both paved and unpaved sections, indicating the detrimental effect of plastic fines on performance, especially when they were exposed to moisture. The presence of a hot mix asphalt cover on top of plastic fines reduces this effect due to lower load levels experienced by the aggregate layers. Finally, sections with QB packed in the voids of large PCR rocks indicated a superior performing construction platform compared to PCR only, which was previously evaluated under similar loading and subgrade conditions.

7.3 SUMMARY OF FINDINGS FROM CELLS 2 AND 3

Three categories of chemically stabilized QB applications were selected and tested for field performance in Cells 2 and 3, for low volume flexible pavement applications with HMA surfacing. The categories are: (1) Blending QB with coarse aggregate fractions of reclaimed asphalt pavement (FRPA) and recycled concrete aggregates (FRCA); (2) Using QB as a cement or fly ash-treated base material; and (3) Using QB as a cement or fly ash-treated subbase (i.e., in inverted pavements). All test sections were stabilized with 3% cement or 10% class 'C' fly ash and constructed on top of an engineered subgrade with a 6% CBR strength.

Satisfactory rut performance was achieved for all chemically stabilized QB layer applications. QB blends with FRCA or FRAP and cement had higher and statistically different unconfined compressive strengths from laboratory tests. They also showed the best rutting performance trends with the highest LWD moduli, lowest FWD deflections, and the highest number of drops per 1 in. (25 mm) of penetration by DCP from field testing. Sections stabilized with fly ash had inferior and more variable performance trends when compared to the cement-stabilized sections. Test sections that utilized two different sources of QB for the cement-stabilized base application did not show any significant difference in performance, which is in agreement with the laboratory unconfined compressive strength (UCS) test results showing no statistical difference for the two QB materials.

The performance monitoring of the stabilized test sections before and after trafficking with APT indicated in general relatively low FWD deflections for the stabilized test sections in Cells 2 and 3. Additionally, measured wheel load deviator stresses on top of the subgrade, recorded for three cement-stabilized test sections in Cells 2 and 3 instrumented with pressure cells, indicated relatively low subgrade pressures of around 2 psi (14 kPa) and thus, low subgrade rutting potential.

7.4 CONCLUSIONS

In light of the sustainable QB layer applications demonstrated for quite satisfactory full-scale field performance trends observed in the construction platform and flexible pavement test sections, the following conclusive remarks can be offered:

- Quarry By-products (QB) were successfully used as a filler material in the voids of large, unconventional, and uniformly graded 'aggregate subgrade' materials to improve strength and reduce potential settlement over a soft CBR=1% subgrade. Satisfactory performance results were achieved for both one-lift and two-lift construction experiences in this research study. Comparisons of rutting progressions with previous studies (with no QB fillers) indicated a significant improvement in performance for aggregate subgrade layers when QB is used as a filler in the large voids of primary crusher run sized aggregate subgrade/rockfill materials.

- The construction platform section with CA06 type dense-graded aggregate subgrade having 15% plastic fines accumulated the highest wheel path rut, and showed the highest rutting rate, possibly during such events when the section was exposed to higher moisture contents from rainwater accumulation. The results from this section indicate the detrimental effect of plastic fines on performance, especially when they were exposed to moisture. The effect of plastic fines on performance was less clearly seen for flexible pavement test sections, where the unbound aggregate layers were exposed to lower load levels/stress states, and were better drained due to the presence of an HMA cover and proximity to the drainage line.

- Sections constructed with QB blended with FRAP/FRCA showed the best performance in terms of the least wheel path rutting progression. No significant difference in performance was observed between the FRAP and FRCA sections. The presence of coarse aggregates increased the layer stiffness and the load carrying capacity of these sections and resulted in better performance.

- The conventional flexible pavement control section (C3S4), having the standard CA06 dense-graded unbound aggregates, was constructed in the field with the lowest HMA thickness and density, and was exposed to the highest water table levels among all the constructed full-scale test sections. Accordingly, the thinnest HMA surfacing in this section (2.75 in. or 70 mm) compared to other sections, accompanied with relatively high levels of HMA porosity resulted in cracks appearing on the pavement surface after 30,000 passes in the transition zone, which increased the exposure of the control section to higher moisture levels. The low HMA density also allowed substantial water infiltration which raised the water table, weakened the base layer and exacerbated the rutting. The pumping of fines under high wheel loads (due to the presence of high moisture levels) expedited the rutting progression due to loss of support under the HMA layer. In conclusion, the C3S4 control section in this full-scale study performed

quite poorly compared to standard conventional flexible sections constructed in Illinois. Therefore, it did not provide a good baseline for comparison to evaluate field performance trends of the targeted sustainable applications of QB in pavements.

- For the chemically stabilized sections in Cells 2 and 3, the test sections stabilized with cement consistently showed better performance than those stabilized with fly ash. Despite this fact, the performance of the fly ash stabilized test sections is still satisfactory. Only the section with fly ash-stabilized QB subbase (C3S3) surpassed the 0.5 in. (12.5 mm) rutting threshold after 135,000 total passes.

- The thickness of subsurface layers and HMA layers had a significant effect on performance trends of the test sections. Thus, sustainable QB applications need to be brought into the IDOT mechanistic-empirical design framework for appropriate thickness design. Note that the thickness of HMA had less effect on performance for the chemically stabilized sections when compared with sections constructed with unbound materials, where the thickness of HMA was one of the major factors affecting performance.

- Cement-stabilized layers of two QB sources (QB2 and QB3) showed similarly good performance. Thus, preliminary results indicate no significant effect of the QB source on performance. This conclusion needs to be further investigated with more QB sources from Illinois tested for performance.

- Inverted pavement sections constructed in Cell 3, i.e. C3S2 and C3S3, in general showed good performance. In particular, C3S2 with a cement-stabilized QB subbase and a dense-graded aggregate base, established quite a satisfactory combination demonstrating the suitability of using cement-stabilized QB in inverted pavement applications.

7.5 RECOMMENDATIONS FOR FUTURE WORK

The field performance evaluations of QB pavement layer applications, investigated in this project, highlighted several potentially successful applications of QB in pavements, both chemically stabilized and unbound applications. However, certain aspects of this study may require further investigation. The following discussion outlines recommendations for further research and research needs:

- There is a need to investigate effective field construction methods for mixing QB with aggregate subgrade for better uniformity. The successful construction of aggregate subgrade/QB layers (PCR/QB) when the QB was added in small increments followed by a vibratory action in this study, suggests that the right practice of vibrating QB into the inherent voids of constructed lifts of aggregate subgrade requires developing an automated technique to spread the QB uniformly and more slowly on the surface, accompanied with continuous vibration. Such a construction method needs to be validated and further investigated.

- There is a likely need to further investigate the effect of QB source for reassurance. Preliminary results indicated no significant effect of QB source. This needs to be further studied by evaluating the performance of QB from more sources across the State of Illinois, and possibly better understanding the particle size and shape distributions of the different QB

sources for investigating the effect of the material composition of the fines (i.e. packing) on performance.

- There is a need to further investigate the effect of mix proportions of QB with coarse recycled aggregates. This study has investigated the performance for sections with QB mixed with coarse fractions of FRAP or FRCA at a blending ratio of 70% QB with 30% FRAP or FRCA. Different mix proportions with other blending ratios that may provide better performance or more sustainable applications need to be studied.

- There is commonly a need to investigate and better evaluate the effect of fly ash source and composition on the fly ash stabilized mixtures. The performance aspects of fly ash stabilized layers can vary widely depending on the source and properties of fly ash, and more detailed investigations on the effect of Class 'C' fly ash source and composition on performance need to be conducted.

- There is a general need to improve construction quality and decrease field variability. The wide fluctuations in the as-constructed thicknesses of pavement layers, particularly HMA, in this study could skew the results of the APT field experiment. This was particularly affecting the control section functionality of the HMA constructed on top of unbound aggregate layers in the conventional flexible pavement test section. Further investigation is needed for improving construction methods and checking construction quality to achieve more consistent pavement layer thicknesses (e.g. surveying, and string lining) and uniform layer properties.

REFERENCES

Arulrajah, A., J. Piratheepan, and M. Disfani. Reclaimed Asphalt Pavement and Recycled Concrete Aggregate Blends in Pavement Subbases: Laboratory and Field Evaluation. Journal of Materials in Civil Engineering, Vol. 26, No. 2, 2013, pp. 349-357.

Arulrajah, A., J. Piratheepan, M. Disfani, and M. W. Bo. Geotechnical and Geoenvironmental Properties of Recycled Construction and Demolition Materials in Pavement Subbase Applications. Journal of Materials in Civil Engineering, Vol. 25, No. 8, 2012, pp. 1077-1088.

ASTM C117-17, Standard Test Method for Materials Finer than 75-μm (No. 200) Sieve in Mineral Aggregates by Washing. ASTM International: West Conshohocken, PA, DOI: 10.1520/C0117-17, www.astm.org, 2017.

ASTM C127, Standard Test Method for Relative Density (Specific Gravity) and Absorption of Coarse Aggregate. ASTM International: West Conshohocken, PA, www.astm.org, 2015.

ASTM C136 / C136M-14, Standard Test Method for Sieve Analysis of Fine and Coarse Aggregates. ASTM International: West Conshohocken, PA, DOI: 10.1520/C0136-04, www.astm.org, 2014.

ASTM C1435 / C1435M, Standard Practice for Molding Roller-Compacted Concrete in Cylinder Molds Using a Vibrating Hammer. ASTM International: West Conshohocken, PA, DOI: 10.1520/C1435_C1435M-14, www.astm.org, 2014.

ASTM C29 / C29M-17, Standard Test Method for Bulk Density ("Unit Weight") and Voids in Aggregate. ASTM International: West Conshohocken, PA, DOI: 10.1520/C0029_C0029M-17A, www.astm.org, 2017a.

ASTM D1632, Standard Practice for Making and Curing Soil-Cement Compression and Flexure Test Specimens in the Laboratory (Withdrawn 2016). ASTM International: West Conshohocken, PA, www.astm.org, 2007.

ASTM D1633, Standard Test Methods for Compressive Strength of Molded Soil-Cement Cylinders (Withdrawn 2016). ASTM International: West Conshohocken, PA, DOI: 10.1520/D1633-00R07, www.astm.org, 2007a.

ASTM D4643, Standard Test Method for Determination of Water (Moisture) Content of Soil by Microwave Oven Heating. ASTM International: West Conshohocken, PA, DOI: 10.1520/D4643-08, www.astm.org, 2008.

ASTM D698, Standard Test Methods for Laboratory Compaction Characteristics of Soil Using Standard Effort (12 400 ft-lbf/ft3 (600 kN-m/m3)). ASTM International: West Conshohocken, PA, DOI: 10.1520/C0698-16, www.astm.org, 2012.

Bennert, T. and A. Maher, The development of a performance specification for granular base and subbase material. Final Report No. FHWA-NJ-2005-003, 2005.

Bennert, T., W. Papp Jr, A. Maher, and N. Gucunski. Utilization of Construction and Demolition Debris under Traffic-Type Loading in Base and Subbase Applications. Transportation Research Record, Journal of the Transportation Research Board, Vol. 1714, 2000, pp. 33-39.

Chesner, W.H., R.J. Collins, and M. MacKay. User Guidelines for Waste and By-product Materials in Pavement Construction. Publication FHWA-RD-97-148. FHWA, U.S. Department of Transportation, 1998.

De Rezende, L. and C. De Carvalho. The Use of Quarry Waste in Pavement Construction. Resources, Conservation and Recycling, Vol. 39, No. 1, 2003, pp. 91-105.

Dumitru, I., T. Zdrilic, and G. Johnson. Further Investigation of Soil Remineralization Using Quarry Fines in Australia. In International Center for Aggregates Research (ICAR) 9th Annual Symposium, 2001.

Huang, Y.H. Pavement analysis and design. Book. Pearsons, 2004

Kalcheff, I. and C. Machemehl Jr. Utilization of Crushed Stone Screenings in Highway Construction. Presented in the 59th Annual Meeting of the Transportation Research Board, Washington, DC, 1980.

Kazmee, H. and E. Tutumluer. Evaluation of aggregate subgrade materials used as pavement subgrade/granular subbase. Final Report. Illinois Center for Transportation/Illinois Department of Transportation, 2015.

Kleyn, E., The Use of the Dynamic Cone Penetrometer (DCP). Transvaal Provincial Administration, 1975.

Kumar, D.S. and W. Hudson. Use of Quarry Fines for Engineering and Environmental Applications. Special Report. National Stone Association, Center for Transportation Research, The University of Texas-Austin, Austin, TX, 1992.

Kumavat, H. R., and V. J. Patel. Factors Influencing the Strength Relationship of Concrete Cube and Standard Cylinder. International Journal of Innovative Technology and Exploring Engineering (IJITEE), 2014, Vol. 3, No. 8, pp. 76-79.

LaHucik, J., S. Schmidt, E. Tutumluer, and J. Roesler. Characterization of Cement Treated Base Course Using Reclaimed Asphalt Pavement, Aggregate By-Products, and Macro-Synthetic Fibers. Proceedings of Geo-Chicago Conference, 2016, pp. 523-533.

Lohani, T. Optimum Utilization of Quarry Dust as Partial Replacement of Sand in Concrete. International Journal of Applied Science and Engineering Research, Vol. 1, No. 2, 2012, pp. 391-404.

MacGregor, J., W. Highter, and D. DeGroot, Structural numbers for reclaimed asphalt pavement base and subbase course mixes. Transportation Research Record: Journal of the Transportation Research Board, Vol. 1687, 1999, pp. 22-28.

Manning, D. Exploration and Use of Quarry Fines. Miro Project Final Report No. 087/MIST2/DACM/01, Mineral Solution LTD, Manchester, United Kingdom, 2004.

McClellan, G., J. Eades, K. Fountain, P. Kirk, and C. Rothfuss. *Research and Techno-Economic Evaluation: Uses of limestone byproducts*. Final Report No. WPI 0510798, Department of Geological Sciences, University of Florida, 2002.

Mishra, D. Aggregate Characteristics Affecting Response and Performance of Unsurfaced Pavements

on Weak Subgrades. PhD Dissertation, University of Illinois at Urbana-Champaign, 2012.

Mohammadinia, A., A. Arulrajah, J. Sanjayan, M. Disfani, M. W. Bo, and S. Darmawan. Laboratory Evaluation of the Use of Cement-Treated Construction and Demolition Materials in Pavement Base and Subbase Applications. Journal of Materials in Civil Engineering, Vol. 27, No. 6, 2014.

Mwumvaneza, V., W. Hou, E. Tutumluer, I. Al-Qadi, and S. Beshears. Characterization and Stabilization of Quarry Byproducts for Sustainable Pavement Applications. Transportation Research Record: Journal of the Transportation Research Board, No. 2509, 2015, pp. 1-9.

Naik, R., N. Rudolph, Y. Chun, C. Fethullah, and W. Bruce. Use of Fly Ash and Limestone Quarry By-products for Developing Economical Self-Compacting Concrete. Proceedings of the International Congress on Fly Ash Utilisation, 4th-7th December, 2005.

Nelson, J., S. Tymkowicz, and M. Callahan. An Investigation of Emulsion Stabilized Limestone Screenings. Departmental Report No. HR-309, Office of Materials, Highway Division, Iowa Department of Transportation, 1994.

Petavratzi, E. and S. Wilson. Incinerated Sewage Sludge Ash in Facing Bricks. Characterization of Mineral Wastes, Resources and Processing Technologies–Integrated waste management for the production of construction material. Publication WRT177/WR0115, 2007.

Petavratzi, E. and S. Wilson. Sustainable Utilisation of Quarry By-products. Minerals Industry Research Organisation, English Heritage, The Department for Environment, Food and Rural Affairs, 2008.

Puppala, A., S. Saride, and R. Williammee. Sustainable Reuse of Limestone Quarry Fines and RAP in Pavement Base/Subbase Layers. Journal of Materials in Civil Engineering, Vol. 24, No. 4, 2011, pp. 418-429.

Puppala, A., S. Saride, S. Sirigiripet, R. Williammee, and V. Dronamraju. Evaluation of Cemented Quarry Fines as a Pavement Base Material. In GeoCongress 2008: Geotechnics of waste management and remediation, 2008, pp. 312-319.

Qamhia, I., H. Kazmee, E. Tutumluer, and H. Ozer. Sustainable Application of Quarry Byproducts Mixed with Large Size Unconventional Aggregates for Improved Performance. In International Congress and Exhibition Sustainable Civil Infrastructures: Innovative Infrastructure Geotechnology". 2017. Springer

Qamhia, I., E. Tutumluer, H. Ozer, and H. Kazmee. Field Performance Evaluation of Pavement Construction Platforms Utilizing Unconventional Large Size Aggregates Packed with Quarry Byproducts, and Higher Fines Aggregate Subgrade Layers. In Airfield and Highway Pavements, 2017a, pp. 334-347.

Qamhia, I., E. Tutumluer, H. Ozer, S. Beshears, H. Shoup, and H. Kazmee. Field Performance Evaluation of Quarry Byproducts Used in Unbound Aggregate Layers Constructed Over Soft Subgrade. Presented in Transportation Research Board 97th Annual Meeting, No. 18-05170, 2018.

Qamhia, I., J. Cheung, W. Hou, V. Mwumvaneza, H. Ozer, and E. Tutumluer. Gradation Effects on the Strength Properties of Cement and Fly Ash Stabilized Quarry By-Products. Proceedings of the Geo-Chicago Conference, Procedia Engineering, 2016. 143: pp. 911-920

Sayed, S.M., J.M. Pulsifer, and R.C. Schmitt, Construction and performance of shoulders using UNRAP base. Journal of materials in civil engineering, Vol. 5, N. 3, 1993, pp. 321-338.

Stokowski, S. Pond Screening from Aggregate Plants: An Industrial Minerals Resource. Proceedings of the 28th Forum on the Geology of Industrial Minerals. West Virginia Geological and Economic survey, Morgantown, WV, 1992.

Stroup-Gardiner, M. and T. Wattenberg-Komas. Recycled Materials and Byproducts in Highway Applications. Volume 4: Mineral and Quarry By-products. NCHRP Synthesis of Highway Practice (Project 20-05, Topic 40-01), Transportation Research Board, 2013.

Townsend, J. M., W.C. Jennings, C. Haycocks, G. M. Neall III, and L.P. Johnson III. A Relationship Between the Ultimate Compressive Strength of Cubes and Cylinders for Coal Specimens. The 18th US Symposium on Rock Mechanics (USRMS), American Rock Mechanics Association, January 1977.

Tutumluer, E., Moaveni, M., and Qamhia, I. Aggregate quality requirements for pavements. National Cooperative Highway Research Program (NCHRP) No. Project 20-05, Topic 48-10. Transportation Research Board, 2018.

Tutumluer, E., H. Ozer, W. Hou, and V. Mwumvaneza. Sustainable Aggregates Production: Green Applications for Aggregate By-Products. Final Report. Illinois Center for Transportation/Illinois Department of Transportation, 2015.

Tutumluer, E., I. Qamhia, and H. Ozer. Field Performance Evaluations of Sustainable Aggregate By-product Applications. Keynote Paper, Proceedings of the International Symposium on Geotechnics of Transportation Infrastructure (ISGTI), Delhi, India, 2018a.

Wood, S.A. and C.R. Marek. Recovery and Utilization of Quarry By-products for use in Highway Construction. International Center for Aggregates Research (ICAR) 3rd Annual Symposium, Vol. 10, 1995.

APPENDIX A: MATERIALS CHARACTERIZATION AND PROPERTIES

Morphological shape properties of aggregate subgrade Primary Crusher Run aggregates (PCR), distributed according to sieve size, were determined using the Enhanced University of Illinois Aggregate Image Analyzer.

Table A.1 Morphological Shape Properties of PCR Aggregate Subgrade Materials

Particle Size		Angularity Index	Flat & Elongated Ratio	Surface Texture
Retained on 76 mm (3 in.)	Average	447.84	1.36	2.37
88 total aggregates	Max	840.00	2.28	4.03
	Min	230.00	1.06	1.38
Retained on 50.8 mm (2 in.)	Average	488.37	2.11	1.54
48 total aggregates	Max	707.83	3.81	2.75
	min	318.46	1.30	0.77
Retained on 38.1 mm (1.5 in.)	average	452.87	2.01	1.38
26 total aggregates	max	686.06	2.69	2.17
	min	327.33	1.40	0.84
Retained on 25.4 mm (1 in.)	Average	401.69	2.37	1.44
21 total aggregates	max	619.58	3.92	3.46
	min	280.78	1.47	0.43
Retained on 12.7 mm (0.5 in)	Average	462.61	2.48	2.29
6 total aggregates	max	663.09	2.98	3.59
	min	370.44	1.61	1.27

Chemical compositions of selected QB materials were measured with X-Ray Florescence (XRF) testing.

Table A.2 Material Composition of the QB Materials, Determined by XRF

XRF Analysis	Chemical Composition (%)							
	CaO	MgO	SiO_2	Al_2O_3	Fe_2O_3	SO_3	K_2O	Others
QB1	81.11	11.29	5.59		0.84	0.5	0.46	0.21
QB2	54.65	36.75	6.17	0.81	0.78	0.33	0.37	0.14
QB3	71.37	10.08	14.35	2.04	0.97	0.25	0.63	0.31

Cross sections and top views of aggregate subgrade/ QB layers were studied in ATREL using the UIUC packing box:

Aggregate subgrade compacted in one lift

Aggregate subgrade compacted in two lifts

| Aggregate subgrade/ QB blends with 20% oven-dried QB, by weight | Aggregate subgrade/ QB blends with 30% oven-dried QB, by weight | Aggregate subgrade/ QB blends with 40% oven-dried QB, by weight |

Continued Next Page

Aggregate subgrade/ QB blends with 30% oven-dried QB, by weight compacted in one lift

Aggregate subgrade/ QB blends with 30% oven-dried QB, by weight compacted in two lifts

Aggregate subgrade/ QB blends with 25% wet QB (moisture content = 2.5%), compacted in two lifts

Aggregate subgrade/ QB blends with 25% wet QB (moisture content = 2.5%), compacted in one lifts over a very soft CBR 1% subgrade

Figure A.1. Selected cross sections and top views for aggregate subgrade and QB blending tests conducted using the UIUC packing box.

APPENDIX B: COMPILATION OF RUTTING PROGRESSION DATA

Rutting Progression for Cell 1S Test Sections (Construction Platforms)
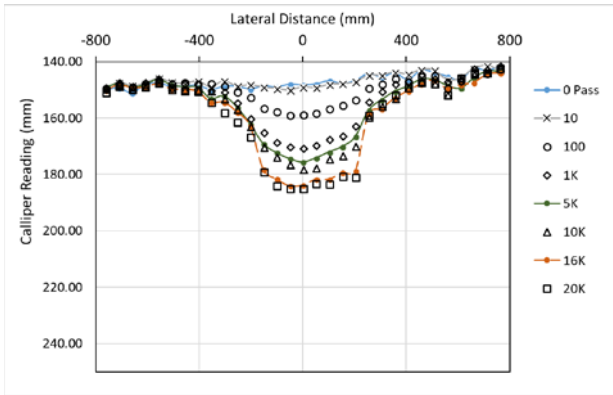
C1S1W: PCR/QB1 in 2 lifts
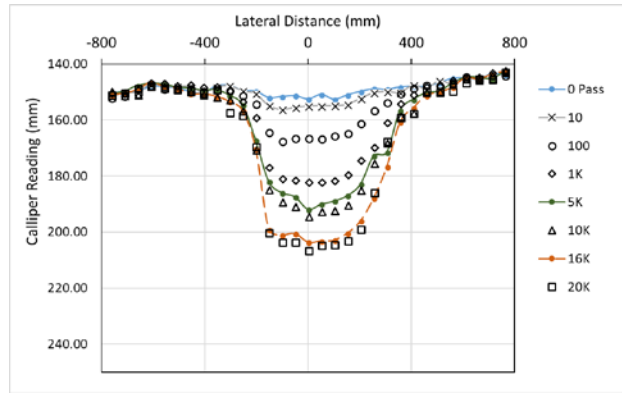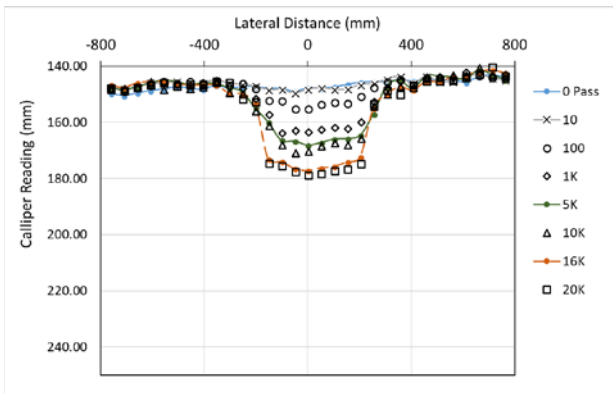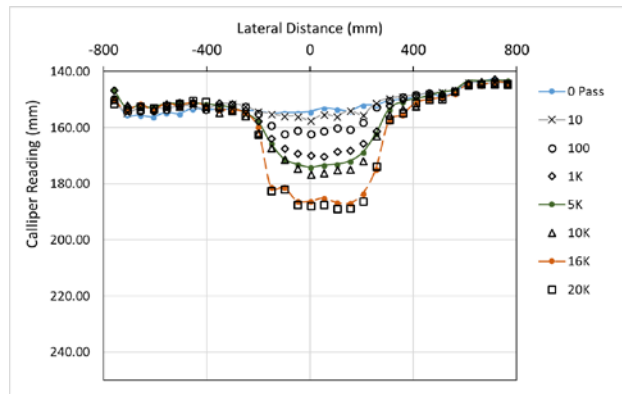
C1S1E: PCR/QB1 in 2 lifts

C1S2W: PCR/QB1 in 1 lift

C1S2E: PCR/QB1 in 1 lift
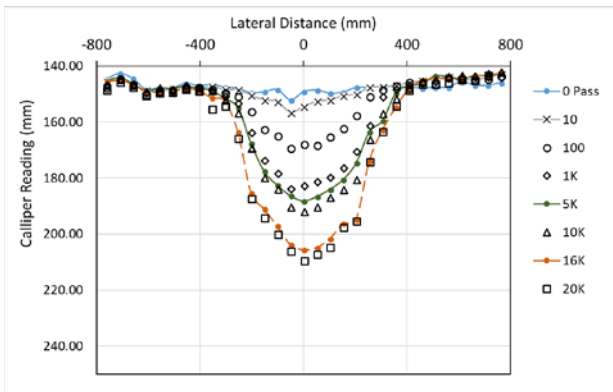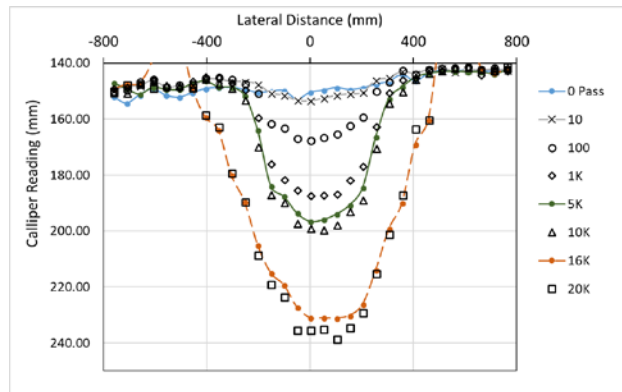
C1S3W: CA06_15PF

C1S3E: CA06_15PF
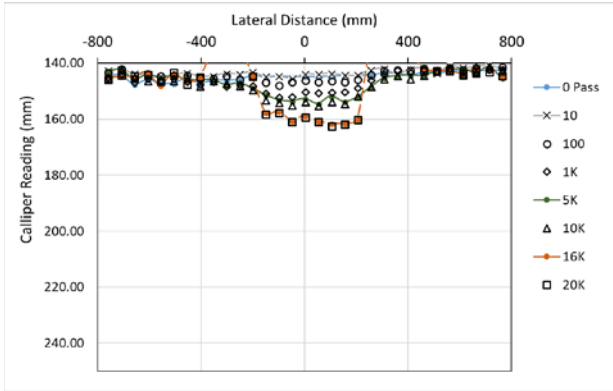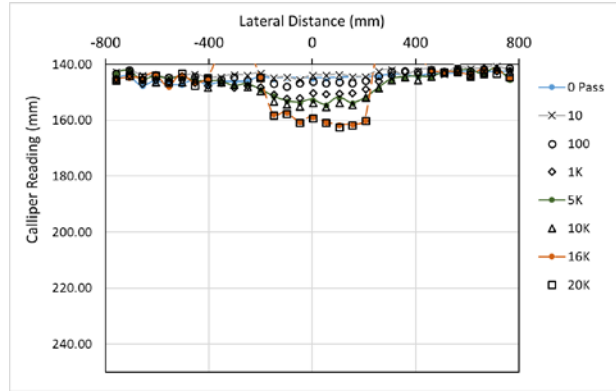
C1S4W: CA06_15NPF   C1S4E: CA06_15NPF

Figure A.2. Rutting Progression for Cell 1S Test Sections. [1 in. = 25.4 mm].
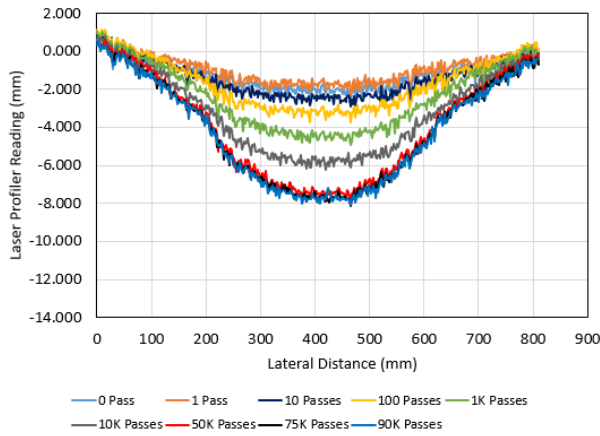
Rutting Progression for Cell 1N Test Sections

C1S1W: PCR/QB1 in 2 lifts
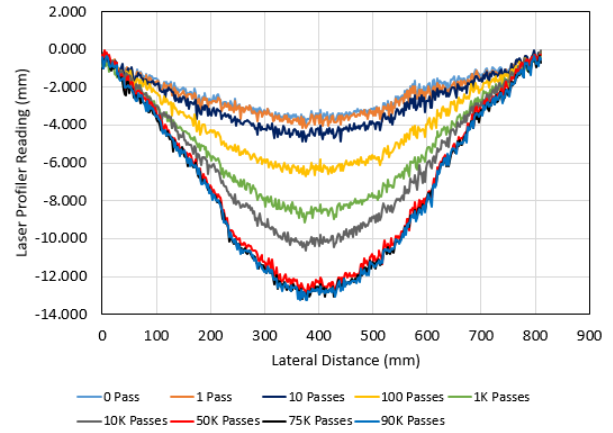
C1S1E: PCR/QB1 in 2 lifts
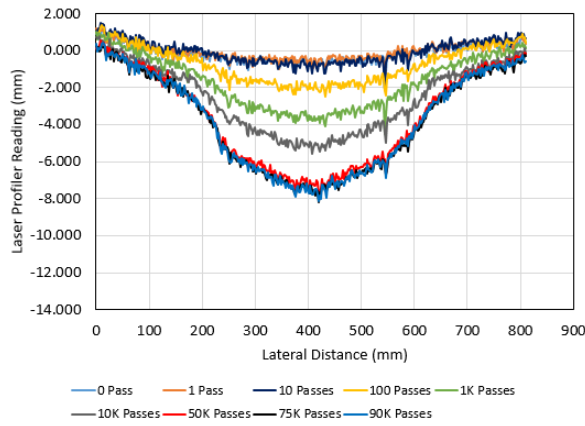
C1S2W: PCR/QB1 in 1 lift
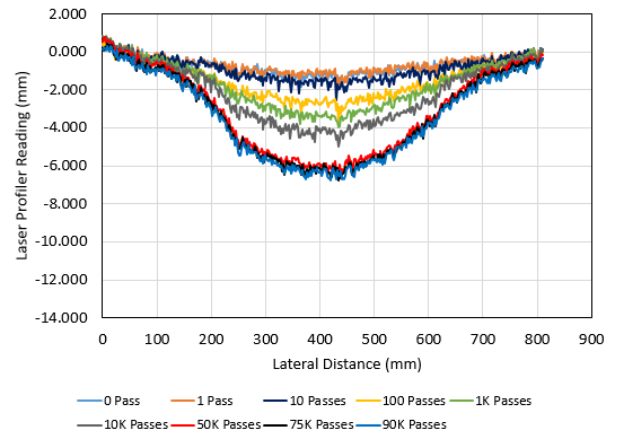
C1S2E: PCR/QB1 in 1 lift
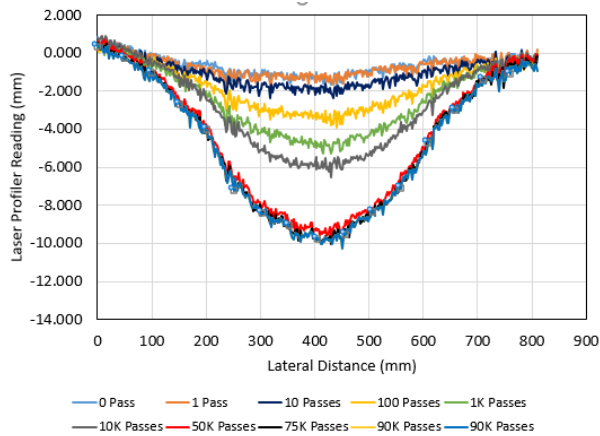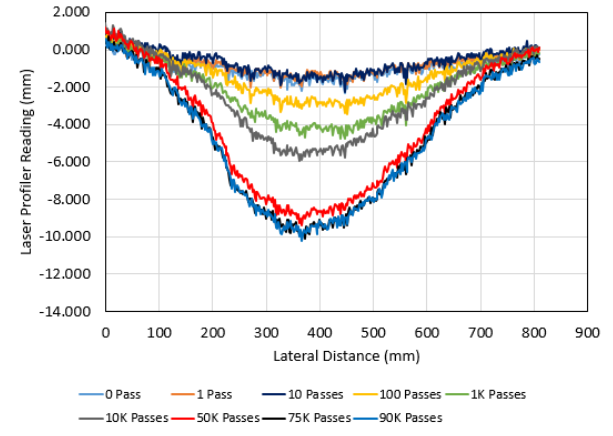
C1S3W: CA06_15PF

C1S3E: CA06_15PF
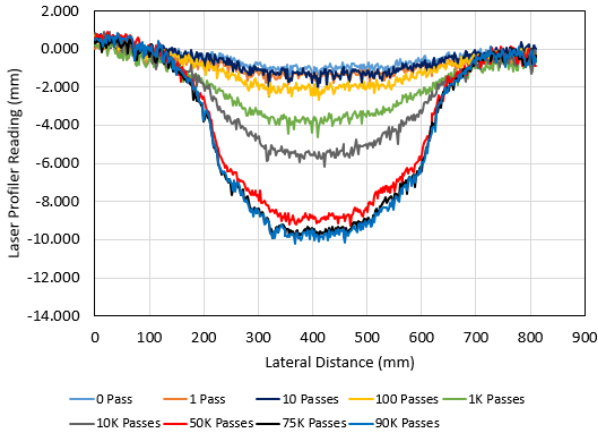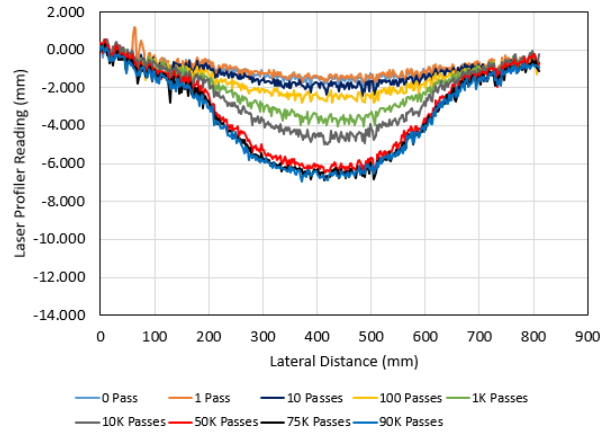
C1S4W: CA06_15NPF   C1S4E: CA06_15NPF

Figure B.1. Rutting Progression for Cell 1N Test Sections. [1 in. = 25.4 mm].

Rutting Progression for Cell 2 Test Sections

C2S1W: QB2 + FRAP + Cement Base

C2S1E: QB2 + FRAP + Cement Base

C2S2W: QB2 + FRCA + Cement Base

C2S2E: QB2 + FRCA + Cement Base

C2S3W: QB2 + FRCA + Fly Ash Base

C2S3E: QB2 + FRCA + Fly Ash Base

C2S4W: QB2 + Cement Base   C2S4E: QB2 + Cement Base

Figure B.2. Rutting Progression for Cell 2 Test Sections. [1 in. = 25.4 mm].
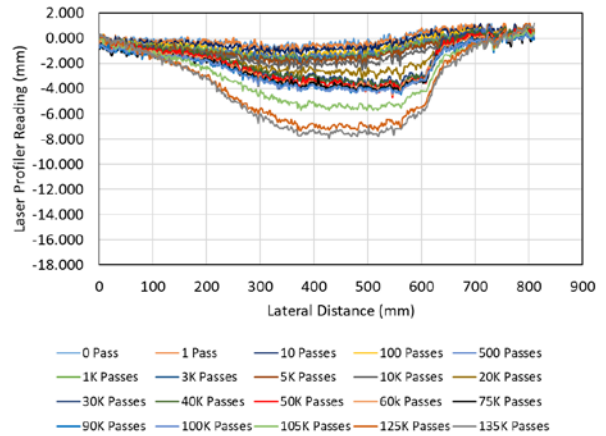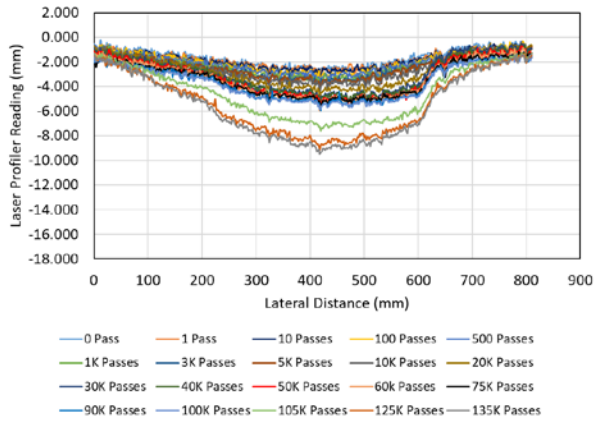
Rutting Progression for Cell 3 Test Sections

C3S1W: QB3 + Cement Base
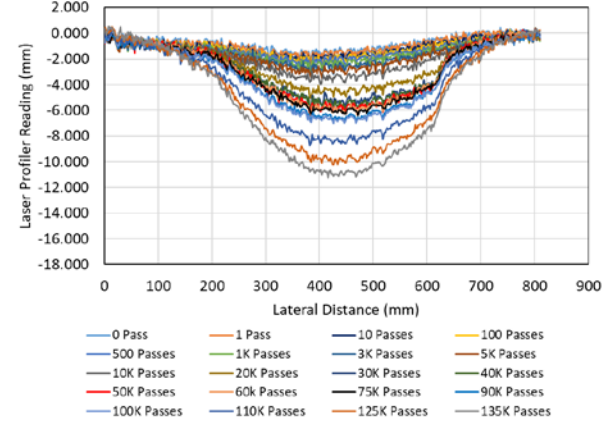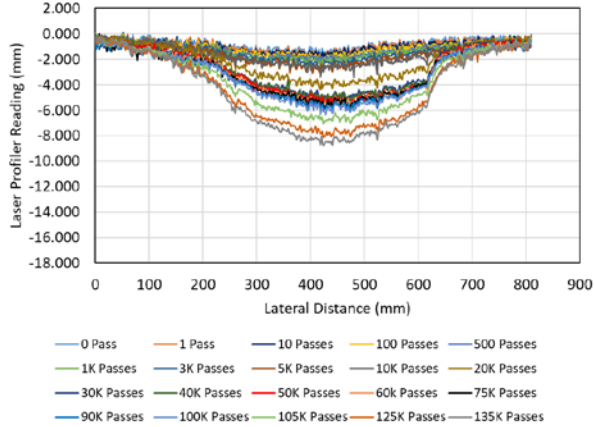
C3S1E: QB3 + Cement Base

C3S2W: QB2 + Cement Subbase and CA06_R Base

C3S2E: QB2 + Cement Subbase and CA06_R Base
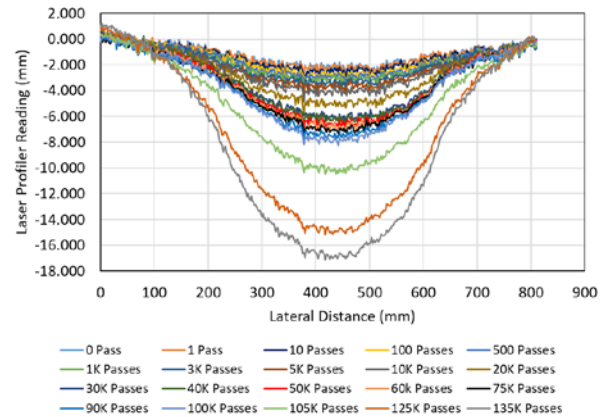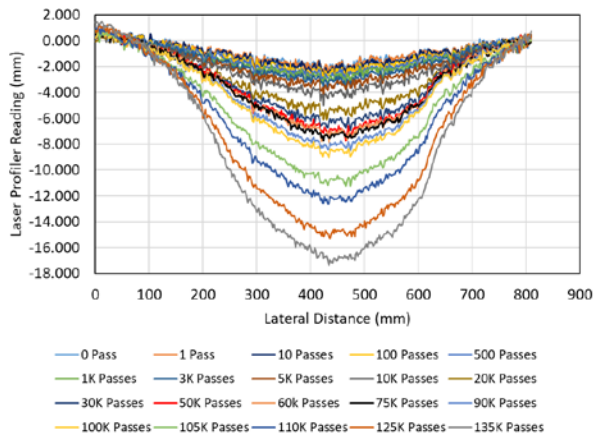
C3S3W: QB2 + Fly Ash Subbase and CA06_R Base

C3S3E: QB2 + Fly Ash Subbase and CA06_R Base
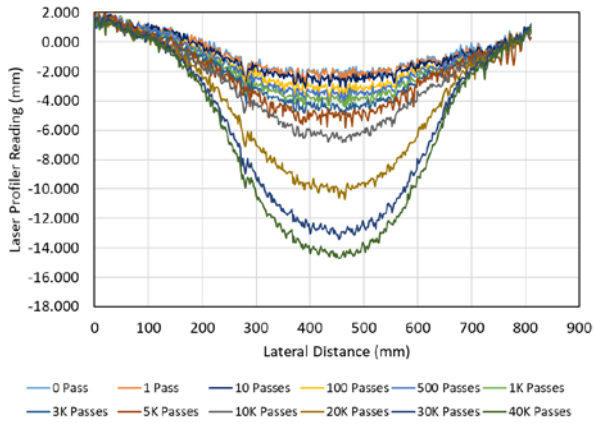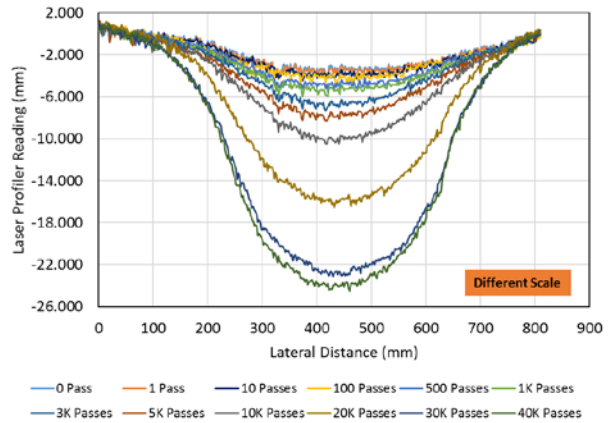
C3S4W: CA06_R Base   C3S4E: CA06_R Base

Figure B.3. Rutting Progression for Cell 3 Test Sections*.[1 in. = 25.4 mm].

* Note difference in y-axis scale from the results of Cell 1N and Cell 2.

APPENDIX C: COMPILATION OF FWD TEST RESULTS

FWD Deflection Basins for Cell 1S Test Sections (Construction Platforms): Deflections measured before trafficking in September 2016
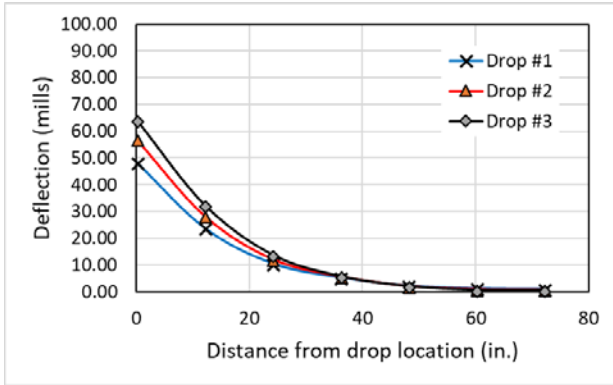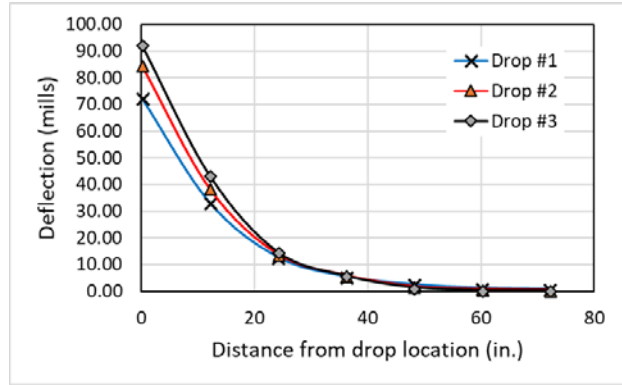
C1S1W: PCR/QB1 in 2 lifts

C1S1E: PCR/QB1 in 2 lifts
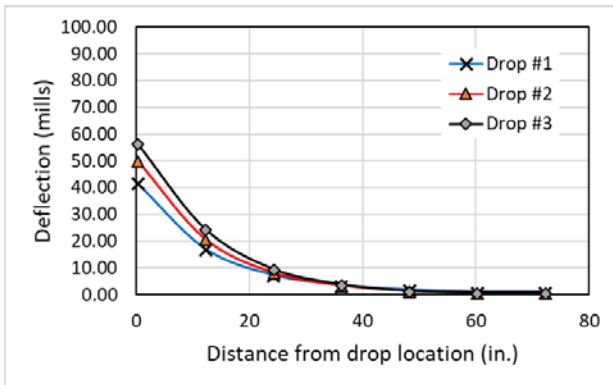
C1S2W: PCR/QB1 in 1 lift
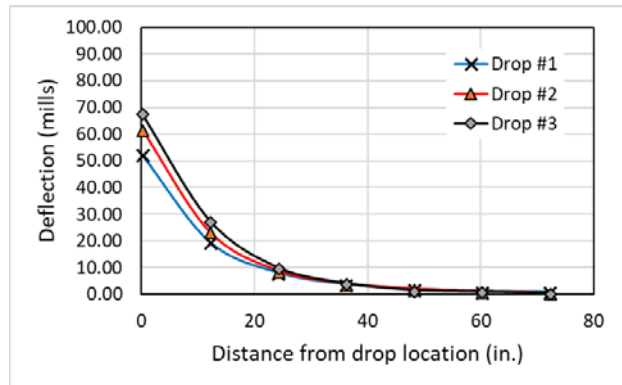
C1S2E: PCR/QB1 in 1 lift
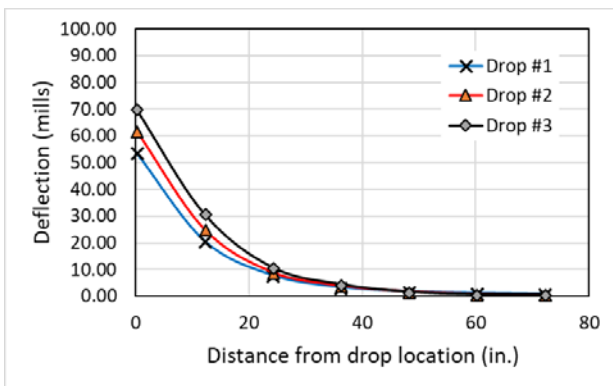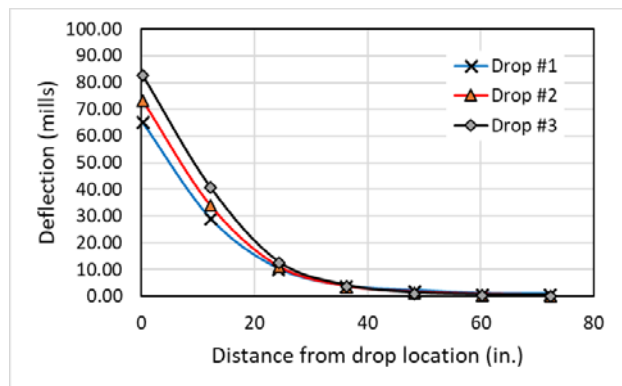
C1S3W: CA06_15PF

C1S3E: CA06_15PF
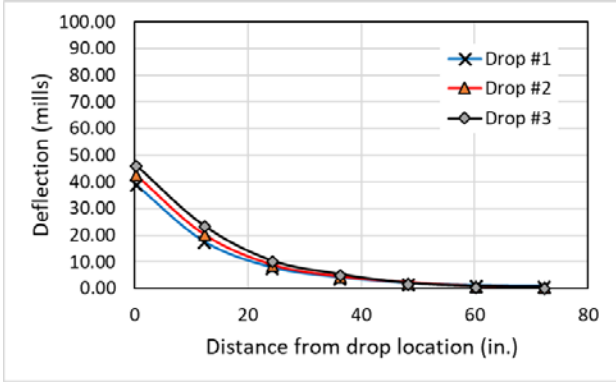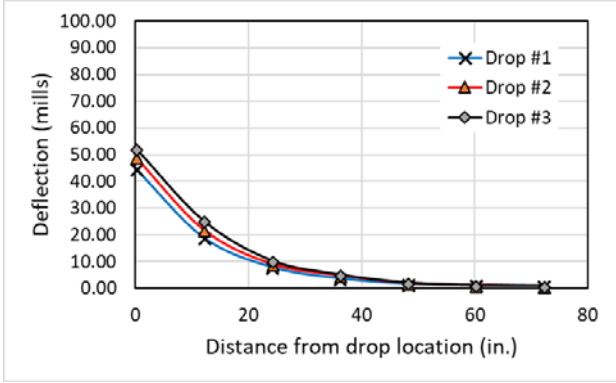
C1S4W: CA06_15NPF   C1S4E: CA06_15NPF

Figure C.1. FWD Deflections for Cell 1S: Before ATLAS Trafficking.

FWD Deflection Basins for Cell 1N Test Sections (Flexible Pavements): Deflections measured before trafficking in September 2016
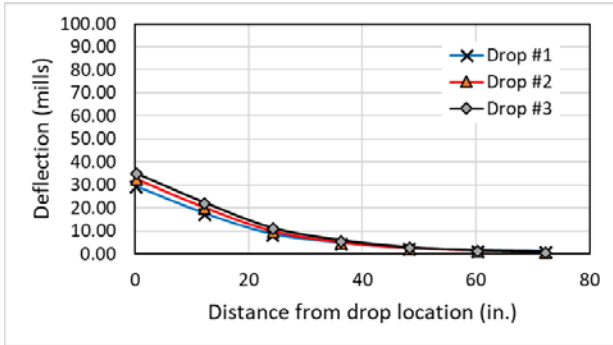
C1S1W: PCR/QB1 in 2 lifts
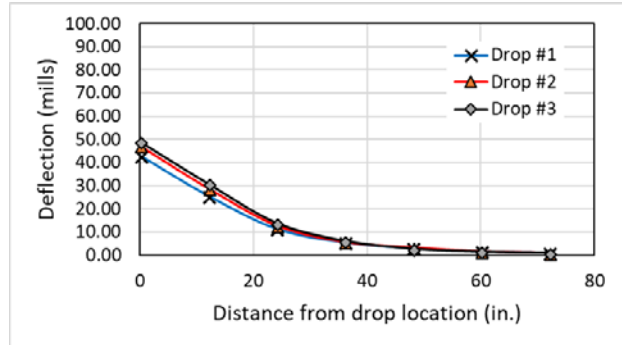
C1S1E: PCR/QB1 in 2 lifts
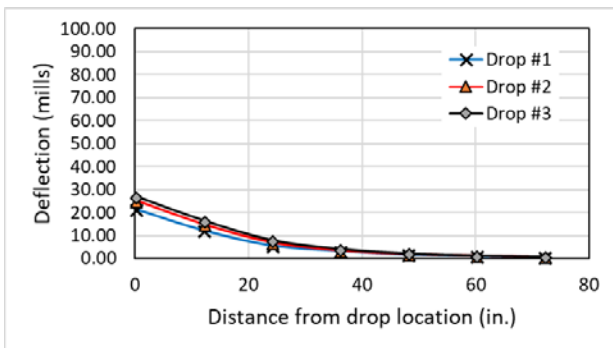
C1S2W: PCR/QB1 in 1 lift
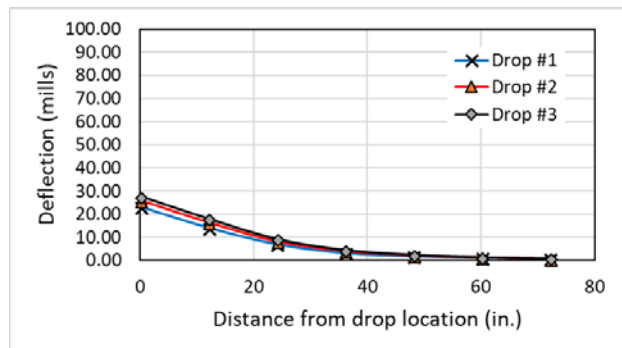
C1S2E: PCR/QB1 in 1 lift
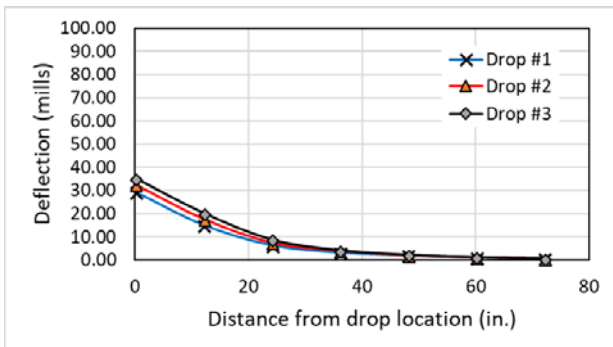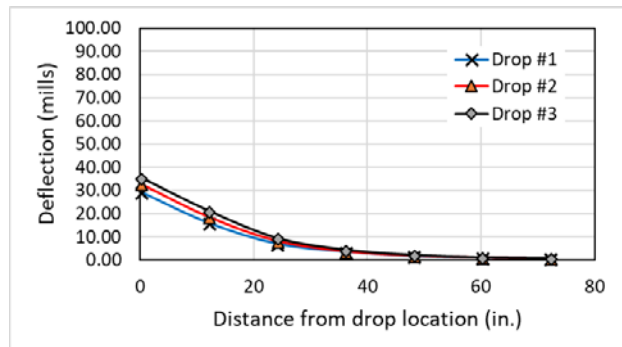
C1S3W: CA06_15PF

C1S3E: CA06_15PF
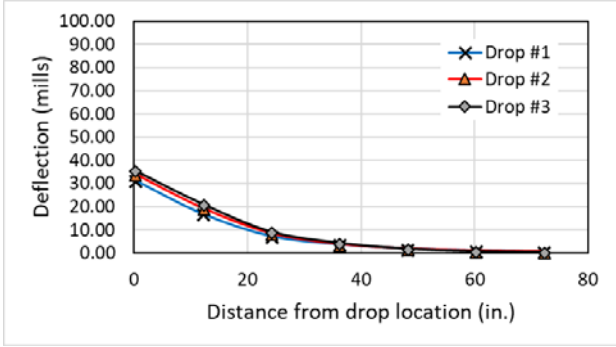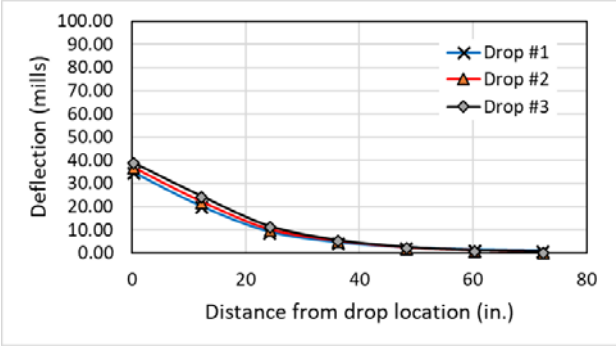
C1S4W: CA06_15NPF   C1S4E: CA06_15NPF

Figure C.2. FWD Deflections for Cell 1N: Before ATLAS Trafficking.

FWD Deflection Basins for Cell 1N Test Sections (Flexible Pavements): Deflections measured after trafficking in May 2017
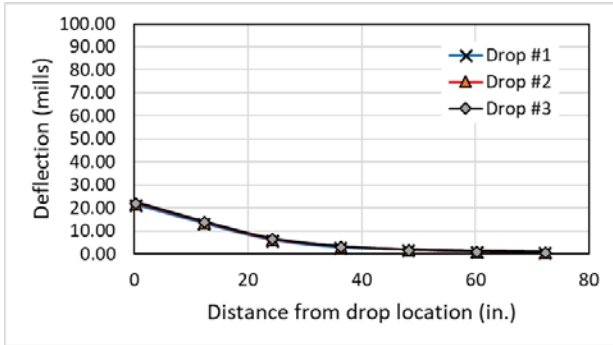
C1S1W: PCR/QB1 in 2 lifts
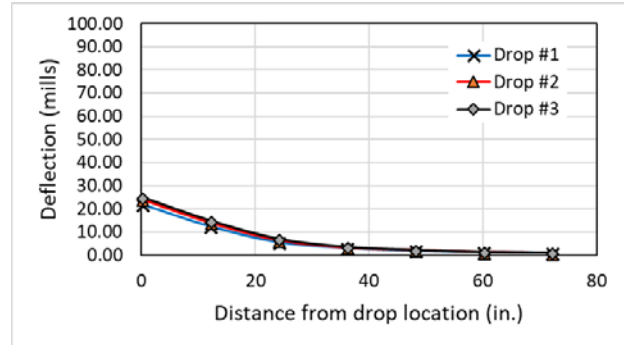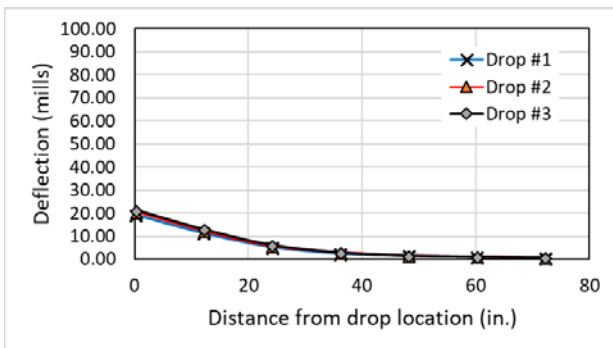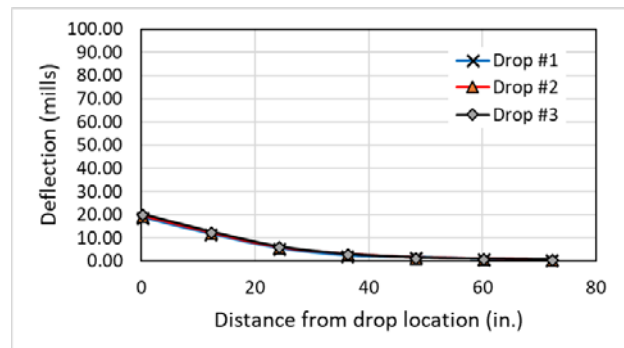
C1S1E: PCR/QB1 in 2 lifts

C1S2W: PCR/QB1 in 1 lift

C1S2E: PCR/QB1 in 1 lift
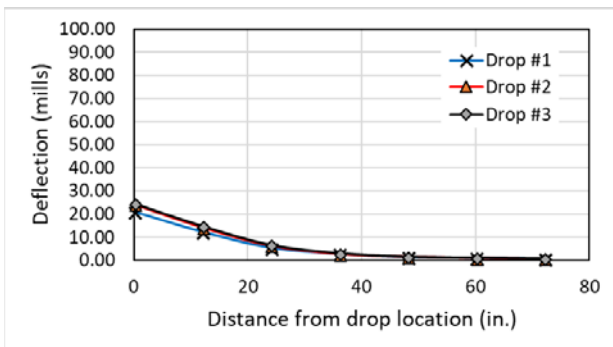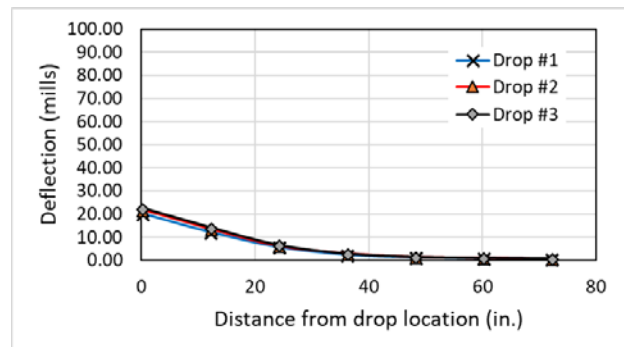
C1S3W: CA06_15PF

C1S3E: CA06_15PF
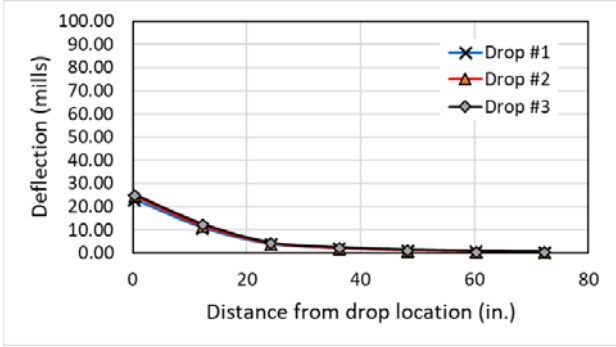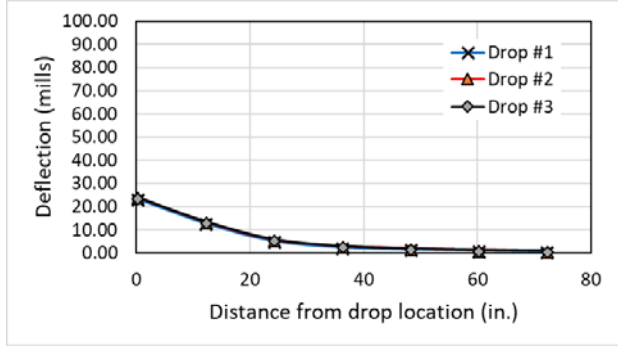
C1S4W: CA06_15NPF   C1S4E: CA06_15NPF

Figure C.3. FWD Deflections for Cell 1N: After ATLAS Trafficking.

FWD Deflection Basins for Cell 2 Test Sections (Flexible Pavements): Deflections measured after construction in September 2016
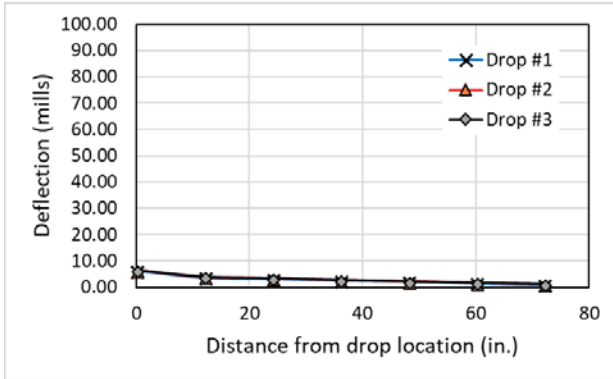
C2S1W: QB2 + FRAP + Cement Base
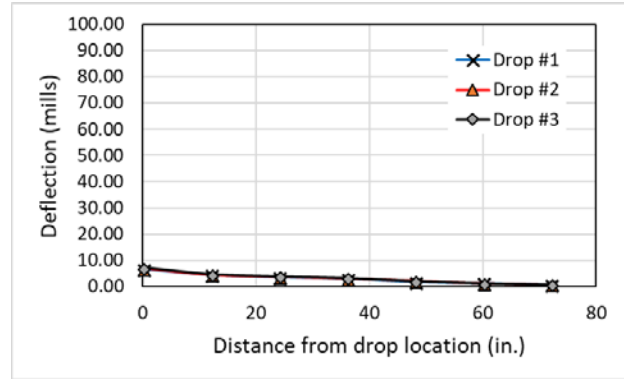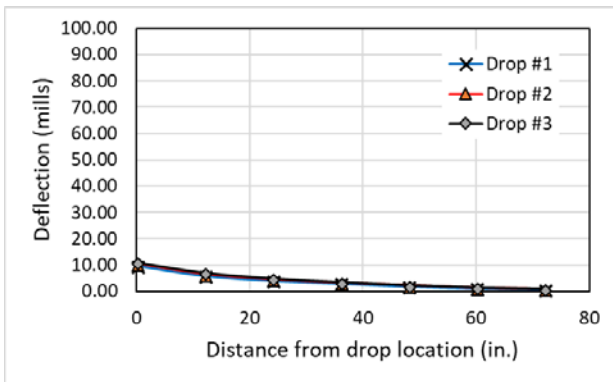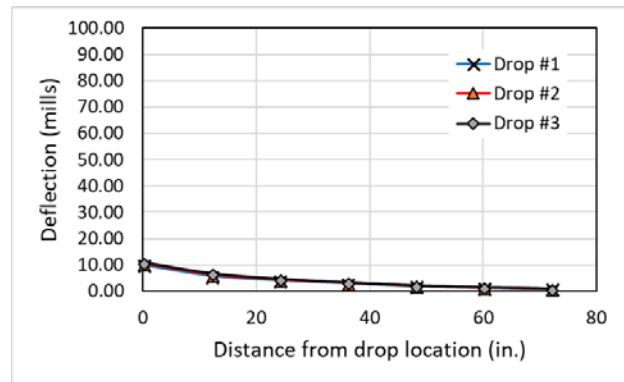
C2S1E: QB2 + FRAP + Cement Base

C2S2W: QB2 + FRCA + Cement Base

C2S2E: QB2 + FRCA + Cement Base
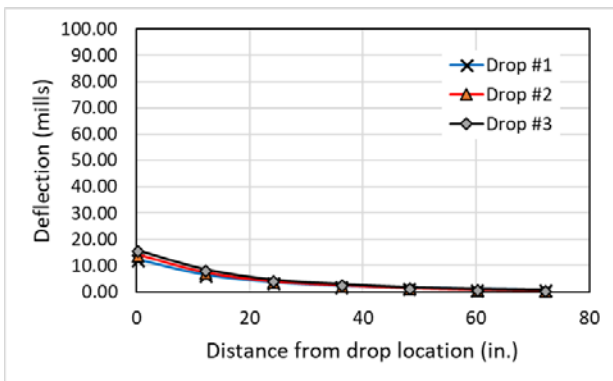
C2S3W: QB2 + FRCA + Fly Ash Base
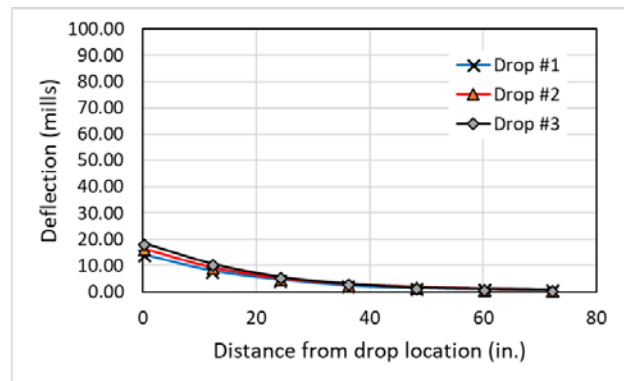
C2S3E: QB2 + FRCA + Fly Ash Base
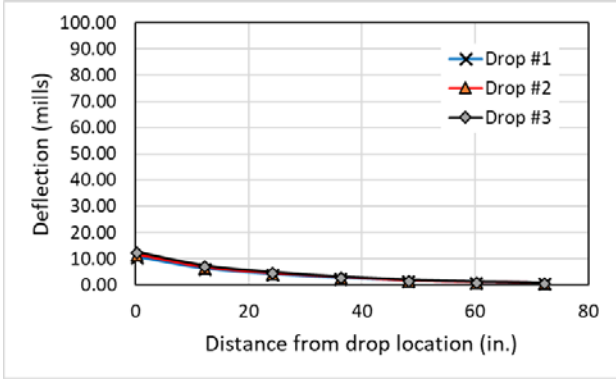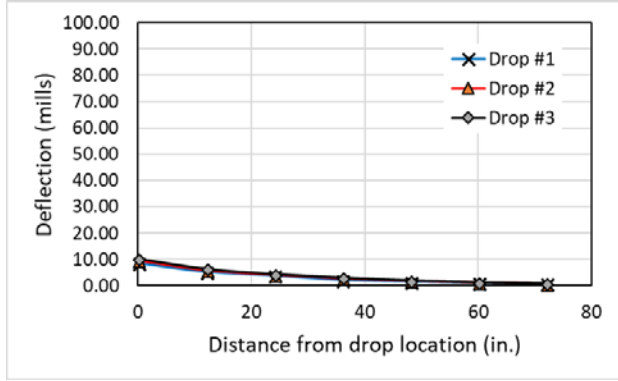
| C2S4W: QB2 + Cement Base | C2S4E: QB2 + Cement Base |

Figure C.4. FWD Deflections for Cell 2: After Construction.

FWD Deflection Basins for Cell 2 Test Sections (Flexible Pavements): Deflections measured before trafficking in May 2017
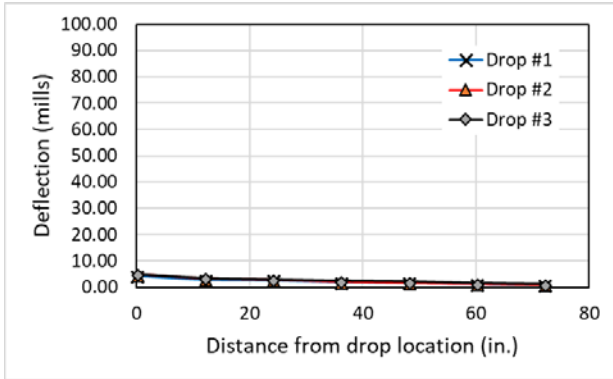
C2S1W: QB2 + FRAP + Cement Base
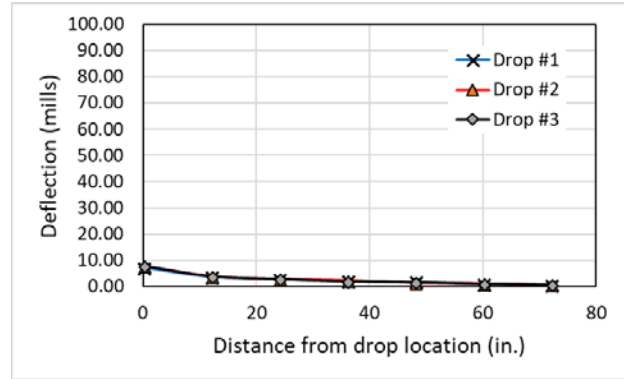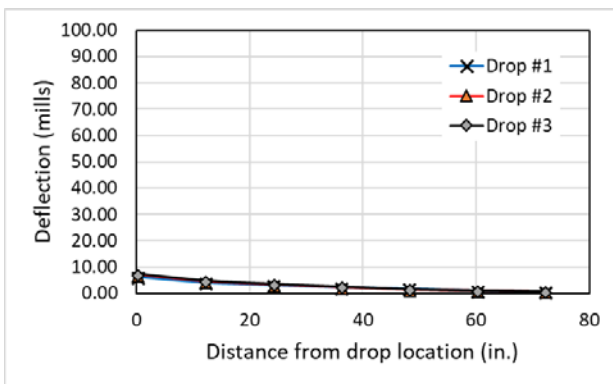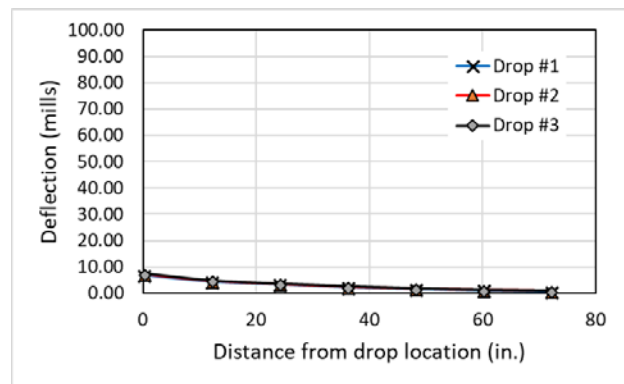
C2S1E: QB2 + FRAP + Cement Base

C2S2W: QB2 + FRCA + Cement Base

C2S2E: QB2 + FRCA + Cement Base
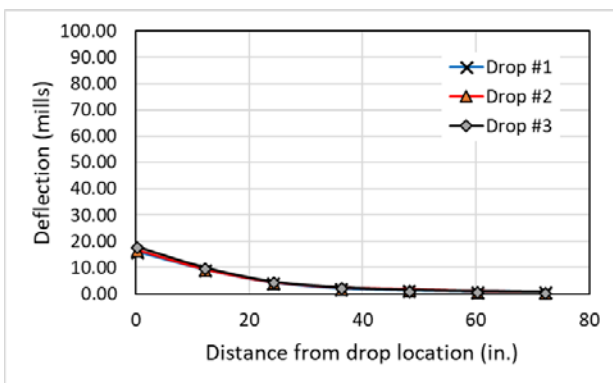
C2S3W: QB2 + FRCA + Fly Ash Base
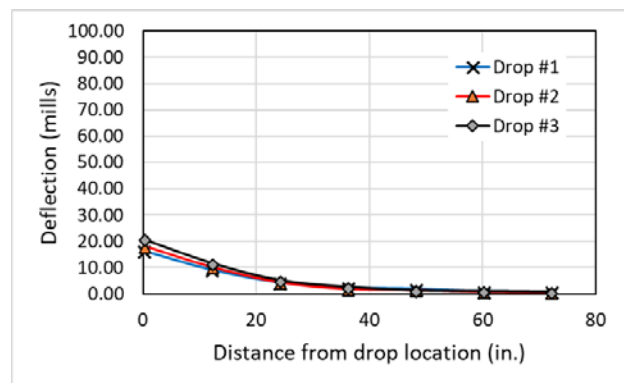
C2S3E: QB2 + FRCA + Fly Ash Base
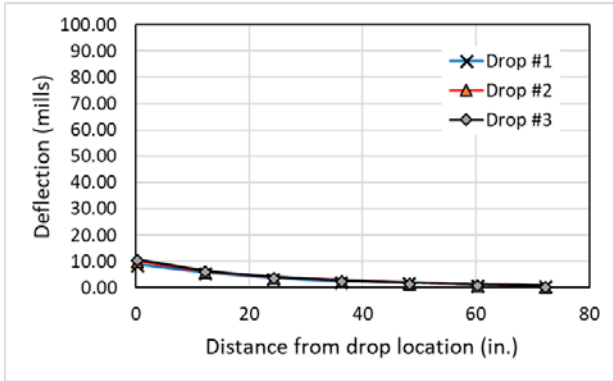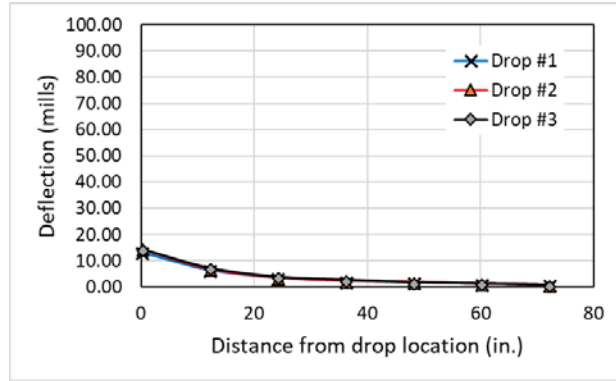
C2S4W: QB2 + Cement Base   C2S4E: QB2 + Cement Base

Figure C.5. FWD Deflections for Cell 2: Before ATLAS Trafficking.

FWD Deflection Basins for Cell 2 Test Sections (Flexible Pavements): Deflections measured after trafficking in October 2017
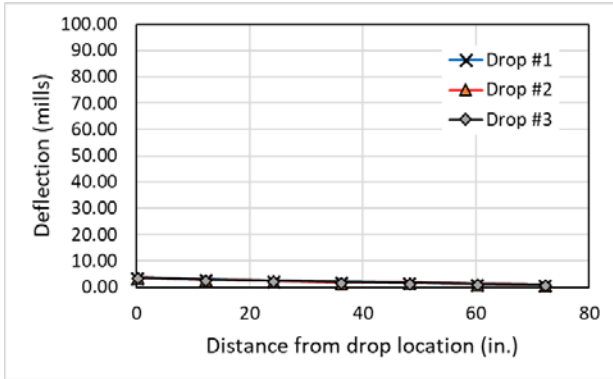
C2S1W: QB2 + FRAP + Cement Base
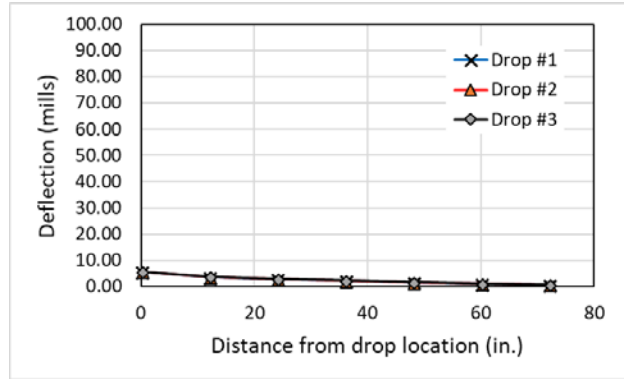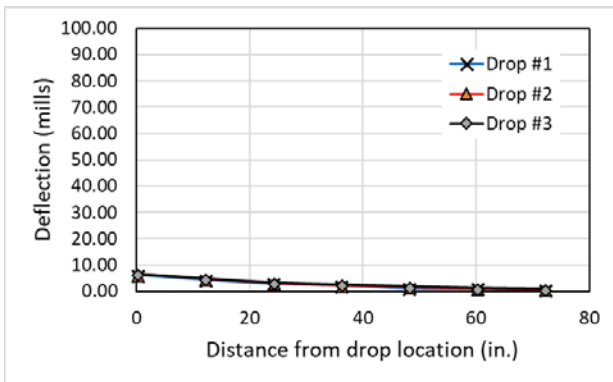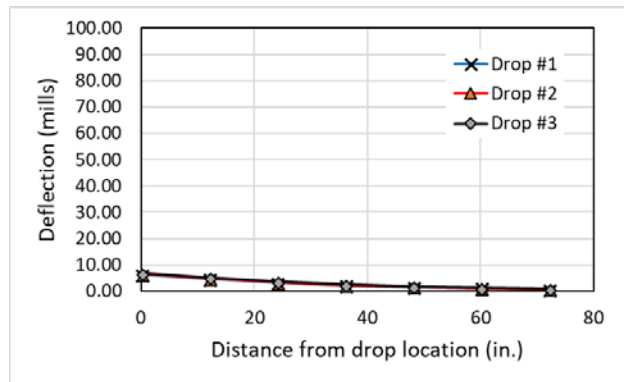
C2S1E: QB2 + FRAP + Cement Base

C2S2W: QB2 + FRCA + Cement Base

C2S2E: QB2 + FRCA + Cement Base
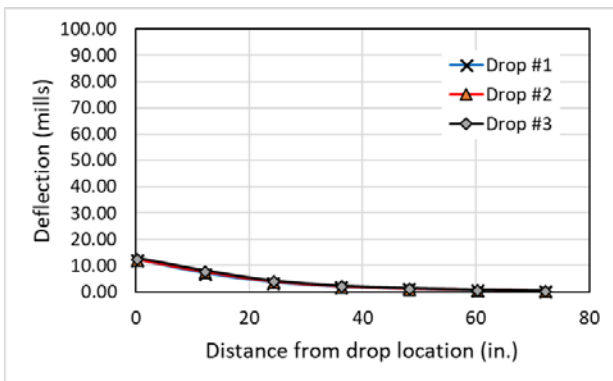
C2S3W: QB2 + FRCA + Fly Ash Base
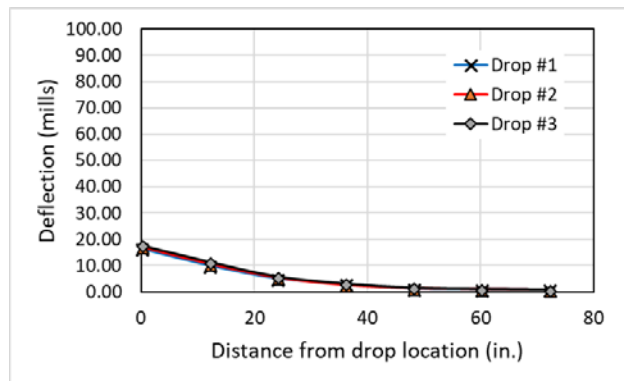
C2S3E: QB2 + FRCA + Fly Ash Base
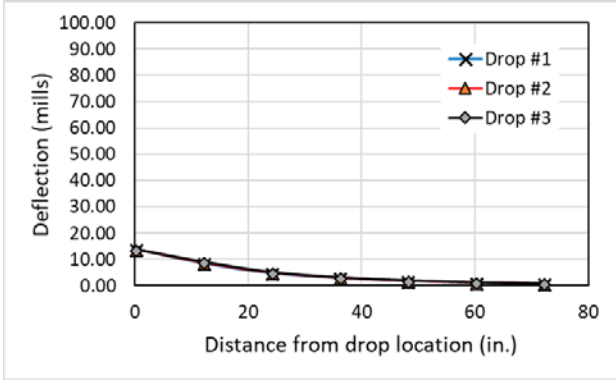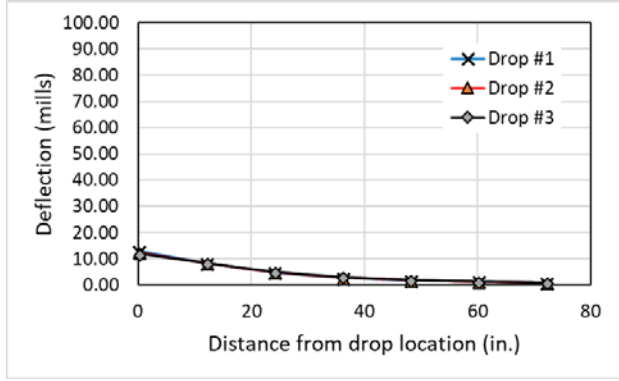
C2S4W: QB2 + Cement Base   C2S4E: QB2 + Cement Base

Figure C.6. FWD Deflections for Cell 2: After ATLAS Trafficking.

FWD Deflection Basins for Cell 3 Test Sections (Flexible Pavements): Deflections measured after construction in September 2016
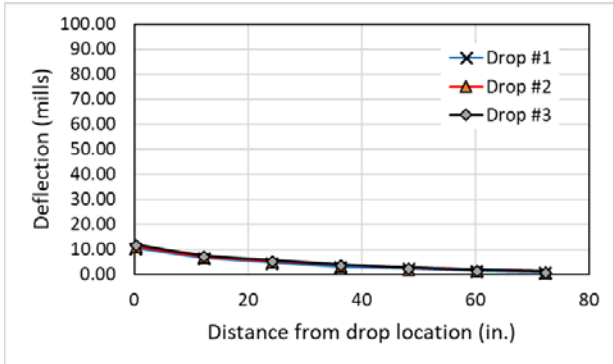
C3S1W: QB3 + Cement Base
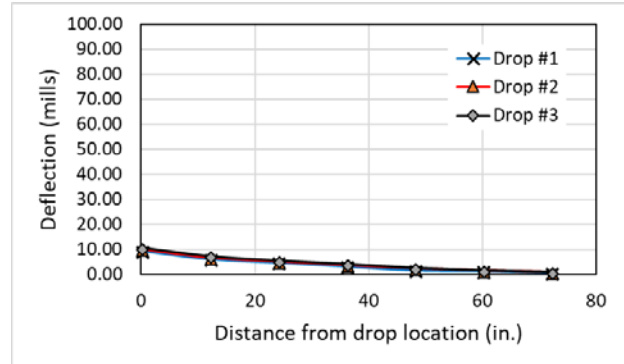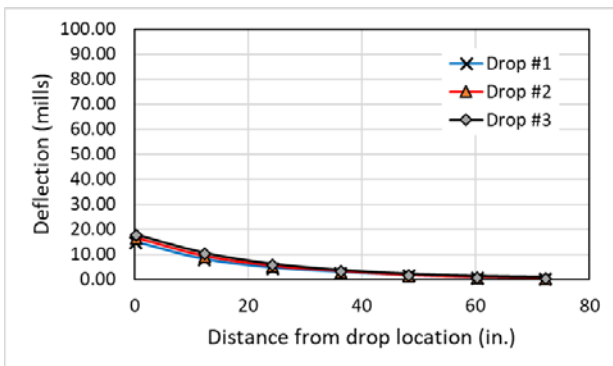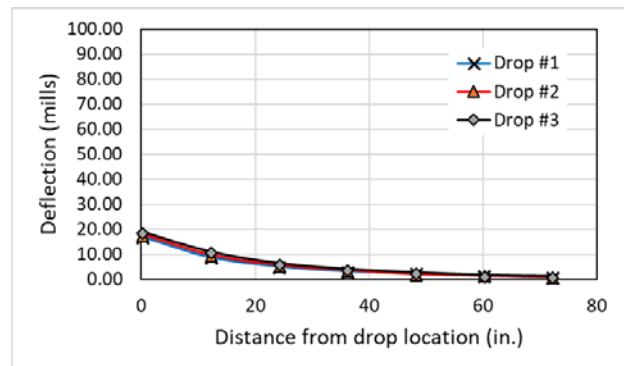
C3S1E: QB3 + Cement Base

C3S2W: QB2 + Cement Subbase and CA06_R Base

C3S2E: QB2 + Cement Subbase and CA06_R Base
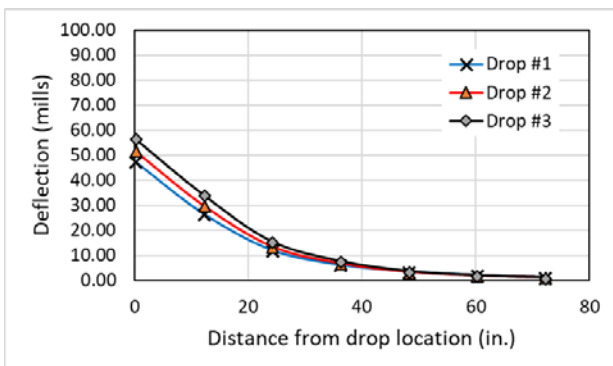
C3S3W: QB2 + Fly Ash Subbase and CA06_R Base
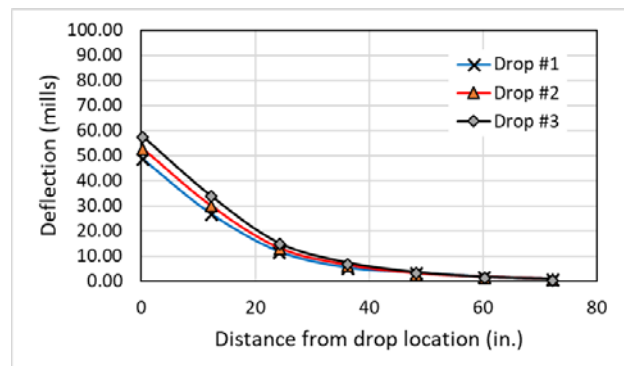
C3S3E: QB2 + Fly Ash Subbase and CA06_R Base
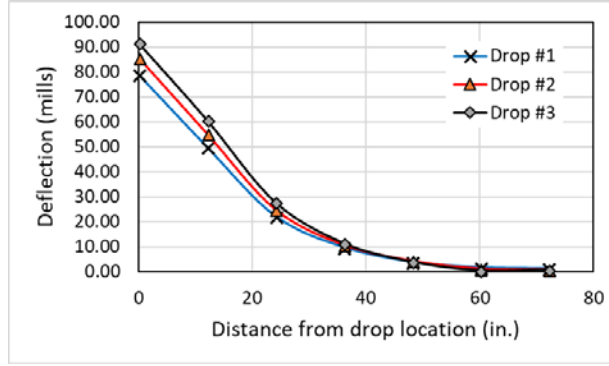
C3S4W: CA06_R Base

Figure C.7. FWD Deflections for Cell 3: After Construction

FWD Deflection Basins for Cell 3 Test Sections (Flexible Pavements): Deflections measured before trafficking in May 2017
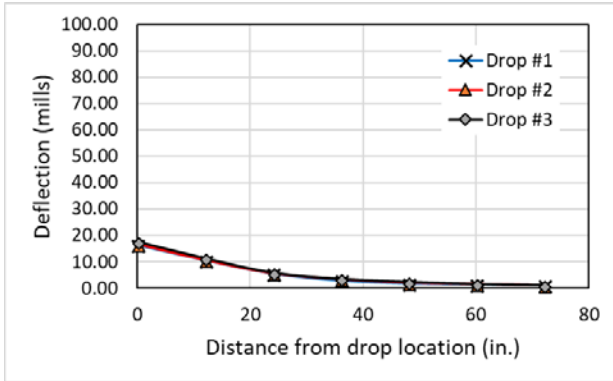
C3S1W: QB3 + Cement Base
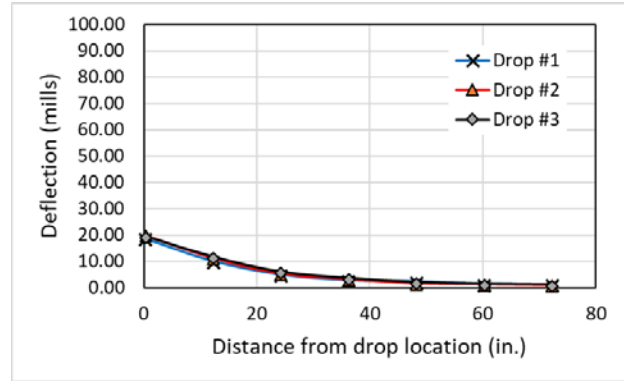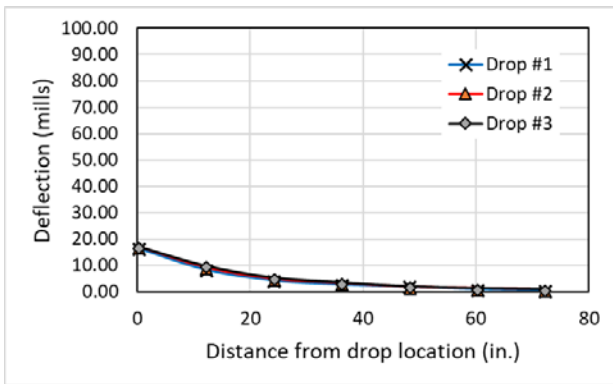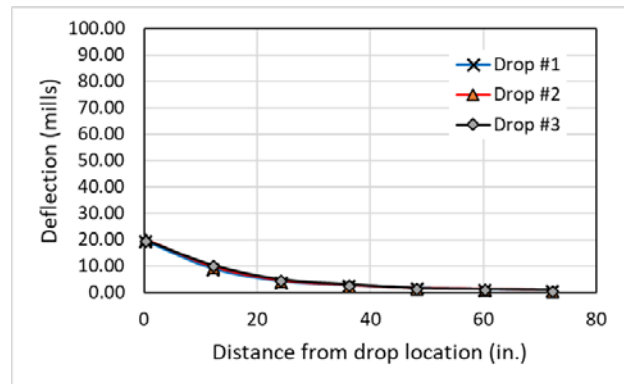
C3S1E: QB3 + Cement Base

C3S2W: QB2 + Cement Subbase and CA06_R Base

C3S2E: QB2 + Cement Subbase and CA06_R Base
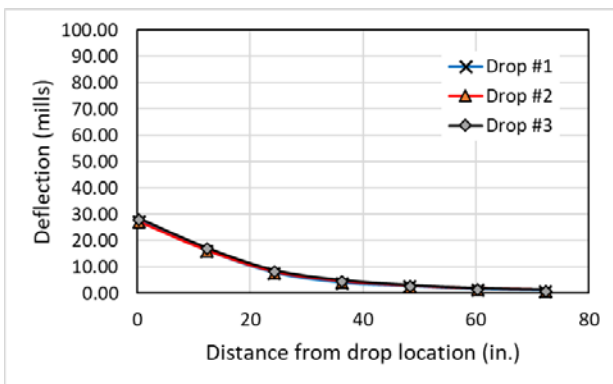
C3S3W: QB2 + Fly Ash Subbase and CA06_R Base
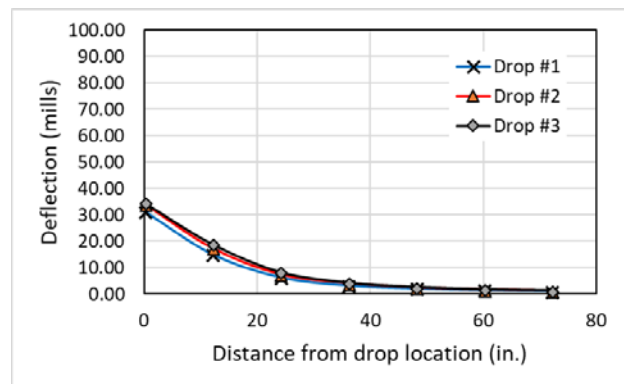
C3S3E: QB2 + Fly Ash Subbase and CA06_R Base
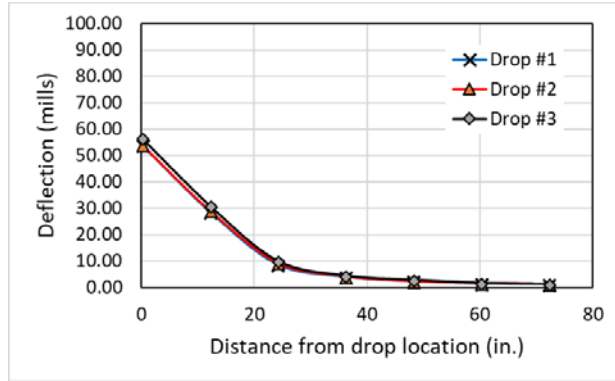
C3S4W: CA06_R Base

Figure C.8. FWD Deflections for Cell 3: Before ATLAS Trafficking.

FWD Deflection Basins for Cell 3 Test Sections (Flexible Pavements): Deflections measured after trafficking in May 2018
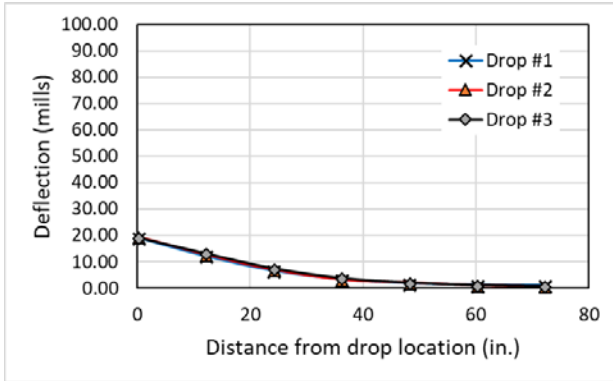
C3S1W: QB3 + Cement Base
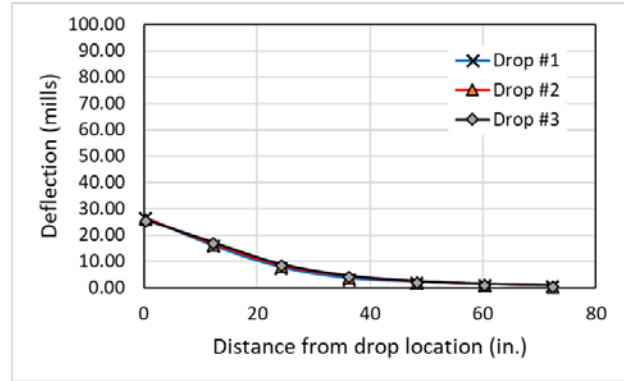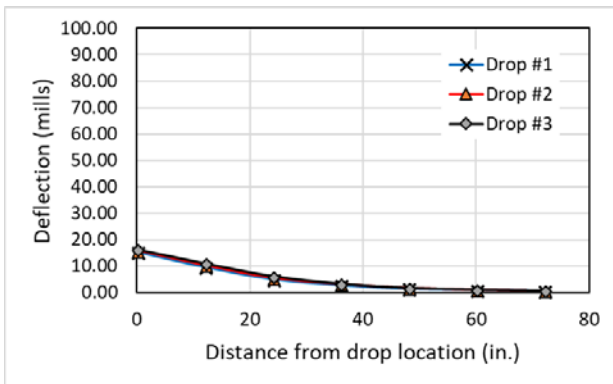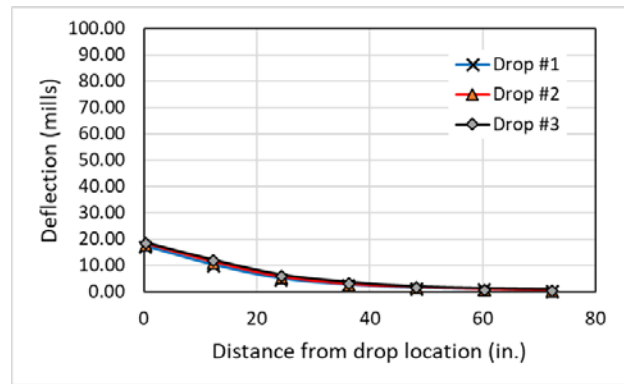
C3S1E: QB3 + Cement Base

C3S2W: QB2 + Cement Subbase and CA06_R Base

C3S2E: QB2 + Cement Subbase and CA06_R Base
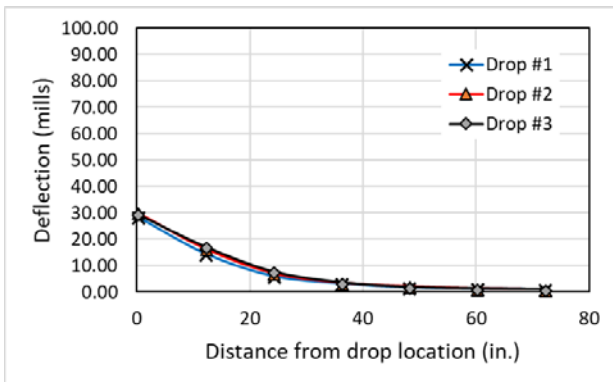
C3S3W: QB2 + Fly Ash Subbase and CA06_R Base
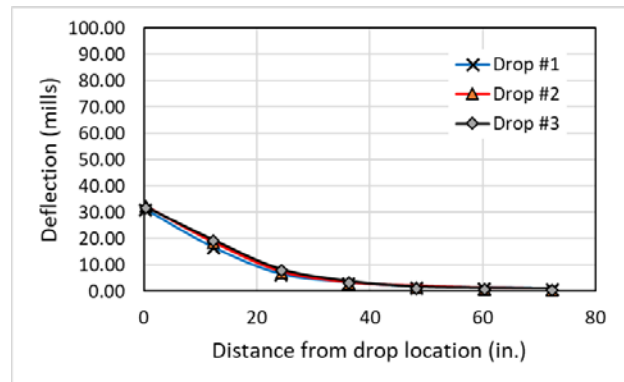
C3S3E: QB2 + Fly Ash Subbase and CA06_R Base
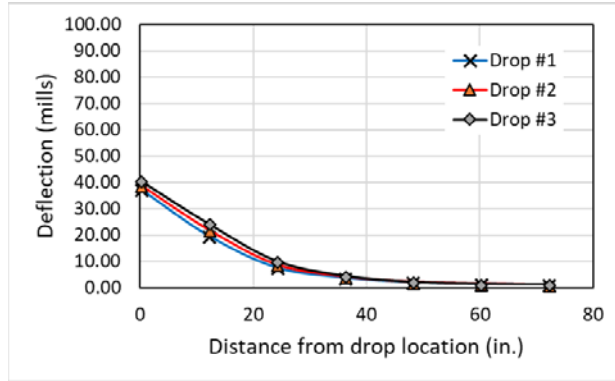
C3S4W: CA06_R Base

Figure C.9. FWD Deflections for Cell 3: After ATLAS Trafficking.

APPENDIX D: IMAGES OF HMA CORES

Images for HMA cores extracted from the wheel path at the measuring points in each Cell / section are presented in this Appendix